Bioresorbable Electrospun Tissue Scaffolds of Poly(ethylene glycol-*b*-lactide) Copolymers for Bone Tissue Engineering

Anand Shreyans Badami

Thesis submitted to the faculty of the
Virginia Polytechnic Institute and State University
in partial fulfillment of the requirements for the degree of

Master of Science
in
Macromolecular Science and Engineering

Aaron S. Goldstein, Chair
Richey M. Davis
Judy S. Riffle
Garth L. Wilkes

October 1, 2004
Blacksburg, VA

Keywords: Polylactide copolymers, poly(ethylene oxide), electrospinning, cell proliferation, differentiation, tissue engineering

Bioresorbable Electrospun Tissue Scaffolds of Poly(ethylene glycol-*b*-lactide) Copolymers for Bone Tissue Engineering

Anand Shreyans Badami

Abstract

Poly(α-hydroxy esters) are a class of biocompatible resorbable polyesters including poly(lactic acid) (PLA) and poly(glycolic acid) (PGA) that are FDA-approved for clinical use. Preliminary tissue culture studies have demonstrated that these poly(α-hydroxy esters) support bone tissue development both in vitro and in vivo, but biocompatibility issues still exist. Tissue scaffolds fabricated from these materials by current methods have biocompatibility limitations because they are chemically and topographically inert to cells. The chemical composition of these scaffolds does not influence cell behavior (i.e. proliferation, differentiation) and their surface topography is on a scale length larger than a cell, which is too large to affect cell adhesion or orientation. It is hypothesized that poly(α-hydroxy ester) tissue scaffolds can be made more bioactive by (1) incorporating poly(ethylene glycol) (PEG) into the polymer interface to promote osteoblastic differentiation and (2) controlling topography to direct cell behavior. The novel processing technique of electrospinning allows the fabrication of nanofiber scaffolds with topographical features the size of focal adhesion contacts capable of influencing cell behavior. Thus, the overall objective of this research project is to characterize electrospun PEG-PLA diblock copolymers as substrates for bone tissue engineering. To accomplish this, PEG-PLLA and PEG-PDLLA diblock copolymers were synthesized with target molecular weights of 42,000 g/mol (PEG:2000, PLLA or PDLLA:40,000). Next, these two polymers and commercially available PLLA and PDLLA were electrospun to form scaffolds with fibers of

diameters 0.14 to 2.1 μm. Finally, cell culture studies were performed to characterize cell morphology, proliferation, and osteoblastic differentiation. Results indicate electrospun fiber scaffolds limit cell spreading and persist in cell culture for two weeks. Analysis of cells cultured over 14 days revealed that there were no differences in cell density between polymers with and without PEG. Cell density increased with fiber diameter, indicating that fiber diameter affects cell adhesion and proliferation and suggesting that cells may migrate into scaffolds with large diameter fibers. In contrast to cell density, ALP activity, an indicator of osteoblastic differentiation, was unaffected by fiber diameter.

Author's Acknowledgements

This thesis would not have been possible without the assistance of several professors at Virginia Tech. I would first like to acknowledge my advisor, Dr. Aaron Goldstein (Department of Chemical Engineering), for his guidance, instruction, and patience throughout my research. I would also like to thank Dr. Judy Riffle (Department of Chemistry) for allowing the use of her lab equipment and supplies, providing guidance about PEG-PLA diblock copolymer synthesis, and ensuring that I always had funding. I am grateful to Dr. Garth Wilkes (Department of Chemical Engineering) for the use of his lab equipment and supplies and for his valuable direction regarding electrospinning. I would also like to thank Dr. Richey Davis (Department of Chemical Engineering) for serving on my graduate committee and providing me with advice about graduate school in general. Additional thanks are also extended to Dr. Tom Ward (Department of Chemistry) and Dr. Ravi Saraf (Department of Chemical Engineering) for allowing the use of their laboratory equipment.

I am also indebted to those graduate students who generously gave of their time and expertise to assist me in my research. To say that my lab mate and friend Michelle Kreke has been extremely helpful to me would be an egregious understatement. I am exceedingly grateful to her for training me in cell culture work, microscopy techniques, and cellular assays as well as the invaluable help and advice she has offered regarding a wide variety of other things too numerous to mention. I truly appreciate how she always finds the time to answer my questions no matter how much she is struggling to perform her research in addition to the myriad of unrelated tasks incessantly thrust upon her. Thanks are also extended to Shane Thompson and Mike Zalich who trained me in the art of polylactide polymerization and Pankaj Gupta who provided electrospinning instruction.

I could not have maintained my sanity and perspective without the help of several additional individuals. Above all, I am indebted to all three persons of the Most Holy Trinity who have graced me more than I deserve. I have been so blessed to have the love and support of my mother and sister, Judy and Ami Badami, as well as my father, the late Shreyans Badami. The career and graduate school advice I have received from Dr. Al Shultz of Rohm and Haas and Dr. Eugene Joseph of 3M is deeply appreciated and I would also like to thank Beth Caba for mentoring me through the MACRO program.

Table of Contents

List of Figures

List of Tables

Chapter 1 Introduction

1.1 Introduction

Poly(α-hydroxy esters) are a class of biocompatible polyesters including poly(lactic acid) (PLA), poly(glycolic acid) (PGA), and poly(lactic-*co*-glycolic acid) (PLGA) that have had extensive clinical use as FDA-approved materials for resorbable sutures, pins, screws, and staples [1-3]. These materials degrade by hydrolysis of ester linkages into low molecular weight molecules that can either be metabolized or cleared through the renal system [4-6]. In addition, they can be readily processed into a variety of structures, while retaining high compressive moduli suitable for bone tissue engineering applications. However, two key issues with the application of these materials must be considered: scaffold architecture and chemistry of the biomaterial interface.

For the purposes of tissue engineering, the polymer must be processed into an open porous structure that fills the tissue deficit while permitting infiltration and development of a new tissue [7]. It is anticipated that the scaffold structure will resorb, leaving behind only new tissue [8] (Figure 1.1.1).

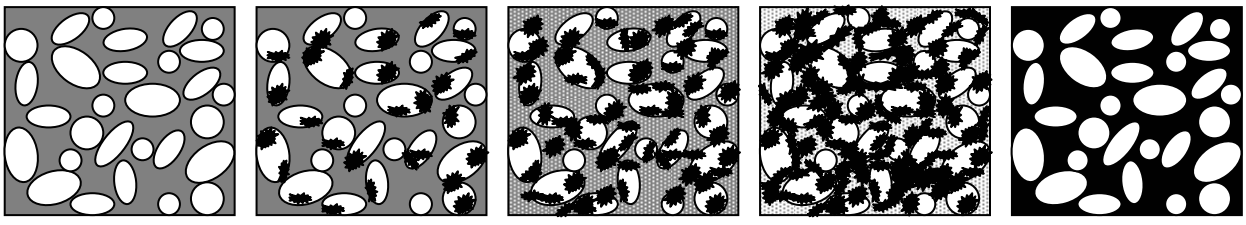

Figure 1.1.1 Diagram of the resorption process of a seeded tissue scaffold.

To date several techniques have been reported to produce porous scaffolds with architectures of open pores (e.g. solvent evaporation [9], phase separation [10-14], freeze drying emulsions [15],

gel casting [16], and gas foaming [17-19]), fused particulates (e.g. compression molding [7, 20-22], solution casting/particulate leaching [17-19], and stereolithography [8, 23]) and fibrous structures (e.g. fused deposition modeling [24] and bonded fiber meshes [25]). All of these techniques produce surfaces with topographical features whose length scales are larger than a cell (greater than 20 microns). It has been shown that biomaterial surfaces with topographical features of 0.5 to 2 microns (the size of focal adhesion contacts) can affect cell adhesion, morphology, and induce cell orientation [26]. This range of feature sizes can be achieved by a novel processing technique of electrospinning [27-29]. This would allow us to characterize the impact of substratum topography on proliferation and osteoblastic differentiation.

Preliminary tissue culture studies have demonstrated that these poly(α-hydroxy esters) support bone tissue development both in vitro and in vivo. However, there remain concerns of material compatibility [30], as evidenced by inflammation and formation of fibrovascular tissue around implanted PLA [31]. In particular, the hydrophobic nature of the polymer may drive denaturation of extracellular matrix proteins (that readily adsorb to the material [32, 33]), which could contribute to the inflammatory response. Because poly(ethylene glycol) (PEG) is considered a hydrophilic biocompatible polymer with minimal inflammatory response, I hypothesize that its incorporation at the polymer interface will enhance scaffold biocompatibility [34]. Further, a novel PEG-PLA diblock copolymer has been recently described that suppresses non-specific protein binding, allowing better adhesion of desired cell types than PLA alone [35].

The overall objective of this research project is to characterize electrospun PEG-PLA diblock copolymers as substrates for bone tissue engineering. In particular, the goals are 1) to determine advanced efficacy of PEG-PLA diblocks for bone tissue development in vitro relative

to PLA, and 2) to identify the impact of nanoscale substrate topography achieved with electrospun fibers on in vitro bone tissue development.

In the following sections a review of the relevant literature for PLA and PEG-PLA synthesis, polymer processing, and bone tissue development for bone marrow stromal cells will be provided. This will be followed by a brief plan of research.

1.2 Poly(lactic acid) Synthesis

Poly(lactic acid) (PLA), also called poly(lactide), is a well-known biodegradable polymer that has been studied with much interest in the past few decades. There are two main pathways by which PLA can be synthesized. The first involves polycondensation of aqueous lactic acid and the second involves ring-opening polymerization of cyclic lactide dimers. PLA synthesized from lactic acid is generally given the name poly(lactic acid), while PLA synthesized from lactide monomer is generally called poly(lactide), however these names are not used consistently throughout the literature [36].

1.2.1 Polycondensation

Polymerization of aqueous lactic acid by polycondensation is a reasonably low-cost, straightforward method of synthesizing PLA [36, 37]. This is accomplished by first removing water to concentrate the solution, which immediately initiates polycondensation and cyclization of the lactic acid molecules. A transesterification catalyst is then added. Suitable catalysts include metals from groups II through V in the periodic table, their oxides, and their salts [38]. The reaction is allowed to proceed at high temperature without removing any intermediate products of the reaction. This reaction scheme is not entirely advantageous because it is difficult to control the endgroups, molecular weight, and molecular weight distribution of the product

[37]. Also, this synthesis method cannot be used to create copolyesters with specific sequences because the monomeric units polymerize in a random order [37, 38].

1.2.2 Ring-Opening

The second method of PLA synthesis utilizes appropriate initiators to perform a ring-opening polymerization on lactide molecules (3,6-dimethyl-1,4-dioxane-2,5-dione), the cyclic dimers created by the dehydratization of lactic acid solution [37]. Each lactide molecule has two chiral β carbons which allow it to have three different forms: D,D-lactide or L,L-lactide (which are both stereoisometric) or racemic D,L-lactide (also called *meso*-lactide) [39] (Figure 1.2.1)

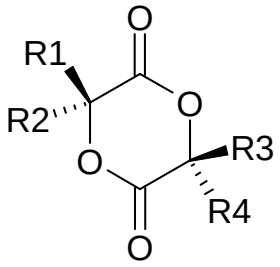

D,D(*R,R*)-lactide	R_1, R_3 = H R_2, R_4 = CH_3
L,L(*S,S*)-lactide	R_2, R_4 = H R_1, R_3 = CH_3
D,L(*R,S*)-lactide (*meso*-lactide)	R_2, R_3 = H R_1, R_4 = CH_3

Figure 1.2.1 Stereoforms of lactide. Adapted from Södergård and Stolt [36].

During lactide ring-opening polymerization, each lactide molecule opens to form a lactic acid dimer (Figure 1.2.2), which adds to the growing chain [40].

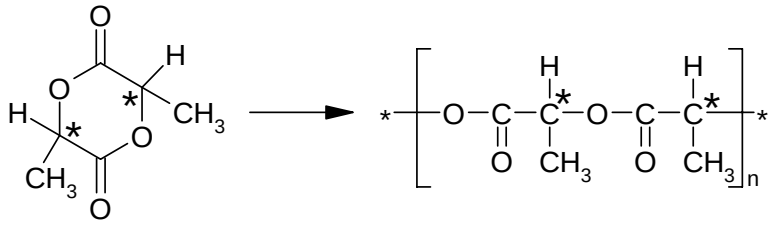

Figure 1.2.2 Lactic acid dimer obtained from lactide monomer. Adapted from Chabot et al. [40].

The poly(lactide) (PLA) that forms is named according to the isomerism of its lactic acid dimers. Poly(D-lactide) (PDLA) is formed from D,D-lactide, poly(L-lactide) (PLLA) is formed from L,L-

lactide, and poly(D,L-lactide) (PDLLA) is formed from D,L-lactide. The two most common forms of PLA are PLLA, which is semicrystalline, and PDLLA, which is amorphous [41, 42]. The ring-opening polymerizations of lactides may be classified by their four different reaction mechanisms and initiator types: anionic polymerizations, cationic polymerizations, coordination-insertion mechanisms, and enzymatic polymerizations [37]. The first three are most prevalent and will be discussed here.

1.2.2.1 Anionic polymerizations

The best way to perform anionic polymerizations of lactides is by using alkali metal alkoxides as initiators [37, 43, 44]. The polymerization is initiated when the nucleophilic anion of the initiator attacks the carbonyl group of the lactide, which prompts the bond between the carbonyl carbon and the endocyclic oxygen next to it to break (Figure 1.2.3a). This oxygen becomes a new anion, allowing propagation of the polymerization to occur in the same manner as the initiation step (Figure 1.2.3b). Anionic polymerization occurs via very basic alkoxides which are capable of deprotonating the monomer in α-position (Figure 1.2.3c). This will inevitably cause racemization to occur as the anion delocalizes over the planar molecule. Chain transfer may also occur if this lactide anion initiates new chains. Since chain transfer will result in molecular weights that are moderate to low (6500 to 38,000 g/mol) , anionic polymerization is not the preferred method polymerizing lactides [37, 44].

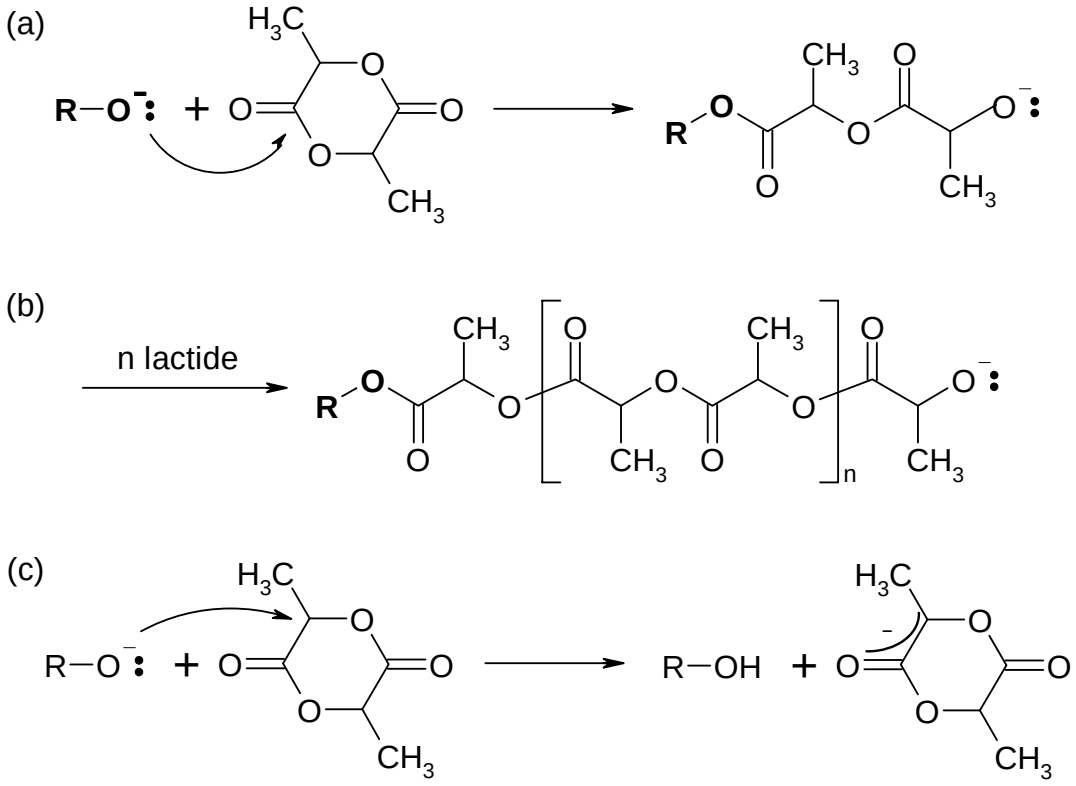

Figure 1.2.3 Reaction scheme and deprotonation mechanism of anionic lactide polymerization: (a) initiation, (b) propagation, (c) chain transfer. Adapted from Kricheldorf [37, 45] and Kricheldorf and Kreiser-Saunders [43, 45].

1.2.2.2 Cationic polymerizations

Cationic polymerization of lactides is performed by using one of a number of initiators which include carbenium ion donors and a few strong acids (e.g. metal fluorides) [37, 45]. The initiation step of cationic polymerization occurs when an exocyclic oxygen of one of the lactide carbonyls is either alkylated or protonated by the initiator, causing the resulting O-CH bond to become positively charged (Figure 1.2.4a). Nucleophilic attack by a second monomer breaks this bond to create another electrophilic carbenium ion (Figure 1.2.4b). The propagation step of this polymerization repeats as nucleophilic attack by additional monomers continues until the polymerization is terminated by a monofunctional nucleophile like water (Figure 1.2.4c). Kricheldorf and Dunsing found that racemization occurred at reaction temperatures above 50°C

[45], but cationic polymerization is not often used to polymerize lactides at lower temperatures because such reactions are slow (over 24 h) and return polymers with moderate to low molecular weights [37, 45].

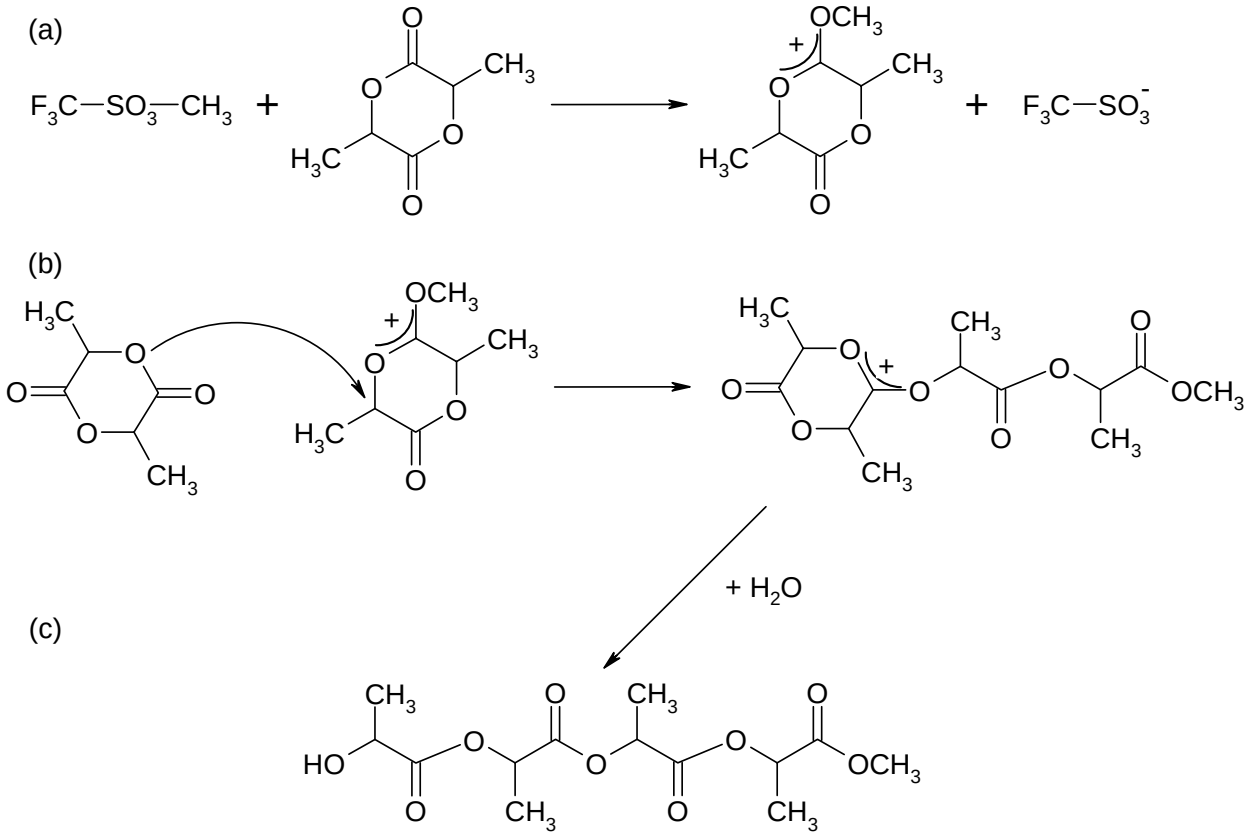

Figure 1.2.4 Reaction scheme for cationic lactide polymerization: (a) initiation, (b) propagation, (c) termination. Adapted from Kricheldorf [37] and Kricheldorf and Dunsing [45].

1.2.2.3 Coordination–insertion mechanisms

The coordination-insertion mechanism, a third method of ring-opening polymerization of lactides, employs metal alkoxide initiators which possess a covalent bond between metal atom and oxygen atom and behave like weak Lewis acids [37, 46]. The first step of the coordination-insertion mechanism occurs when one of the exocyclic oxygens of the lactide becomes temporarily coordinated with the metal atom of the initiator, increasing the nucleophilicity of the alkoxide part of the initiator as well as the electrophilicity of the lactide carbonyl group

(Figure 1.2.5) [37, 46, 47]. In the second step, the acyl-oxygen bond (between the carbonyl group and the endocyclic oxygen) of the lactide is broken and the lactide chain produced is inserted into the metal-oxygen bond of the initiator [37, 46, 47]. The alkoxide end of the initiator becomes a dead chain end while the chain growth of this "living" polymerization continues as additional lactide molecules are opened and inserted into the bond between the metal atom and its adjacent oxygen atom [46]. The non-reacting endgroup of the growing chain can be easily varied by reacting the initiator in situ with an alcohol or phenol (Figure 1.2.5) [37]. As initiation begins, this alcohol or phenol will become an ester endgroup. Bioactive molecules having at least one hydroxyl group can be incorporated into the polymer endgroup this way.

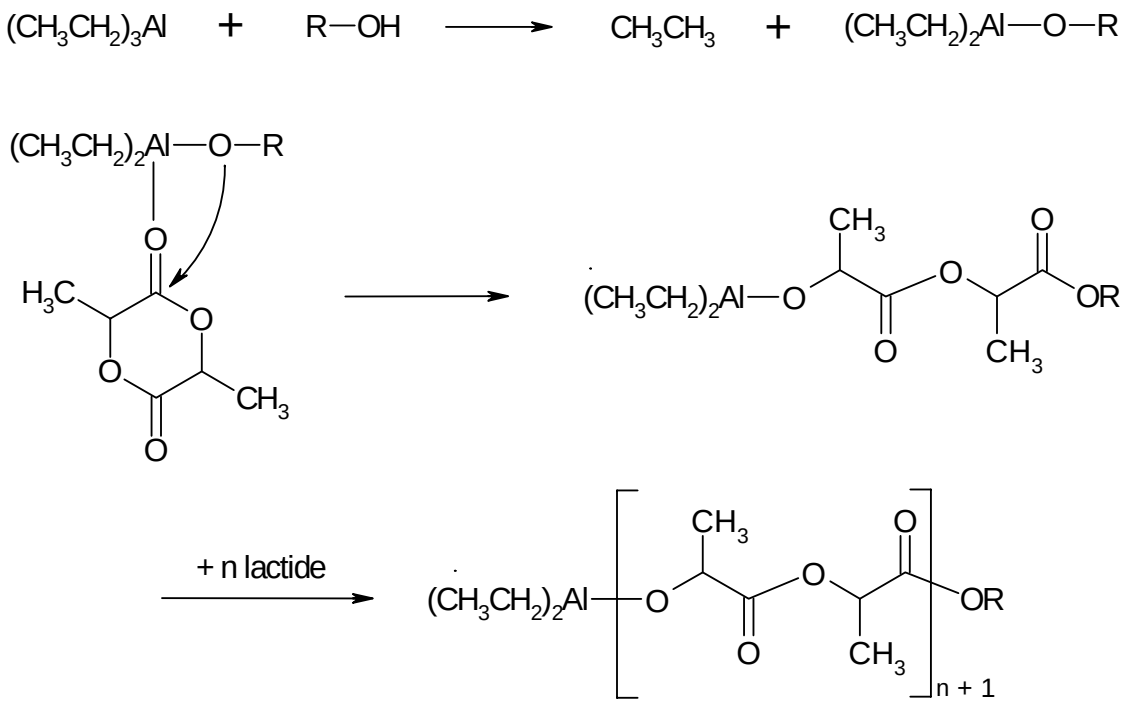

Figure 1.2.5 Coordination insertion mechanism. Adapted from Kricheldorf [37].

By modifying the ratio of monomer to initiator, this coordination-insertion mechanism allows for the control of molecular weights over a broad range (low to high) [37]. High number-average molecular weights (>200,000 Da) [48] are easier to obtain by this method than in anionic or

cationic polymerizations because there is a much lower probability of side reactions. Furthermore, the probability of racemization occurring at high temperatures is limited because these initiators are covalent instead of ionic. Transesterification may be caused by covalent metal alkoxides at temperatures around 100°C, but occurs less frequently with aluminum alkoxides than with tin alkoxides, making aluminum alkoxides more appropriate in synthesizing block copolyesters while tin alkoxides are better suited for synthesizing randomly sequenced copoly(lactones) [47]. Alkoxides of tin [49-51], aluminum [52], zinc [40, 53], magnesium [37], zirconium [37], and titanium [37] are common initiators used in this polymerization, and transition metal compounds of iron [54], lead [55], bismuth [55], and yttrium [56] have also been reported at catalysts.

The most commonly used initiator for ring-opening polymerization of lactides is tin(II) 2-ethylhexanoate (often abbreviated $SnOct_2$) (Figure 1.2.6).

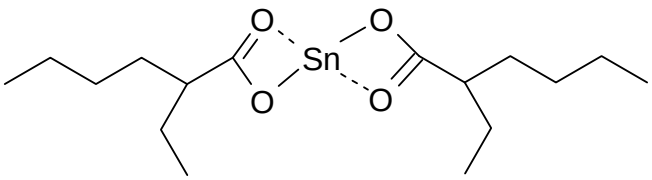

Figure 1.2.6 Structure of tin(II) 2-ethylhexanoate ($SnOct_2$). Adapted from Nijenhuis et al. [49].

There are three main reasons why $SnOct_2$ is the catalyst of choice for lactide polymerizations: low risk of racemization, high efficiency, and relatively low toxicity [50]. The risk of racemization is so low that poly(L-lactide) that is 99% optically pure can be synthesized at high temperatures (150°C) with reaction times of a few hours [50]. As a catalyst, $SnOct_2$ is so efficient that even when the monomer to catalyst ratio exceeds 11,000 [46] it still enables the reaction to progress to complete conversion [50]. $SnOct_2$ is considered to have a toxicity much lower than other heavy metal salts, indicated by its allowed use as a food additive in multiple

countries [50]. Despite this, catalysts containing tin have been shown to be cytotoxic, so great care must be taken when purifying polymers for biomedical use synthesized using such catalysts [57]. Recent studies regarding the mechanism of $SnOct_2$-catalyzed lactide polymerizations indicate that when alcohol is added in a 2:1 or less alcohol to monomer ratio, the alcohol acts as a coinitiator in the reaction [37, 51]. The alcohol replaces one of the octanoate groups of the $SnOct_2$ and the polymerization progresses as opened lactide rings insert themselves into the Sn-OR bond of the resulting alkoxide (Figure 1.2.7) [36, 37, 41, 51].

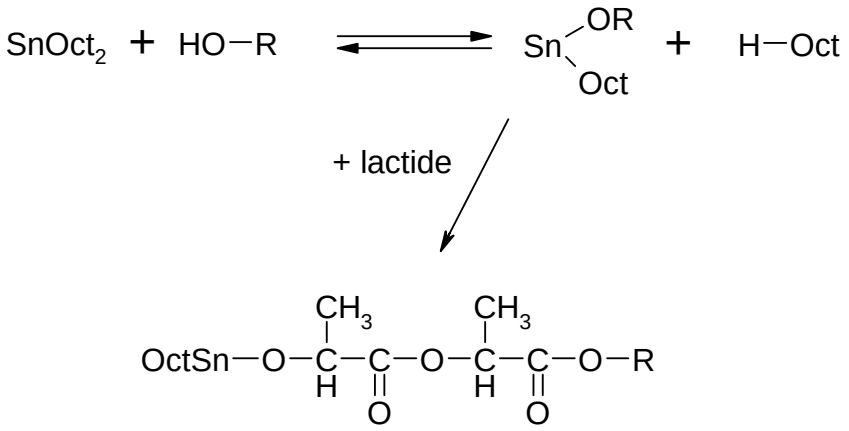

Figure 1.2.7 Reaction scheme for ring-opening polymerization of lactides with $SnOct_2$. Adapted from Kricheldorf [37].

1.3 Poly(ethylene oxide-*b*-lactide) (PEO-PLA) Copolymers

Poly(ethylene oxide-*b*-lactide) (PEO-PLA), or poly(ethylene glycol-*b*-lactide) (PEG-PLA) copolymers are attractive candidates for use as biomaterials for bone tissue scaffolds because their component blocks, polylactide (PLA) and poly(ethylene oxide) (PEO) are both biocompatible. PLA, as mentioned previously, is a widely accepted resorbable polymer which has been used in absorbable sutures since the late 1960s [1], developed for use as orthopedic plates, screws, and pins [2], and shown to be compatible with bone [4, 5]. The other component block, poly(ethylene oxide) (PEO), also called poly(ethylene glycol) (PEG), is a nondegradable

hydrophilic polymer with extremely low toxicity [58] and good biocompatibility [59, 60]. PEO molecules which have molecular weights of 20,000 Da or less and possess hydroxyl end groups are called poly(ethylene glycol) (PEG) molecules [61], although this nomenclature is not universally used throughout the literature. Copolymerizing hydrophobic PLA with hydrophilic poly(ethylene oxide) (PEO) to make PEO-PLA copolymers [62-64] is an effective way to enhance the biocompatibility of hydrophobic PLA [35].

1.3.1 Synthesis of PEO

The synthesis of PEO-PLA copolymers requires the polymerization of both PEO and PLA. Regardless of the method employed, the first step of the process is to synthesize PEO, which can be synthesized by anionic polymerization [65]. Anionic polymerization of ethylene oxide can be initiated by a number of species including oxides, alkoxides, hydroxides, and metal alkyls and aryls. Potassium hydroxide is a very common initiator traditionally used in the synthesis of PEO (Figure 1.3.1).

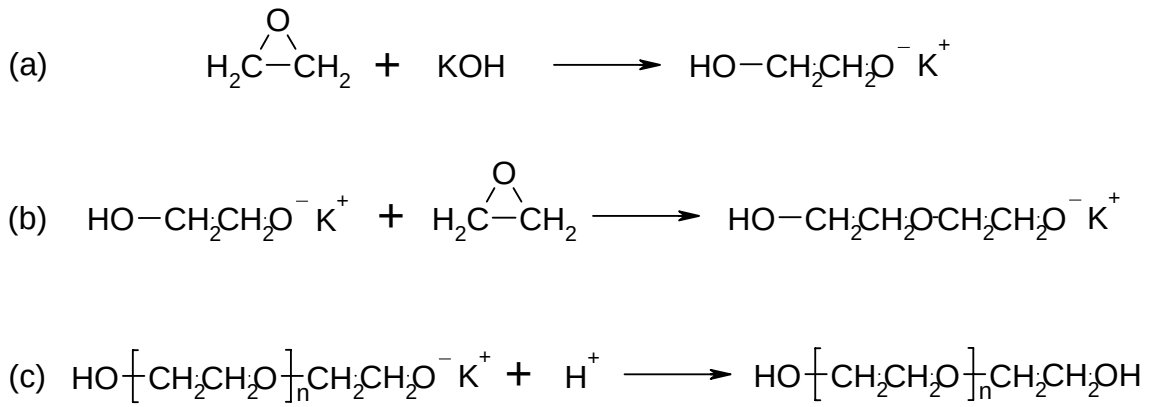

Figure 1.3.1 Reaction scheme for anionic polymerization of ethylene oxide: (a) initiation, (b) propagation, (c) termination. Adapted from Chanda [65].

Masson et al. have reported two specialized ways in which PEO can be synthesized by anionic polymerization [66]. In the first way, a monofunctional initiator is chosen to control the

molecular weight of the polymer. Either the potassium alkoxide of methoxyethanol or diphenylmethylpotassium are used as initiators for the anionic PEO polymerization [66]. Following the polymerization, an unsaturated electrophile is added to deactivate the active sites of the monofunctional "living" PEO polymer. Masson and coworkers chose methacrylic chloride as a deactivator because its unsaturated bonds cannot be attacked by the alkoxide of the PEO chain [66]. The final structures of the two structures described are presented below (Figure 1.3.2).

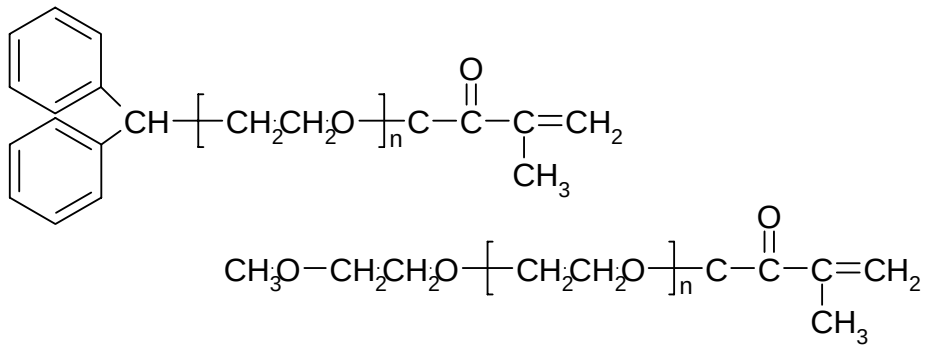

Figure 1.3.2 PEO macromers initiated by diphenylmethylpotassium (top) and the potassium alkoxide of methoxyethanol (bottom). Adapted from Masson et al. [66].

The second way of polymerizing PEO utilizes an unsaturated initiator to initiate ethylene oxide polymerization [66, 67]. Masson et al. selected p-isopropenylbenzyl alcoholate as an initiator because it is easily prepared and its activated double bond reacts by addition onto ethylene oxide without difficulty [66]. Furthermore, its double bonds are not attacked in any side reactions by the PEO alkoxide because the alkoxide has a low nucleophilicity [66]. Benzyl chloride or proton donors are used to deactivate the PEO alkoxide following completion of the polymerization (Figure 1.3.3) [66].

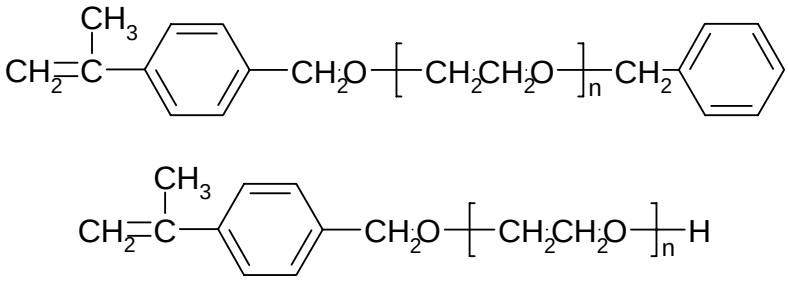

Figure 1.3.3 PEO macromers initiated by p-isopropenylbenzyl alcoholate and deactivated with benzyl chloride (top) or protons (bottom). Adapted from Masson et al. [66].

1.3.2 Functionalizing PEO molecules during synthesis

Numerous methods have been developed to functionalize PEO molecules with various end groups other than hydroxyl groups during synthesis [67-71]. Monomethyl ether of PEG (mPEG) has only one derivatizable chain end and is often used in applications where monofunctionality is desired and cross-linking is not [68]. Many syntheses have been devised to derivatize PEG with a variety of functional groups including halide, sulfonyl, amino, hydrazido, thiol, carboxyl, aldehyde, and epoxide groups [68]. Two main pathways are followed when derivatizing PEG; either a hydroxyl group of the PEG is converted by reaction to form a new functional group, or a bifunctional molecule is reacted with the hydroxyl group of a PEG molecule to form a linkage at one end while leaving the other functional end free [68]. Alternatively, PEG can be synthesized using a functionalized initiator. Ishizu et al. developed a method to synthesize PEO macromonomers with tertiary amino endgroups (Figure 1.3.4) [67].

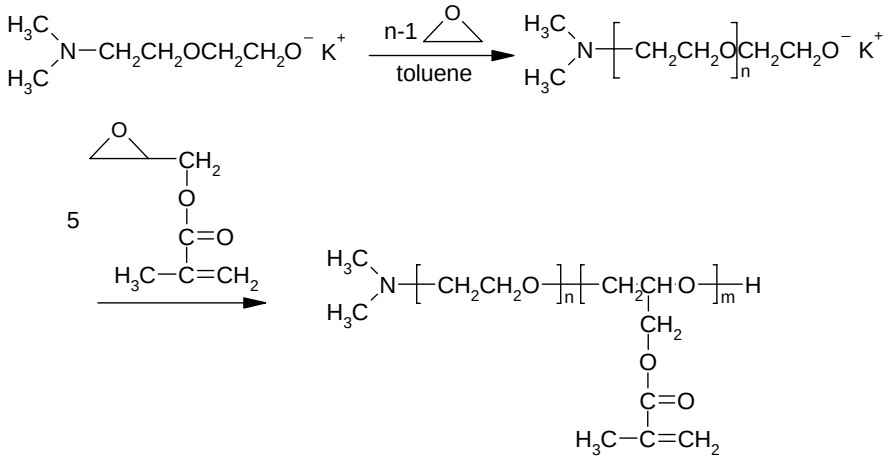

Figure 1.3.4 Synthetic scheme for synthesis of PEO macromonomers with tertiary amino endgroups. 2-[2-N,N-dimethylamino)ethoxy]ethanol potassium alkoxide initiates the living anionic polymerization of ethylene oxide in toluene at 20 °C for 140h, the temperature is raised to 60 °C for 100h, then functionalized macromonomers are made by a solution of glycidyl methacrylate. Adapted from Ishizu et al. [67].

In addition to monofunctional PEG, a series of syntheses have been developed to create heterobifunctional PEOs with two different functional groups on opposite ends: α-methoxy-ω-amino PEO [69], α-hydroxy-ω-amino PEO [69-71], and α-hydroxy-ω-formyl PEO [72].

1.3.3 Copolymerization of PEO with PLA

Once polymerized PEG has been obtained, it can be copolymerized with PLA by polymerizing lactic acid or lactide monomer using PEG as an initiator [61, 73, 74]. PEG and PLA can be copolymerized into diblock, triblock, multiblock, and star block copolymers [75]. PEO-PLA block copolymers can be polymerized via polycondensation [76-78], ring-opening polymerization [79-83], and anionic polymerization [84, 85]. Polycondensation of lactic acid using various molecular weights (M_w = 600-6000) of dihydroxy-terminated PEO initiators and phosphoric acid and SbO_3 catalysts was performed by Cohn et al. [76-78] to synthesize ABA triblock copolymers with poly(lactic acid) A-blocks and PEO B-blocks. Lactide polymerizations using multi-arm PEO (e.g. 4- or 8-arm PEO) initiator and stannous octoate or aluminum

triethylene catalyst have been performed to synthesize star-block copolymers having block copolymer arms radiating from a central core [86, 87].

Alternatively, ring-opening polymerization of lactide monomer with PEO is a common way of synthesizing PEO-PLA block copolymers [73, 75, 79-81]. PLA-PEO-PLA triblock copolymers are synthesized by using PEO to initiate a ring opening polymerization of lactide monomer in two directions (Figure 1.3.5), while PEO-PLA diblock polymers may be synthesized by using monomethylether PEG (mPEG) to initiate a ring-opening polymerization of lactide monomer in one direction [73, 75].

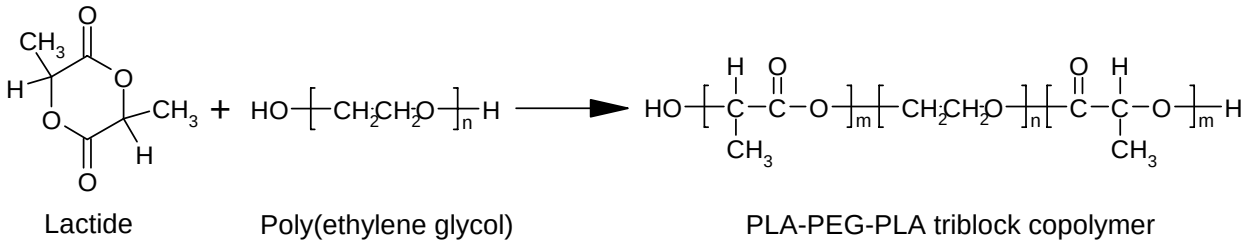

Figure 1.3.5 Ring-opening polymerization of lactide using dihydroxy PEG as an initiator. Adapted from Li and Vert [73].

Deng et al. synthesized ABA triblock copolymers of PEO and PDLLA with a narrow polydispersity by performing a bulk ring-opening polymerization with stannous chloride catalyst at 170-200 °C [79]. Kricheldorf and Meier-Haack synthesized ABA triblock copolymers from PEO and L-lactide by bulk ring-opening polymerization using metal oxides and stannous octoate as catalysts [80]. Among the catalysts they tested, the only metal oxide that achieved high conversion and low racemization was SnO. However, stannous octoate achieved even higher conversion with less racemization than SnO [80].

Finally, anionic polymerization is a third way to synthesize PEO and PLA copolymers. Jedlinski et al. prepared ABA triblock copolymers anionically using sodium poly(ethylene glycol)ate in THF at 25 °C [84]. Kricheldorf and Boettcher anionically synthesized AB diblock

and ABA triblock copolymers of mPEG or PEO and lactide using potassium tert-butoxide catalyst in toluene at 50 or 80 °C [85].

The ratio of PEO to PLA obtained during the synthesis of PEO-PLA copolymers influences the solubility and structure of the copolymers in aqueous environments. In general, the water solubility of PEO-PLA diblock and PLA-PEO-PLA triblock copolymers increases as the PEO/PLA ratio of the copolymers increases and the molar mass decreases [73]. However, PEO-PLA diblock copolymers will self-assemble spontaneously in water into a spherical micelle of a few hundred molecules (Figure 1.3.6) which has a core of densely packed hydrophobic PLA blocks and a dense PEO brush shell which radiates from the core [88]. Micellar structures of PEO-PLA diblock copolymers are especially suited as vehicles to deliver hydrophobic drugs to cells and tissues.

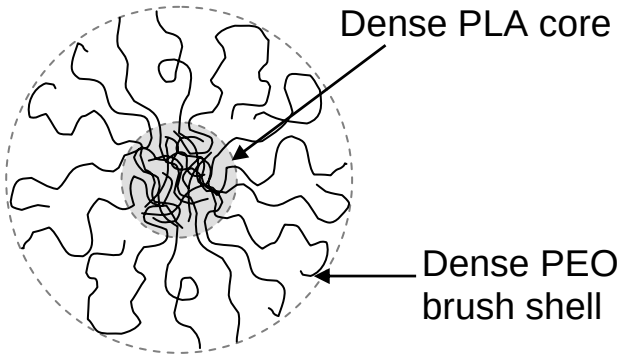

Figure 1.3.6 Diagram of a polymeric micelle comprised of PEO-PLA diblock copolymers. Adapted from Kwon et al. [88].

1.3.4 Functionalizing PEO-PLA block copolymers with bioactive moieties

Although PEO-PLA block copolymers support cell adhesion and tissue development [35, 89, 90], incorporation of bioactive groups into the polymer or at the polymer surface offers a means to control cell behavior and tissue function [91]. For example, immobilization of cell adhesion peptides can help stimulate cell attachment and spreading on biomaterials [91-94]. Binding bioactive molecules covalently to functional groups on the ends of polymers avoids the

drawbacks (e.g. high processing temperatures [95] and non-uniform coatings [96]) of other functionalization methods such as chemical vapor deposition [95, 97] and coating with functionalized polymers [98]. For example, Tessmar et al. [99] sought to create a polymer which could first be processed as desired and then made to be biomimetic by covalently linking biochemical groups to its surface. Consequently, they synthesized a diblock copolymer with amine reactivity at one end (*N*-succinimidyl tartrate monoamine poly(ethylene glycol)-*b*-poly(D,L-lactic acid)) (Figure 1.3.7) by reacting the amine reactive linker disuccinimidyl tartrate with monoamine poly(ethylene glycol)-*b*-poly(D,L-lactic acid) [99]. They also reacted a thiol reactive linker, *N*-succinimidyl 3-maleinimido propionate with poly(ethylene glycol)-*b*-poly(D,L-lactic acid) to create a thiol reactive diblock copolymer [100]. The amine reactive diblock copolymer was shown to bind with insulin and the thiol reactive diblock copolymer was shown to bind with somatostatin, demonstrating the ability of these functionalized polymers to bind with proteins to form biomimetic molecules [100].

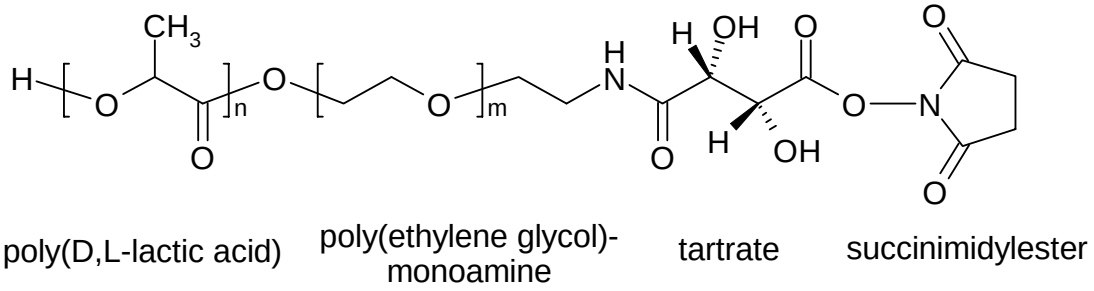

Figure 1.3.7 Chemical structure of amine reactive N-succinimidyl tartrate monoamine poly(ethylene glycol)-block-poly(D,L-lactic acid). Adapted from Tessmar et al. [99].

1.4 Scaffold Preparation Techniques

Bioabsorbable porous polymeric scaffolds are an essential component of engineered tissue because they provide a template for tissue regeneration by providing a surface for attachment where developing cells can localize while reserving space into which new tissue will

grow as it develops [7]. An ideal scaffold possesses five characteristics [8]. First, it possesses the appropriate three-dimensional shape and size suitable for repair at the implant site. Second, it possesses mechanical properties similar to those of the tissue into which it is implanted so that it can support local stresses until new tissue develops. Third, the surface of the scaffold has a chemistry that promotes attachment, proliferation, and differentiation of cells. Fourth, the scaffold material displays bioresorbability or biodegradability that can be adjusted to match the rate of cell and tissue growth. Fifth, the scaffold is porous with an architecture of interconnected pores that enable growth of cells and tissues into the scaffold and permit adequate transport of nutrients and oxygen. A porosity greater than 90% is preferable for bone tissue scaffolds [17, 101] and the ideal range of pore diameters for bone tissue scaffolds of 100-350 μm has been suggested [101]. Polymeric scaffolds have been processed into porous structures by many methods, including phase transitions (e.g. solvent evaporation [9], phase separation [10-14], freeze drying emulsions [15], gel casting [16]), incorporation of leachable porogens (e.g. compression molding [20], gas foaming [7, 22], and solution casting/particulate leaching [17-19, 21, 102-105], rapid prototyping (e.g. stereolithography [8, 23], fused deposition modeling [24]), and fiber deposition (e.g. bonded fiber meshes [25], and electrospinning [27-29]). Furthermore, some fabrication techniques involve a combination of methods.

1.4.1 Solvent Evaporation

Solvent evaporation is the most elementary method of fabricating porous polymer films. This method has been used to make polymeric synthetic skin from a 20/80 wt% mixture of polylactide and polyurethane [9]. Five to ten layers of a polymer solution (between 8 to 15 wt %) are cast onto a motorized polytetrafluoroethylene (PTFE) roller, and then the solvent is allowed to evaporate. When a membrane of adequate thickness has been formed, the membrane

is wetted with ethanol to reduce its adhesion to the roller, cut off the roller, and allowed to dry. This results in a membrane with pores between 40 and 200 μm in diameter interconnected with smaller pores 5 to 20 μm in diameter [9]. The small pore sizes attainable by solvent evaporation techniques usually range from 1 to 20 μm [17], which is on the order of the dimensions of individual mammalian cells and therefore too small to permit tissue formation. In addition, a number of shortcomings exist with using solvent evaporation for scaffold preparation [8]. First, a long time period may be required for the organic solvent to evaporate. Second, skin layers that may form during solvent evaporation will reduce the interconnectedness of pores in the film. Third, variations in the solvent evaporation rate will cause pore walls and edges to vary in thickness and length.

1.4.2 Phase Separation

Phase separation techniques use differences in solvent partitioning between polymer rich and polymer-poor phases to form porous films and scaffolds. Techniques for phase separating polymer solutions include immersion precipitation, air-casting, phase separation, and precipitation from the vapor phase [10-14]. In immersion precipitation, a thin film – cast from a polymer solution – is immersed in a non-solvent, which causes the formation of pores through phase separation and gelation in solution. The morphology of the final porous film is a function of both the initial polymer solution concentration and the chemistry of the immersion bath. This technique has been used to create porous PLLA films for cell culture [10]. Limitations of phase separation include the use of toxic organic solvents and the generation of pores that are too small and too few for tissue engineering applications. For example, Zoppi et al. [10] report pore sizes of 5 to 10 μm in PLLA films produced by immersion precipitation [8].

In addition to immersion precipitation, tissue scaffolds can also be made via temperature-induced phase separation/sublimation (TIPS) [17, 106]. The method begins by first creating a polymer solution (e.g. PDLLA/PLGA in dioxane [17]) which is poured into a mold at room temperature [17, 106]. This solution is frozen quickly and a vacuum is applied to sublime the solvent. The solvent leaves behind a porous polymeric foam whose density is a function of the original polymer solution. After the solvent is removed by this freeze-drying process, the temperature is slowly returned to room temperature. Temperature induced phase separation/sublimation retains water-soluble agents during scaffold creation that would otherwise be lost by solution casting/salt leaching methods [17]. TIPS methods yield pore sizes ranging from 50 μm to 400 μm, but choosing the correct solvent/polymer combinations and processing parameters is essential for obtaining pore diameters greater than 100 μm [17]. Alternatively, the polymer solution can be sprayed or cast into an already cold mold instead of being chilled in the mold. This approach has been shown to produce pore sizes of 100 μm and 50 μm for foams made from 1 and 5 wt % PLLA in naphthalene, respectively [11].

1.4.3 Freeze-Drying Emulsions

Freeze-drying emulsions is a scaffold technique created by Whang et al. [15, 107] similar to TIPS. In this technique, a water/polymer solution emulsion is created, placed in a mold, frozen, and freeze-dried to produce a pattern of interconnected pores with porosities greater than 90%. Pore sizes average 15 to 35 μm in diameter with maximum pore sizes exceeding 200 μm. Average pore size can be increased by increasing the volume fraction of the water in the emulsion and molecular weight of the polymer.

1.4.4 Gel Casting

Another technique used to make porous scaffolds is gel casting, which utilizes gelation and solvent extraction to create porous polymer scaffolds [16]. This technique begins by dissolving semi-crystalline and/or amorphous bioresorbable polymers in a poor solvent (e.g. PLA and/or poly(glycolide) (PGA) in ethyl acetate or acetone). This solution (2.5-15% (w/v)) is poured into a mold where it is allowed to form into a gel. Following gelation, the gel is removed from the mold and immersed into a non-solvent (e.g. methanol), which extracts the solvent and promotes the precipitation of the polymer from the gel. The microporous structure that results is then allowed to dry, resulting in a material with a thickness of 5 to 10 mm, which is greater than most solvent cast films. If the original polymer solution contains certain non-gelling amorphous or semi-crystalline polymers (e.g. 70/30 PLGA or polycaprolactone, respectively), water may also be used to extract the organic solvent. Coombes and Heckman [16] point out that it is imperative to remove any organic solvent or non-solvent from the porous structure to prevent the recoiling of amorphous polymer chains which may lead to shrinkage and collapse of the microporous structure. They reported that immersing the gels in water to extract solvent and non-solvent before the gels had air-dried effectively reduced the amount of shrinkage in the porous structures. In addition, the sizes of the irregularly shaped pores obtained were less than 5 μm for gels fabricated with some amount of semi-crystalline polymer (i.e. PLLA or PLLA/(50/50) PLGA blend) and less than 1 μm for gels of amorphous polymers (i.e. (50/50) PLGA) [16].

1.4.5 Compression Molding

Another method of scaffold fabrication is compression molding. In this process, polymer pellets (or pieces of solvent cast polymer films) and porogens (e.g. salt crystals) are loaded into a

die, heated above the melting temperature (for semi-crystalline polymers) or glass-transition temperature (for amorphous polymers), and compressed into a solid disc [20]. This disc can be processed into a scaffold by either gas foaming or particulate leaching. This method has been used for 50/50 (mole ratio) poly(D,L-lactic-co-glycolic acid) (PLGA) to form porous scaffolds (up to 93% porosity) with large interconnected pores (100 μm) [20].

1.4.6 Gas Foaming

Gas foaming is another method by which polymeric tissue scaffolds can be made. Nam et al. report the preparation of PLLA scaffolds by gas foaming via two separate ways: vacuum drying and hot aqueous solution [22]. The first way involves mixing ammonium bicarbonate salt (100-500 μm) into a polymer solution to form a paste that is cast in a disc-shaped mold and then air-dried. Gas foaming is initiated by drying under a vacuum for two weeks, then a warm water bath is used to remove any remaining salt. The second way involves mixing sieved ammonium bicarbonate salt (180-300 μm or 300-500 μm) into a viscous polymer solution, casting this paste into molds, partially evaporating the solvent at atmospheric pressure, then immersing the samples into hot water (90°C) until gas bubble generation ceases. In both cases, the sizes of the resulting highly interconnected pores are similar to and dependent upon ammonium bicarbonate salt size—200 to 300 μm for vacuum drying and 200 to 500 μm for hot aqueous solution. Porosities were around 90% and increased as the salt/polymer weight ratio was increased. Gas foaming methods suffer from skin layers and partially collapsed pore structures, which are the same drawbacks noted with solvent evaporation methods [8].

Mooney et al. devised a method of making porous scaffolds without organic solvents by utilizing compression molding and gas foaming [20]. Compression molded 50/50 PLGA (made without salt crystals) is placed into a high pressure chamber pressurized with carbon dioxide.

The polymer is allowed to equilibrate in this chamber for three days at room temperature. At the end of this time the chamber is depressurized quickly causing the carbon dioxide to no longer be dissolved in the polymer. A multitude of gas cells form and grow to create a porous polymer sponge with pores around 100 μm and porosities up to 93%. Some of these pores are interconnected while others are closed in the interior of the scaffold matrix. Pore formation is not observed when crystalline polymers are used because gas is solubility in them is much lower than in amorphous polymers. This method is advantageous because it avoids organic solvents, which can be toxic to cells and tissues and can denature biologically active factors (e.g. growth factors) if they remain in the polymer scaffold after fabrication [13, 20]. Nevertheless, with the exception of organic solvents, the gas foaming method still shares the same drawbacks with solvent evaporation.

1.4.7 Solvent Casting/Particulate Leaching

Another scaffold preparation method is solvent casting/particulate leaching [102]. Salt crystals (i.e. sodium chloride (NaCl)) or soluble sugar crystals of a fixed size are mixed into a polymer solution, which is then cast into a film [17]. A porous membrane is created by using water to leach the salt out of the polymer film. The size of the salt particles and the fraction of them in the solution have been shown to affect porosity and pore size. Pore diameters of 100-500 μm and porosities of 87-91% have been reported using this method. Salt crystals are not the only type of porogen that can be used in this technique. For example, porous poly(L-lactide) PLLA films can be fabricated by solution casting PLLA and poly(ethylene oxide) PEO blended films, then extracting the PEO using distilled water [18]. Porosity and pore size of the film can be controlled by changing the fraction of PEO in the polymer blend. Unfortunately, the leaching

process can remove water-soluble bioactive molecules (e.g. growth factors, drugs) from the scaffolds [17]. This can be prevented by utilizing phase separation techniques.

A variation of solvent casting/particulate leaching is solvent casting/compression molding/particulate leaching [21]. This method has been used to create porous scaffolds of 75/25 PLGA. The polymer and salt crystals are dissolved in solution and cast into a film which is broken into pieces. These pieces are placed into a cylindrical Teflon® mold and subjected to axial compression (1.4 MPa) at a temperature of 100 °C maintained by a band heater (Figure 1.4.1a). Once cooled the foams are immersed in water to leach out the salt crystals (Figure 1.4.1b). Mercury intrusion porosimetry indicated that this method can achieve porosities from 71 to 89%. Low porosities suffered from poor interconnectivity of pores, while foams with high porosities displayed diminished mechanical properties [21].

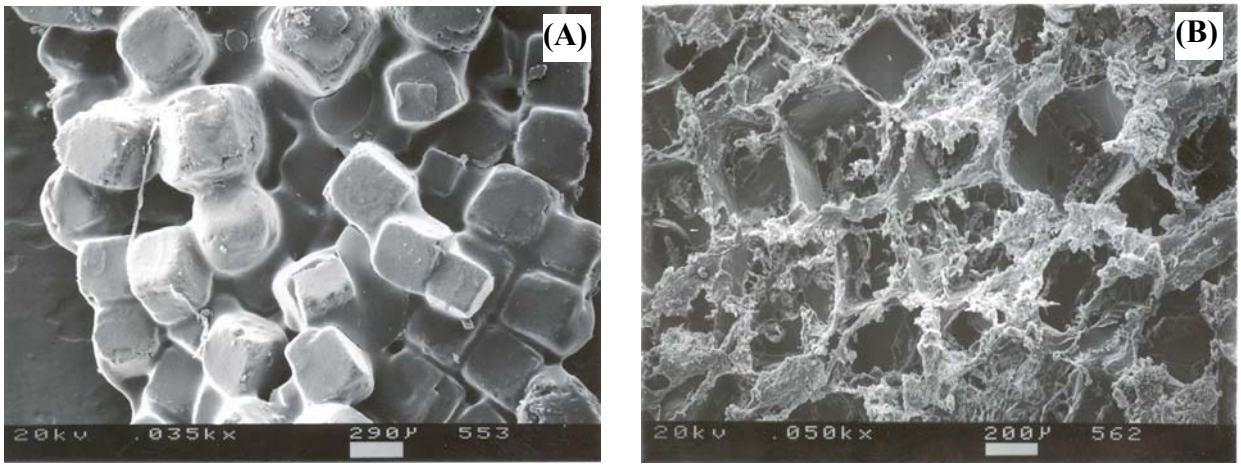

Figure 1.4.1 Scanning electron microscopy images of (A) a compression molded PLGA/salt composite and (B) a scaffold formed after the particulate leaching of a compression molded PLGA/salt composite [108].

In another variation of this particulate leaching technique, hard paraffin microparticles [103] and lipid microparticles [104] have been used as porogens to prepare macroporous polymer foams. This is performed in three steps (Figure 1.4.2) [103]. The first step is creating a viscous polymer solution and blending it with hydrocarbon porogen (e.g. paraffin, beeswax)

particles (300 μm to 500 μm in diameter). In the second step, this mixture is compacted in a Teflon® mold. The polymer solvent and porogen are extracted in the third step using a hydrocarbon solvent, in which the polymer is immiscible. As the solvent and porogen are extracted, a porous polymer network is formed.

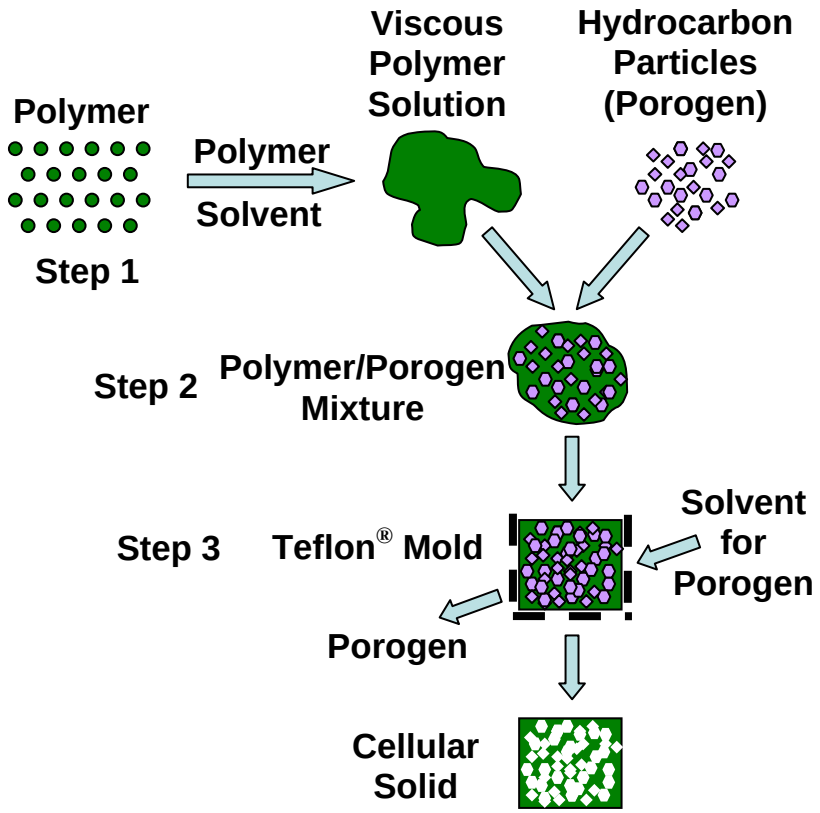

Figure 1.4.2 Diagram of steps involved in fabrication of macroporous polymer foam scaffold. Adapted from Shastri et al. [103].

Another variation of this process is the solvent casting/extrusion process developed by Widmer et al. [105]. In this method, the polymer/salt composite was melted and extruded through a die. A porosity of 83% was obtained for a 90% weight fraction of salt crystals between 150 and 300 μm in diameter. Pore size increased with salt crystal size while porosity remained constant, but as extrusion temperature increased, polymer molecular weight and pore diameter decreased, while porosity remained constant.

There are three main drawbacks of particulate leaching techniques [8]. They include irregularly shaped pores and residual porogens (e.g., salt, paraffin) in the polymer matrix. In addition, porogen dispersion may not be uniform. Finally, porogens may agglomerate to produce larger pores. –

1.4.8 Stereolithography

A number of relatively new manufacturing techniques which fall under the umbrella of rapid prototyping, or solid free form fabrication, are capable of creating scaffolds via computer aided manufacturing based on computer aided designs [8]. One example of these techniques is stereolithography [8, 23]. This involves the use of a UV laser to initiate chemical crosslinking of polymer resin. The laser, which is moveable in the X-Y plane, fuses the resin in a spatially-dependent manner to form a single slice of the desired object. A thin layer of fresh resin is then spread over the surface and the process is repeated. As the resin polymerizes, it bonds to the polymer slices deposited below it. This process continues until fused three-dimensional object is achieved. Currently, the 3D printing resolution of stereolithography devices (0.1 mm) is limited by how thin they can slice an object. As rapid prototyping techniques like stereolithography evolve, they will be very promising for future fabrication of solvent-free scaffolds having uniform morphology, pore size, and interconnectedness over their entire volume unlike currently produced scaffolds [8].

1.4.9 Fused Deposition Modeling

A second rapid prototyping technique used for computer-controlled design and fabrication of scaffolds is fused deposition modeling (FDM) [24]. Like other rapid prototyping methods, FDM uses computer-designed models to fabricate three-dimensional structures. In this

technique a molten thermoplastic polymer is melt-extruded as a filament and deposited onto a platform in precise patterns in the X-Y plane. After each layer is deposited, the platform descends along the Z-axis and the next layer is deposited on top of the previous one. FDM eliminates the need for organic solvents. Using a filament of poly(ε-caprolactone) and a series of processing parameters, Zein et al. [24] produced scaffolds with porosities ranging from 48-77%, pores with regular honeycomb geometries, channel sizes of 160-700 μm, and filament diameters of 260-370 μm by varying the processing parameters of roller speed, layer thickness, direction of deposition, and FDM head speed.

1.4.10 Bonded Fiber Meshes

Although non-woven fiber meshes (i.e., felts) provide high porosity, they typically possess low mechanical properties. To increase the mechanical strength, Mikos et al. [25] developed a technique to thermally fuse adjacent fibers without damaging the overall scaffold architecture. These bound fiber meshes are fabricated utilizing two polymers which are immiscible with each other in the melt, referred to as polymer A and polymer B (e.g. poly(glycolic acid) (PGA) and poly(L-lactic acid) (PLLA), respectively). Fibers of polymer A are placed in a solution of polymer B either by immersion or by pouring the solution over the fibers loaded into a mold. The solvent chosen for polymer B must be a non-solvent for polymer A (e.g. dichloromethane). Once the fibers are in the solution, the solvent is allowed to evaporate to form a polymer-polymer composite consisting of polymer A fibers imbedded in a matrix of polymer B. This composite is heated above the melting point of polymer A, causing the fibers to bond with each other within the polymer B matrix. After the composite returns to room temperature, polymer B is dissolved using a non-solvent for polymer A, leaving only the bonded fiber mesh comprised of polymer A. Mikos et al. showed that this technique retained

porosities as much as 0.81 and area/volume ratios up to 0.05 μm^{-1} without disrupting the chemistry or shape of the fibers used.

1.4.11 Electrospinning

Electrospinning is a technique by which scaffolds of nanoscale polymer fibers can be fabricated by subjecting a polymer solution to an electric field (Figure 1.3.7) [27]. Electrospinning begins with a polymer solution loaded in a syringe fitted with a capillary needle [27]. An electric field is applied to solution within the capillary, usually via an electrode mounted inside the needle which is connected to a high voltage power source [27, 28]. As the electric field increases, a charge builds at the tip of the capillary and develops into a repulsive force which eventually exceeds the force of the polymer's surface tension and a charged jet of polymer solution is emitted from the capillary tip [27]. As the jet leaves the tip, it thins considerably and it may experience a fluid instability resulting in bending of the jet and even whip-like motion [109]. Since the charge on this jet allows its path to be guided by an electric field, a metal screen is often used to collect the charged polymer fiber that forms when the solvent evaporates from the polymer jet [27]. This fiber deposits itself randomly as it contacts the screen, forming a non-woven material [27]. Electrospinning may be used to create fibers with diameters ranging from 50 nm to 5 μm [27]. The diameters of electrospun fibers may be controlled by varying the parameters of the electrospinning process, which include electric field voltage, distance between the capillary tip and the collection screen, solution feeding rate, and solution parameters (e.g. concentration, solvent, surface tension, viscosity, polymer molecular weight) [27, 28]. It has been shown that fiber diameter varies proportionally with voltage and solution feeding rate [28]. The temperature, humidity, and air flow within the electrospinning chamber also have some effect on the fiber morphology [27, 29]. Zong et al. determined that

solution concentration and the amount of salt added to the polymer solution (charge density) are the primary parameters that influence fiber diameter [28]. Similarly, Boland et al. demonstrated that a direct correlation exists between polymer concentration and electrospun fiber diameter [110]. Electrospinning has been used to fabricate nanofiber meshes from a variety of polymers including poly(glycolic acid) [110], poly(ethylene-co-vinylacetate) [111], poly(D,L-lactide-co-glycolide) [112, 113], poly(ethylene oxide) [27, 114], poly(vinyl chloride)/Estane® [115], poly(vinyl chloride)/poly(vinylidiene fluoride) [115], poly(D,L-lactic acid) [28], poly(L-lactic acid) [28, 111], poly(ethylene-co-vinyl alcohol) [111], poly(ε-caprolactone) [116, 117], and silk [118].

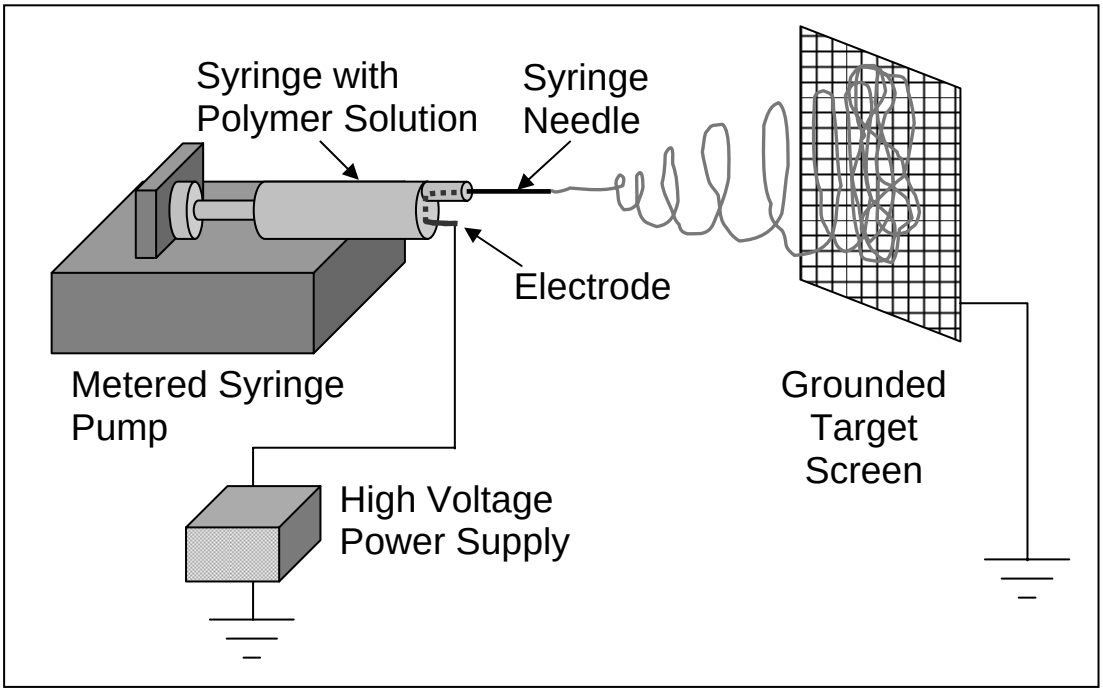

Figure 1.4.3 Schematic diagram of electrospinning apparatus.

1.5 Characterization of PLAs, PGAs and PLGAs

1.5.1 Degradation rate under aqueous conditions

In aqueous environments, aliphatic polyesters like PLA, PGA, and PLGA are insoluble but degrade hydrolytically [119-122]. This degradation can either be homogeneous (occurring at the polymer surface) or heterogeneous (occurring in the bulk of the polymer) [123], depending on the size of the polymer matrix, its degradation rate, and the diffusivity of water within the polymer [124]. Hydrolysis, which is pH sensitive, occurs as ester linkages of the molecules are randomly cleaved to form carboxylic acid and hydroxyl chain ends following the reaction [125]:

$$R\text{-}COO\text{-}R' + H_2O \rightarrow RCOOH + R'OH$$

Degradation rate is primarily a function of water uptake [126]. Consequently, differences in water uptake in PLA, PGA, and PLGA are the reasons these polymers have different degradation rates. The ability of water to access the ester bonds of a polymer is influenced by molecular weight, local pH, bulk sample dimensions, crystallinity, and glass transition temperature [127-132]. Even the catalyst used to synthesize a polylactide can affect the rate of its water uptake; poly(D,L-lactide) has been shown to be much more hydrophilic when synthesized using zinc metal compared to when it is made via stannous octoate [133].

The degradation time of an aliphatic polyester is a function of the initial molecular weight [6]. Viewed through the lens of molecular weight changes, three stages have been defined for the hydrolysis of PLA and PGA and their copolymers once water uptake occurs [6]. In stage one there is no significant loss in weight of the polymers, but there is a swift decrease in molecular weight as the polymer chains are randomly cleaved. During the second stage, molecular weight continues to decline as oligomers formed during stage one begin to hydrolyze into monomers. At this time, weight loss of the polymer begins when internal degradation has advanced so far that

oligomers can permeate through the surface of the polymer and are dissolved in the surrounding media [119]. This happens around a molecular weight of 15,000 or less [121]. Finally in stage three the total hydrolysis of oligomers into monomers of lactic and glycolic acid is complete [6].

Local pH and bulk sample dimensions impact the degradation rate of an aliphatic polyester [119-121, 125, 134, 135]. Pitt et al. [121] discovered that the carboxylic acid chain ends of oligomers formed as byproducts of hydrolytic degradation accelerate the rate of degradation. As a result, hydrolytic degradation of aliphatic polyesters can best be described by a diffusion-reaction mechanism [119, 125, 134, 135]. First, hydrolysis of a polyester begins homogeneously as water uptake occurs and the polymer chains are cleaved into oligomers. Next, the oligomers at or near the surface may be diluted by the surrounding medium or diffuse into it, if soluble, while those at the center are trapped inside the polymer. Finally, the accumulating carboxylic acid chain ends of these trapped oligomers cause local acidity to increase and further autocatalyze ester hydrolysis. Consequently, it has been demonstrated by Vert et al. [119, 120, 134] that large samples of PLA or PLGA will have higher degradation rates in their interior compared to their surface, causing them to degrade heterogeneously from the inside out. Polymers with amorphous regions in their centers may become hollow during hydrolysis before total degradation occurs. Similarly, Grizzi et al. [135] observed that large objects degrade faster than very small ones. In phosphate buffer pH 7.4 at 37 °C, tiny microspheres and cast films degraded via surface (homogeneous) erosion while the hydrolysis of large millimetric beads and compression-molded plates made of the same polymers occurred by bulk (hetereogeneous) erosion [135].

The degree of crystallinity and the glass transition temperature of an aliphatic polyester also dictate its rate of water uptake and ultimately its degradation rate. Two stages have been

identified in the hydrolytic degradation of semicrystalline polyesters [136]. In the first stage, water penetrates into the amorphous regions, whose unoriented, mobile chains allow water to permeate them more easily than denser crystalline regions and hydrolysis begins. These amorphous regions hydrolyze faster when they are above their glass transition temperature than below. When the majority of the amorphous regions have been degraded, the second stage begins as the crystalline regions begin degrading from their surfaces to their interiors. This is why the hydrolysis rate of semicrystalline PLLA is slower than that of amorphous PDLLA. For the same reason, PLLA hydrolyzes slower than amorphous PGA [120, 127, 137]. Consequently, copolymers of PLLA and PDLLA or PGA will degrade more slowly as the fraction of PLLA present increases and more quickly as the fraction of PDLLA or PGA increases. Li observed that the amount of L-lactide, D-lactide, and glycolide in different PLLA, PDLLA, and PGA polymers determined the time required (anywhere from 3 to 110 weeks) for those polymers to lose one half of their initial mass when incubated in phosphate buffer pH 7.4 at 37 °C [127]. Devices made of copolymers of lactide and glycolide have been observed to change from translucent to completely white by 6 weeks in vivo as amorphous regions degrade and the semicrystalline regions crystallize [138]. One reason for this is that polymers containing L-lactide units increase in crystallinity as they degrade because their amorphous regions degrade first [139]. It is difficult to compare degradation times of polymeric devices from several independent studies because the polymers may differ in molecular weight, surface area, and porosity [39]. Generally, biodegradation times of polylactides range from 18-24 months for poly(L-lactide), to 12-16 months for poly(D,L-lactide), and between 150 days and 50-60 days for D,L-lactide-*co*-glycolide polymers with varying copolymer ratios [39].

1.5.2 Mechanical strength and changes in mechanical strength during degradation

The mechanical strength of an aliphatic polyester is a function of a number of factors including composition, crystallinity, residual monomer, and molecular weight [119, 140-143]. The composition of lactides is determined by the relative amounts of D-lactide and L-lactide units present. Units of D-lactide within a poly(L-lactide) polymer backbone will yield diminished mechanical properties sooner than L-lactide units will because units of D-lactide accelerate degradation [140, 141]. This leads to considerably reduced mechanical properties when a polylactide is comprised of more than 10% D-lactide [140, 141]. More L-lactide units in a polylactide increase its crystallinity, which lowers impact strength and elongation at break because the brittleness of a polymer increases with crystallinity [139]. Residual monomer may accelerate the decrease in mechanical strength of a polymer because as it diffuses out of the polymer, it leaves behind a microporous structure which is theorized to accelerate water permeability and subsequent degradation [142]. Consequently, polymers containing residual monomer may display increased rates of molecular weight loss and actual weight loss compared to polymers without residual monomer [142].

Mechanical strength decreases as degradation occurs, with semicrystalline polymers weakening faster than amorphous ones. Nakamura et al. measured bending strength changes in vivo for amorphous copolymers of PLA with PDLLA or PGA and semicrystalline homopolymer PLLA samples and found that although the semicrystalline PLLA had a larger initial bending strength, it lost its mechanical strength much faster than the copolymer samples [142]. The PLLA lost over 50% of its initial bending strength after 3 months in vivo, while the copolymers retained over 90% of their initial bending strength. Li et al. [134] observed a similar phenomenon in the storage modulus of semicrystalline and amorphous PLA specimens. When

amorphous regions hydrolyze, the low molecular weight oligomers that form may recrystallize, which increases the crystallinity of a polymer and further reduces its mechanical properties (e.g. tensile strength) [144]. In addition, once the amorphous regions between crystalline regions are hydrolyzed, they are no longer able to interconnect the crystalline regions and maintain the strength of the material, causing tensile strength of a polylactide to decrease during hydrolysis.

The amount of time it takes an aliphatic polyester like PLA, PGA, or PLGA to lose its mechanical strength can vary. Degradation induced changes in mechanical strength of an aliphatic polyester do not coincide with a simultaneous loss of mass. Since only the monomeric products of degradation (i.e. lactic acid, glycolic acid) are soluble, random chain scission of the polymer chains causes a large decrease in molecular weight and mechanical properties before dissolution of monomer causes a noticeable decrease in sample mass [126]. Li et al. [134] observed that after eight months amorphous and semicrystalline PLA samples still possess 40 and 20% of their initial storage moduli values, respectively. Cordewener et al. [139] examined the degradation of poly(96L/4D-lactide) (PLA96) in both pH 7.4 PBS at 37 °C and in rats, concluding that tensile strength, elastic modulus, elongation at break, and impact strength all displayed a major decrease within the first three weeks of degradation and were no longer measurable by seven weeks. Reed and Gilding [122] observed the degradation of PGA sutures and concluded that while only ~20% of initial tensile strength is lost in the first two weeks, most of the strength was completely gone within four weeks. They noted the PGA embrittled with degradation because its elongation and tensile strength decreased simultaneously. Li et al. [120] measured the storage modulus (E') of lactide-glycolide copolymers (75/25 mole ratio), and reported that storage modulus was maintained for one week then declined uniformly until week seven when it was no longer measurable.

1.6 Bone Marrow Stromal Cells

1.6.1 Potential of bone marrow stromal cells

Adult stem cells are attractive components in regenerative medicine because they can proliferate extensively while retaining the potential to develop into multiple tissue types [145, 146]. Although a true mesenchymal stem cell (MSC) with capacity for indefinite self-renewal and potential to form into all tissue types of the mesodermal germ line has not been identified, the bone marrow stromal cell (BMSC) has emerged as a primitive cell type with many of the attractive properties of a MSC [145]. It possesses a high proliferative capacity, can differentiate into osteoblasts, chondrocytes, fibroblasts, and myoblasts of the mesodermal germ line as well as endothelial cells and neurons in vitro, and become incorporated into bone, muscle, and cartilage tissues in vivo [145, 146]. Two paradigms for the application of this cell type to the repair of musculoskeletal defects have been explored. The first involves the delivery of the primitive undifferentiated cells within a biomaterial scaffold into the defect site. The second involves the in vitro culture of BMSCs within the biomaterial scaffold under conditions that induce tissue development followed by the implantation of the tissue equivalent.

The remaining sections will focus on the latter paradigm with the goal of achieving a bone tissue equivalent in vitro.

1.6.2 Factors influencing osteoblastic differentiation of bone marrow stromal cells

The introduction of various induction factors into the growth medium of BMSCs can prompt them to commit to a particular lineage and progress toward terminal differentiation. For the process of osteoblastic differentiation into bone three separate stages have been identified: proliferation, extracellular matrix maturation, and mineralization of the extracellular matrix

[147]. Markers of osteoblastic phenotype include production of osteopontin (OP), osteocalcin (OC), and type I collagen as well as increased alkaline phosphatase (ALP) activity [148, 149]. As the BMSCs progress through the three stages of differentiation, the markers are upregulated at difference times, acquired, and/or lost [150]. For example, OP peaks twice during proliferation then later once more before other matrix proteins, while OC is upregulated about the same time as mineralization occurs, and mineralization is well advanced when ALP peaks [150]. Bone nodule formation and bone sialoprotein expression during matrix mineralization are additional indicators of differentiation into the osteoblastic phenotype [151].

Dexamethasone is a synthetic glucocorticoid with anti-inflammatory properties [152] that has been shown to induce osteoblastic phenotype expression in human bone marrow stromal cells [153-155]. Increases in alkaline phosphatase (ALP) activity and matrix mineralization have been shown to increase with continuous addition of dexamethasone to cell culture [153, 154, 156]. The degree of osteoblastic phenotype expressed in response to dexamethasone is dependent upon the amount and timing of dexamethasone addition [156, 157].

Other agents that have been demonstrated to affect pre-osteoblastic differentiation are L-ascorbic acid (AA) and β-glycerolphosphate [153, 158]. Maniatopoulos et al. [153] observed that AA and β-glycerolphosphate are necessary in culture for the extracellular matrix to assemble and mineralize in the form of mineralized bone-like nodules. Jaiswal et al. [159] showed that the matrix mineralization, osteocalcin (OC) production, ALP activity, and morphology of MSCs are all influenced by the presence of dexamethasone, ascorbic acid or L-ascorbic acid-2-phosphate, and β-glycerolphosphate in the culture medium. The amount of differentiation in response to dexamethasone, AA, and β-glycerolphosphate has been found to also be a factor of the age of the cells upon exposure [155].

1.6.3 In vitro studies of bone tissue development in poly(α-hydroxy ester) scaffolds

Numerous efforts have been made to promote bone tissue development in vitro by culturing osteoblast-like cells on synthetic biodegradable poly(α-hydroxy esters) [21, 160-162]. Ishaug et al. [160] demonstrated that rat osteoblasts adhere and proliferate on PLLA, 75/25 PLGA, 50/50 PLGA, and PGA films with an increase in ALP activity observed on 75/25 PLGA similar to that observed on tissue culture polystyrene controls. Ishaug et al. [161] determined that three-dimensional (3-D) foam scaffolds of 75/25 PLGA made by solvent casting/particulate leaching are feasible materials for regenerating bone tissue with autogenous osteoblasts. Foam scaffolds were fabricated in three pore sizes of 150-300, 300-500, and 500-710 μm. Significant increases in cell number, mineralized matrix deposition, and ALP activity of adult rat bone marrow stromal cells seeded on all the PLGA foams revealed that the proliferation and differentiation of the cells were sustained over 56 days of culture. A similar subsequent study with neo-natal rat calvarial osteoblasts indicated that PLGA is an appropriate scaffold material to support the growth and differentiation of osteoblasts of different origins [162]. Goldstein et al. [21] showed that as the porosity of PLGA scaffolds made by solvent casting/particulate leaching increases, so does the potential for adherent osteoblasts to collapse the scaffold structure, thereby undesirably reducing its volume.

Research has shown that fluid flow curing culture improves the properties of osteoblasts growing on poly(α-hydroxy ester) scaffolds. In an attempt to promote cell growth in the interior and not just the periphery of 3-D scaffolds, Goldstein et al. [163] cultured osteoblastic stromal cells seeded on porous PLGA foam disks in a spinner flask, perfusion flow system (Figure 1.6.1), and a rotary flask.

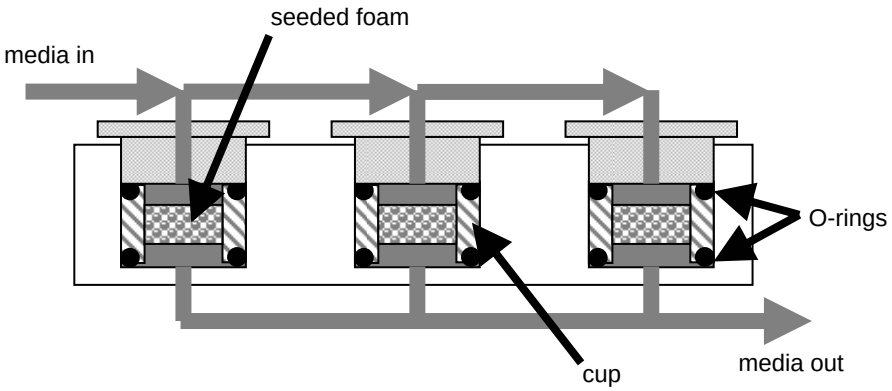

Figure 1.6.1 Diagram of a perfusion flow system. Media delivered from a constant hydrostatic head device is distributed between the cylindrical foams loaded in the system. The cup and pair of O-rings surrounding the foam in each chamber prevent media leakage around the foam or out of the system. The "media in" and "media out" flowrates are monitored by flow meters and manually controlled by small clamps. Adapted from Goldstein et al. [89].

While cells cultured in all three convective cultures performed at least as well as those in static culture, the cells cultured in the perfusion flow system were more evenly distributed throughout the scaffold displayed higher values for ALP activity than the cells in the other culture systems. These results showed that osteoblastic cells seeded on PLGA foams display improved properties when cultured with flow, especially a perfusion flow system.

Surface chemistry of poly(α-hydroxy ester) scaffolds, specifically the addition of hydrophilic poly(ethylene glycol) (PEG), has also been demonstrated to influence the properties of cultured osteoblasts. Göpferich et al. [89] examined the adhesion, proliferation, and differentiation of osteoblasts cultured on films of poly(D,L-lactic acid) (PLA) compared to diblock copolymers of PLA and PEG. They found that FBS protein adsorption and cellular proliferation were inversely proportional to hydrophilicity of the surface, with greater proliferation on the PLA than the PEG-PLA films. However, the PEG-PLA diblock copolymer surfaces yielded cells with higher levels of differentiation and metabolic activity. Lieb et al. [90] also noted enhanced differentiation on the diblock copolymers and determined that increasing the amount of PEG decreased the amount of adsorbed protein on the copolymer surface and

consequently decreased cell adhesion and altered cell shape. These results showed that cell-surface interactions can be tuned by adjusting the amount of PEG copolymerized with PLA.

1.7 Initial Research Plan

1.7.1 Project Description

This project involves the fabrication, characterization, and application of tissue scaffolds of hydrophilic-hydrophobic PEG-PLA diblock copolymers. The scope of this research can be conceptualized in three different steps. The first step involves synthesizing diblock copolymers comprised of hydrophobic PEG and hydrophilic PLA polymers (i.e. PEG-PLLA and PEG-PDLLA). The second step entails electrospinning the synthesized diblock copolymers and commercially available PLLA and PDLLA into non-woven fiber scaffolds of varying fiber diameters. The third step of the project is to characterize the influence of scaffold fiber diameter and PEG content on cell proliferation and osteoblastic activity.

1.7.2 Hypotheses

This plan of research is intended to test two hypotheses. The first hypothesis is that increasing the content of PEG in the tissue scaffolds will result in more hydrophilic, less adhesive surfaces that will decrease proliferation but increase differentiation of osteoprogenitor cells. The second hypothesis is that electrospun scaffolds formed of fibers with diameters of 100 nm to 5 μm will modulate cell adhesion and proliferation by regulating formation of focal adhesion contacts and restricting cell spreading.

1.7.3 Experimental Approach

*1.7.3.1 Synthesis of Poly(ethylene-*b*-lactide) Diblock Copolymers*

PEG will be used to initiate ring-opening polymerizations of L-lactide and D,L-lactide monomers with stannous octoate catalyst to synthesize PEG-PLLA and PEG-PDLLA, respectively. Proton Nuclear Magnetic Resonance (^{1}H-NMR) will be used to analyze the reagents involved in the synthesis and monitor the conversion of the lactide monomer. Gel Permeation Chromatography (GPC) will be used to measure the molecular weights of the synthesized copolymers.

1.7.3.2 Electrospinning Bioresorbable Tissue Scaffolds

The synthesized PEG-PLA diblock copolymers and commercially available PLLA and PDLLA will be processed into three-dimensional scaffolds by electrospinning. Electrospinning parameters will be identified and varied to obtain scaffolds with different fiber diameters. Scanning Electron Microscopy (SEM) will be used to characterize the topography of the electrospun fibers.

1.7.3.3 Cell Culture on Electrospun Polymer Scaffolds

The MC3T3-El osteoprogenitor cell line will be cultured on the electrospun polymer scaffolds to determine how the fiber topography impacts cell function. Immunofluorescence studies will be performed during culture to measure the morphology of the cells on the fiber scaffolds and to determine if the polymer fibers degrade during culture. In addition, this research will quantify the influence of hydrophilic PEG blocks and fiber diameter on the growth and differentiation of MC3T3-E1 osteoblastic cells. DNA assays will be performed to measure changes in cell number (proliferation) over time while another assay will measure ALP activity,

an early marker of osteoblastic differentiation. These tests would bring closure to the synthesis, processing, characterization, and testing of PEO-PLA diblock copolymer scaffolds.

Chapter 2 Synthesis of Poly(ethylene glycol-b-lactide) Diblock Copolymers

2.1 Introduction

Poly(ethylene glycol-*b*-lactide) (PEG-PLA) copolymers are attractive candidates for use as biomaterials for bone tissue scaffolds because of the characteristics of their component blocks, polylactide (PLA) and poly(ethylene glycol) (PEG). PLA is a widely accepted resorbable polymer which has been used in absorbable sutures since the late 1960s [1], developed for use as orthopedic plates, screws, and pins [2], and shown to be compatible with bone [4, 5]. Poly(ethylene glycol) (PEG), also called poly(ethylene oxide) (PEO), is a nondegradable hydrophilic polymer with extremely low toxicity [58] and good biocompatibility [59, 60]. I hypothesize that hydrophilic PEG covalently bonded to PLA will enhance the biocompatibility of the hydrophobic polymer [164]. Similar results were seen by Koegler and Griffith [34] who observed enhanced osteoblastic differentiation on porous scaffolds of PLA blended with varying amounts of PEO. Their findings suggest that copolymerizing PEG with PLA may stimulate bone tissue development by enhancing osteoblastic differentiation. The goal of this research was to synthesize monomethylether poly(ethylene glycol-*b*-lactide) diblock copolymers for use in fabricating bioresorbable tissue scaffolds. For these studies monomethylether PEG was used to initiate ring-opening polymerization of D,L-lactide, and L-lactide. A target molecular weight of 40 kDa was selected so that the resultant materials could be compared to commercially available poly(D,L-lactide) (PDLLA) and poly(L-lactide) (PLLA).

This chapter describes the initial synthesis of PEG-PLLA and PEG-PDLLA diblock copolymers, and a replicate synthesis of both polymers with the aim of increasing polymer molecular weight by reducing moisture by more thoroughly drying the starting materials and

apparatus. The polymer products were characterized by proton nuclear magnetic resonance (^{1}H NMR) spectroscopy and gel permeation chromatography (GPC).

2.2 Materials and Methods

2.2.1 Materials

Materials were obtained from Sigma-Aldrich (St. Louis, MO) unless otherwise specified. L-lactide (Purac) and D,L-lactide (Polysciences, Warrington, PA) were recrystallized in ethyl acetate (EMD Chemicals, Gibbstown, NJ) before use. Toluene (EMD Chemicals) was either used as received or dried by distillation just prior to use. Monomethylether poly(ethylene glycol) (PEG) was dissolved in toluene and dried by removing a water-toluene azeotrope before use. Tin(II) 2-ethylhexanoate (stannous octoate) was diluted with dry toluene to a working concentration of either 0.019 g/mL or 0.018 g/mL. Methanol (EMD Chemicals), dichloromethane (EMD Chemicals), and 2-propanol (EMD Chemicals) were used as received. Chloroform (EMD Chemicals) and chloroform-*d* ($CDCl_3$; Cambridge Isotope Laboratories, Andover, MA) were used as received.

2.2.2 Synthesis of PEG-PLLA copolymer

PEG-PLLA copolymer was synthesized by using monomethylether poly(ethylene glycol) (PEG; $M_n \approx 2000$ g/mol) to initiate a ring-opening polymerization of L-lactide monomer using stannous octoate catalyst.

2.2.2.1 Recrystallization of lactide monomer

Ethyl acetate (100 mL) was placed in a 150-mL beaker and heated to boiling. L-lactide monomer (21.03 g) was placed into a beaker with a magnetic stir bar. When the boiling ethyl

acetate began to reflux, it was added slowly and sparingly into the monomer beaker on a hot plate with stirring so that the monomer dissolved in a minimum amount of solvent. The dissolved monomer was removed from heat and allowed to cool at ambient temperature while the remaining solvent was placed in an ice bath. The equilibrated monomer solution was placed into the ice bath to equilibrate (~1 h). The resulting crystals in the beaker were scraped into a filter funnel and vacuum filtered. The beaker was rinsed with the chilled solvent to recover as many crystals as possible. After the bulk solvent was removed, the lactide monomer crystals were transferred to a flame-dried 250-mL round-bottom flask, which was stoppered with a septum and heated under vacuum in a stirred oil bath at 40 °C overnight. ^{1}H NMR analysis was performed on the recrystallized monomer after drying to confirm the absence of water and ethyl acetate.

2.2.2.2 Flame drying reaction flask

To minimize the moisture present during the reaction, a 100-mL, round-bottom, reaction flask was flame dried. The flask was stoppered with a septum and suspended on a ring stand. With a nitrogen purge line attached, the outside surface of the flask was heated uniformly with the flame of a Bunsen burner until the flame turned orange. The flask was allowed to cool under nitrogen purge before use.

2.2.2.3 Calculating the stoichiometry of the reaction

The L-lactide monomer crystals (16.08 g) were added with a magnetic stir bar to the flame-dried 100-mL round-bottom reaction flask and purged with nitrogen. Since the desired PLLA number average molecular weight (M_n) was 40,000 g/mol, a 10% higher target molecular weight of 44,000 g/mol was used for stoichiometric calculations so that the reaction need only

progress to 90% conversion. Since the molecular weight of a ring-opened polylactide equals the ratio of grams monomer/moles initiator, 16.08 g monomer required 3.66 * 10^{-4} mol PEG to yield a 44,000 g/mol polylactide. ^{1}H NMR analysis determined the M_n of the PEG to be 2018 g/mol, so 0.738 g PEG was required to initiate the reaction. Approximately 2 mL of toluene solvent was required for every gram of lactide. Finally, to ensure a catalyst concentration of 200 ppm Sn, a volume of 0.46 mL of a 0.019 g Sn/mL stannous octoate catalyst solution (8.91 * 10^{-3} g Sn) was required for a mass of 44.56 g of the lactide monomer, PEG, and toluene solvent.

2.2.2.4 Drying PEG and polymerization reaction

PEG (0.738 g) was dissolved in an excess of toluene (40 mL) in a two-neck 250-mL, round-bottom flask equipped with a magnetic stir bar and a Dean Stark trap filled with toluene and topped with a condenser. Heating tape was wrapped around the arm of the trap connected to the flask and its temperature was controlled by a variac set at 55%. The solution was heated in an oil bath at 130 °C with stirring and allowed to reflux. Excess toluene (8 mL) was drained from the Dean Stark trap and the system was refluxed until at least the same volume of toluene condensed in the trap. ^{1}H NMR analysis was performed on the PEG and L-lactide monomer to confirm the absence of water. The dried PEG solution was transferred by syringe from the 250-mL round-bottom flask to the 100-mL reaction flask, and heated in an oil bath at 100 °C with stirring to dissolve the recrystallized L-lactide monomer. Stannous octoate was added by syringe to a final concentration of 200 ppm Sn (0.46 mL of the catalyst solution) to initiate the reaction. Reaction progress was monitored by ^{1}H NMR. The reaction was terminated after ~90% conversion (~11 h) by cooling the mixture to room temperature.

2.2.2.5 Isolation of product

The product crystallized out of solution during cooling and was redissolved by adding 30 mL chloroform with stirring. Polymer was then precipitated by slowly dribbling 25 to 35% of the polymer solution into 500 mL of stirred methanol. The resultant precipitate was vacuum filtered, and the process repeated until the entire product was precipitated and filtered. The filtered polymer was transferred to a 250-mL round-bottom flask, which was stoppered with a septum, and dried under vacuum in a stirred oil bath at 45 °C overnight. ^{1}H NMR analysis was performed on the dried product to confirm the absence of methanol and toluene.

2.2.3 Synthesis of PEG-PDLLA copolymer

PEG-PDLLA copolymer was synthesized by using monomethylether poly(ethylene glycol) (PEG; $M_n \approx 2000$ g/mol) to initiate a ring-opening polymerization of D,L-lactide monomer using stannous octoate catalyst.

2.2.3.1 Recrystallization of lactide monomer

D,L-lactide monomer (20.99 g) was recrystallized from ethyl acetate following the same procedure used to recrystallize the L-lactide monomer used in the synthesis of PEG-PLLA copolymer (section 2.2.2.1).

2.2.3.2 Flame drying reaction flask

To minimize the moisture present during the reaction, a 100-mL round-bottom reaction flask was flame dried following the same procedure used to flame dry the reaction flask used in the synthesis of PEG-PLLA copolymer (section 2.2.2.2).

2.2.3.3 Calculating the stoichiometry of the reaction

Stoichiometric calculations were performed as described in section 2.2.2.3. For 17.23 g of D,L-lactide monomer crystals, 0.790g PEG, 34.5 mL toluene, and 0.53 mL stannous octoate catalyst solution (0.018 g Sn/mL) were calculated to be necessary.

2.2.3.4 Drying PEG and polymerization reaction

PEG (0.790 g) was dried using a Dean Stark trap following the same procedure used to dry the PEG used in the synthesis of PEG-PLLA copolymer (section 2.2.2.4), except that the system was refluxed for 2 h longer than the time required for the toluene in the trap to return to its original level after draining to allow for additional drying. The dried PEG solution was transferred to the 100-mL reaction flask via cannula and heated in an oil bath at 100 °C with stirring to dissolve the D,L-lactide monomer. Stannous octoate was added by syringe to a final concentration of 200 ppm Sn (0.53 mL of the catalyst solution) to initiate the reaction. Reaction progress was monitored by ^{1}H NMR. The reaction was terminated after ~90% conversion (7.75 h) by cooling the mixture to room temperature.

2.2.3.5 Isolation of product

The viscous product solution was diluted by adding 30 mL chloroform with stirring. A fraction of the polymer solution was precipitated by slowly dribbling the solution into 400 mL of stirred 2-propanol, and then the precipitated polymer was vacuum filtered. This was repeated seven times until the entire product was precipitated and filtered. The filtered polymer was transferred to a 250-mL round-bottom flask which was stoppered with a septum and heated under vacuum in a stirred oil bath at 40 °C overnight. ^{1}H NMR analysis was performed on the dried product to confirm the absence of 2-propanol and toluene.

2.2.4 Synthesis of PEG-PLLA copolymer (repeated)

PEG-PLLA copolymer was synthesized a second time by using monomethylether poly(ethylene glycol) (PEG; $M_n \approx 2000$ g/mol) to initiate a ring-opening polymerization of L-lactide monomer using stannous octoate catalyst. The goal of this second synthesis was to increase the molecular weight of the final product by further minimizing any water present during the reaction.

2.2.4.1 Recrystallization of lactide monomer

L-lactide monomer (21.03 g) was recrystallized from ethyl acetate following the same procedure for the previous synthesis of PEG-PLLA copolymer (section 2.2.2.1). ^{1}H NMR analysis was performed on the recrystallized monomer after drying to confirm the absence of water and ethyl acetate.

2.2.4.2 Flame drying reaction flask

A 100-mL round-bottom reaction flask and a 50-mL round-bottom flask were flame dried following the same procedure used in the previous synthesis of PEG-PLLA copolymer (section 2.2.2.2).

2.2.4.3 Calculating the stoichiometry of the reaction

Stoichiometric calculations were performed as described in section 2.2.2.3. For 15.58 g of L-lactide monomer crystals, 0.714g PEG, 31 mL toluene, and 0.48 mL stannous octoate catalyst solution (0.018 g Sn/mL) were calculated to be necessary.

2.2.4.4 Drying PEG and polymerization reaction

In an effort to further reduce the moisture present, the PEG was dried twice using two different methods. First, 0.714 g PEG were added to a flame-dried 50-mL round-bottom reaction flask which was stoppered and heated under vacuum at 80 °C in a stirred oil bath for 63 h. Second, an excess of dry toluene (40 mL) was syringed into the flask with the dried PEG and heated to 60 °C with stirring to dissolve the PEG. The dissolved PEG was transferred via cannula to a flame-dried two-neck 250-mL round-bottom flask equipped with a magnetic stir bar and a flame-dried Dean Stark trap topped with a condenser. An additional 5 mL dry toluene was added to the 50-mL flask to facilitate the transfer of all of the PEG. The PEG was dried using the Dean Stark trap following the same procedure used to dry the PEG used in the synthesis of PEG-PLLA copolymer (section 2.2.2.4), except that the trap was filled with dry toluene (25 mL), the system was refluxed for 2 h longer than the time required for the toluene in the trap to return to its original level after draining to allow for additional drying, and a nitrogen purge line into the two-neck flask with a vent in the condenser was employed to facilitate the condensation of toluene in the trap. The PEG solution was transferred via cannula into the 100-mL reaction flask and heated in an oil bath at 100 °C with stirring to dissolve the L-lactide monomer. Stannous octoate was added by syringe to a final concentration of 200 ppm Sn (0.48 mL of the catalyst solution) to initiate the reaction. Reaction progress was monitored by ^{1}H NMR. The reaction was terminated after ~90% conversion (10.6 h) by cooling the mixture to room temperature.

2.2.4.5 Isolation of product

The product crystallized out of solution during cooling and was redissolved by adding 30 mL chloroform with stirring. The polymer product was precipitated and filtered following the same procedure for the isolation of the PEG-PLLA in section 2.2.2.5. The filtered polymer was

dried in a vacuum oven at 40 °C for over 24 h. ^{1}H NMR analysis was performed on the dried product to confirm the absence of methanol and toluene.

2.2.5 Synthesis of PEG-PDLLA copolymer (repeated)

PEG-PDLLA copolymer was synthesized a second time by using monomethylether poly(ethylene glycol) (PEG; $M_n \approx 2000$ g/mol) to initiate a ring-opening polymerization of D,L-lactide monomer using stannous octoate catalyst. The goal of this second synthesis was to increase the molecular weight of the final product by further minimizing any water present during the reaction.

2.2.5.1 Recrystallization of lactide monomer

D,L-lactide monomer (20.92 g) was recrystallized from ethyl acetate following the same procedure used to recrystallize the L-lactide monomer used in the first synthesis of PEG-PLLA copolymer (section 2.2.2.1), except that the lactide monomer crystals were transferred to a flame-dried 250-mL round-bottom flask, which was stoppered with a septum and heated under vacuum in a stirred oil bath at 45 °C for 122 h.

2.2.5.2 Flame drying reaction flask

A 100-mL round-bottom reaction flask was flame dried following the same procedure used in the first synthesis of PEG-PLLA copolymer (section 2.2.2.2).

2.2.5.3 Calculating the stoichiometry of the reaction

Stoichiometric calculations were performed as described in section 2.2.2.3. For 18.07 g of D,L-lactide monomer crystals, 0.829 g PEG, 36 mL toluene, and 0.56 mL stannous octoate catalyst solution (0.018 g Sn/mL) were calculated to be necessary.

2.2.5.4 Drying PEG and polymerization reaction

In an effort to further reduce the moisture present, the PEG was dried twice using different methods. First, 0.829 g PEG were added to a flame-dried two-neck 250-mL round-bottom flask and placed under vacuum at room temperature overnight (>12 h). A Dean Stark trap was attached to the round-bottom flask, the assembly was flame dried, and dry toluene was syringed into the Dean Stark trap to fill it. The septum of the trap was removed to add a condenser onto the trap after the dry toluene was added. The PEG was dried using the Dean Stark trap following the same procedure used to dry the PEG used in the synthesis of PEG-PLLA copolymer (section 2.2.2.4), except that 4 mL toluene were drained from the trap, the system was refluxed for 1.25 h longer than the time required for the toluene in the trap to return to its original level after draining to allow for additional drying, and a nitrogen purge line into the two-neck flask with a vent in the condenser was employed to facilitate the condensation of toluene in the trap. The PEG solution was transferred to the 100-mL reaction flask via cannula and heated in an oil bath at 100 °C with stirring to dissolve the D,L-lactide monomer. Stannous octoate was added by syringe to a final concentration of 200 ppm Sn (0.56 mL of the catalyst solution) to initiate the reaction. Reaction progress was monitored by ^{1}H NMR. The reaction was terminated after ~90% conversion (~4.2 h) by cooling the mixture to room temperature.

2.2.5.5 Isolation of product

The viscous product solution was diluted by adding 30 mL chloroform with stirring. A fraction of the polymer solution was precipitated by slowly dribbling the solution into 400 mL of stirred methanol, and then the precipitated polymer was vacuum filtered. This was repeated several times using a total of 2 L methanol until the entire product was precipitated and filtered. The filtered polymer was transferred to a 250-mL round-bottom flask that was stoppered with a

septum and heated under vacuum in a stirred oil bath at 40 °C overnight. ^{1}H NMR analysis was performed on the dried product to confirm the absence of methanol and toluene. The dried polymer was dissolved in dichloromethane and reserved in a sealed jar at room temperature.

2.2.6 Instrumentation and characterization

^{1}H NMR was used to confirm the absence of water at 1.55 to 1.60 ppm, ethyl acetate peaks at 1.26, 2.05, and 4.12 ppm, methanol at 3.49 ppm, and toluene at 2.36, 7.17, and 7.25 ppm. Reaction progress was monitored by ^{1}H NMR by observing the change in chemical shift of chiral protons from 4.95 to 5.25 ppm. Monomer and polymer samples were dissolved in $CDCl_3$ and analyzed with a Varian Unity 400 spectrometer operating with a relaxation delay of 1.0 s, pulse angle of 26.1°, acquisition time of 3.7 s, and a frequency of 399.94 MHz.

Molecular weights and polydispersity indices were estimated using a Waters 2690 Gel Permeation Chromatograph (GPC; Waters Corporation, Milford, MA) equipped with four Waters Styragel® HR columns (Models HR 0, HR 2, HR 3, and HR 4), an online Viscotek 100 differential viscometric detector (Viscotek, Houston, TX), and a Viscotek laser refractometer. Chloroform was the mobile phase with a flow rate of 1.0 mL/min at 25 °C. A calibration plot constructed from polystyrene standards was used to determine the molecular weights of the samples via a universal calibration.

2.3 Results

2.3.1 Synthesis of PEG-PLLA copolymer

A ring-opening polymerization of L-lactide monomer initiated by monomethylether poly(ethylene glycol) (PEG; $M_n \approx 2000$ g/mol) with stannous octoate catalyst was successfully employed to synthesize a PEG-PLLA copolymer (Fig. 2.3.1).

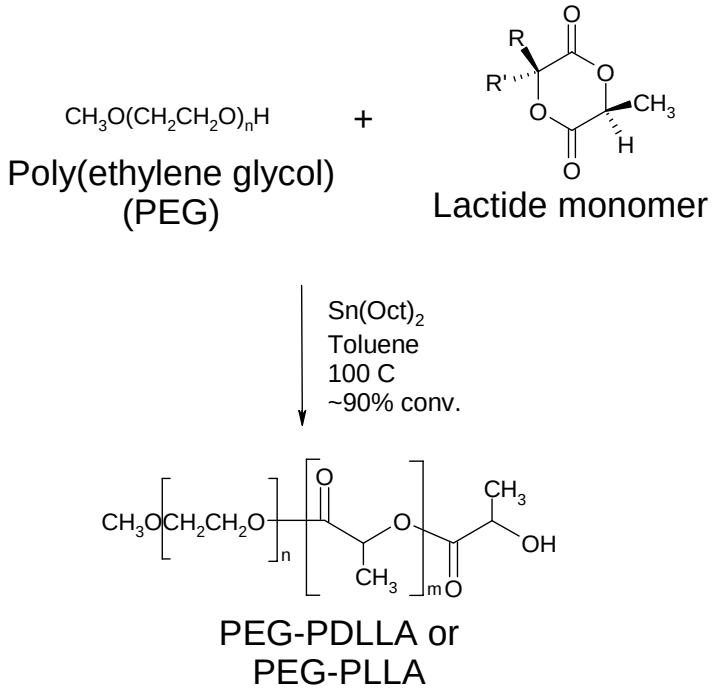

Figure 2.3.1 Synthesis of PEG-PDLLA and PEG-PLLA. For D,L-lactide, R = H and R′ = CH_3; for L-lactide, R = CH_3 and R′ = H.

^{1}H NMR analysis performed on the recrystallized monomer after drying (Figure 2.3.2) confirmed the absence of ethyl acetate and water relative to the $CDCl_3$ solvent (Fig. 2.3.2 inset).

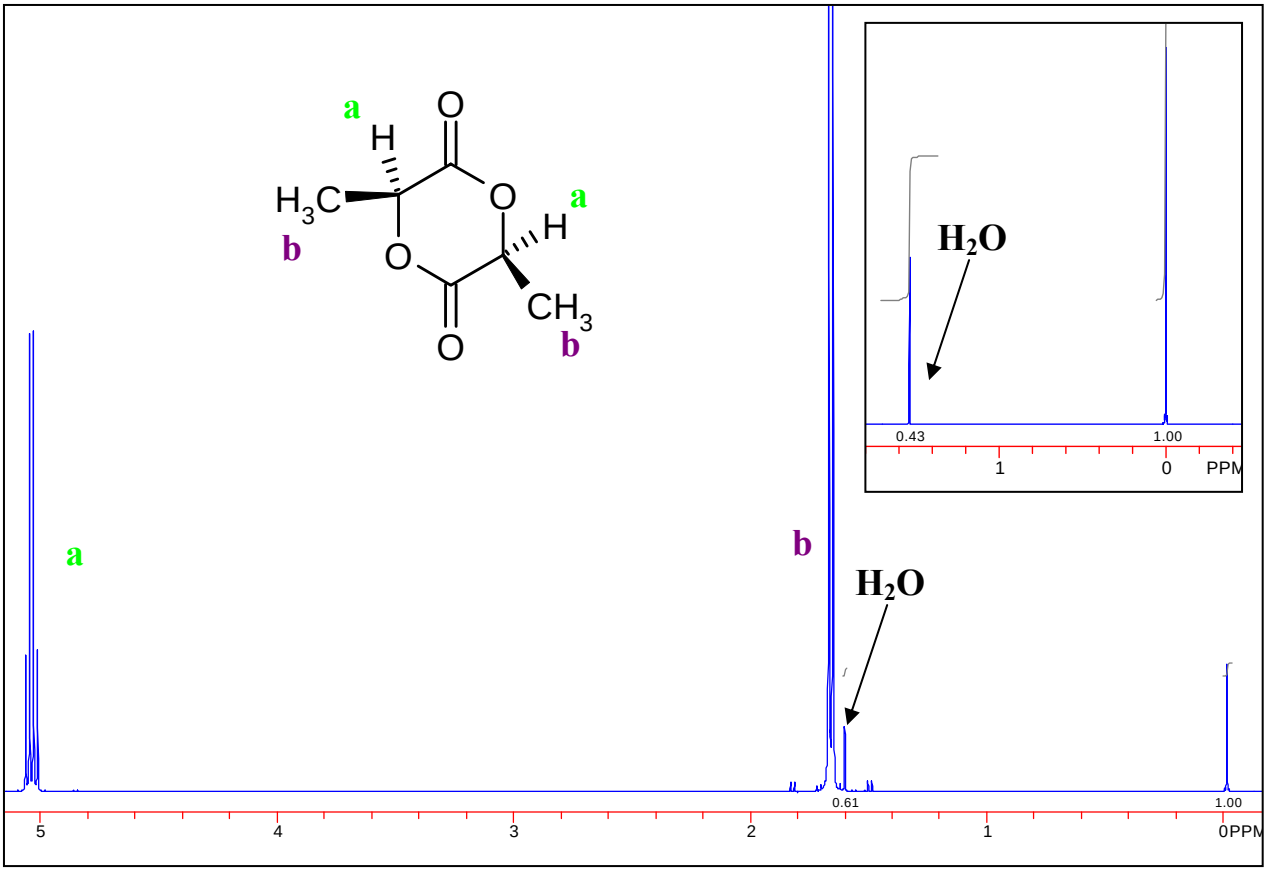

Figure 2.3.2 ^{1}H NMR spectrum of recrystallized L-lactide monomer after drying.

^{1}H NMR analysis of the PEG before drying (Fig. 2.3.3) was used to determine the number average molecular weight (M_n) of the PEG, which was approximately 2018 g/mol. Reaction progress of the polymerization was monitored by ^{1}H NMR by observing the change in chemical shift of chiral protons from 4.95 to 5.25 ppm. The percent conversion calculated from these spectra (Figure 2.3.4) allowed the reaction speed to be estimated so that it could be terminated after ~90% conversion (~11 h).

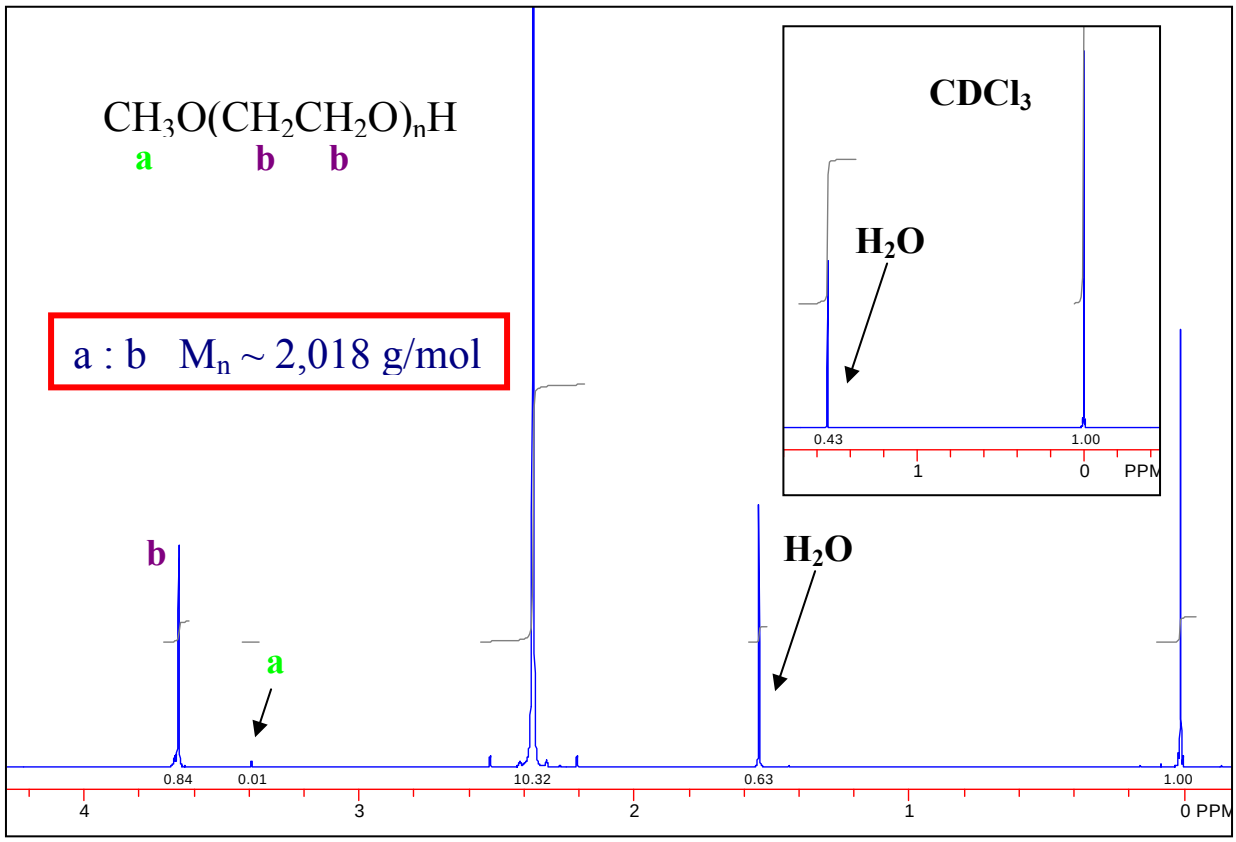

Figure 2.3.3 ^{1}H NMR spectrum of monomethylether poly(ethylene glycol) after drying.

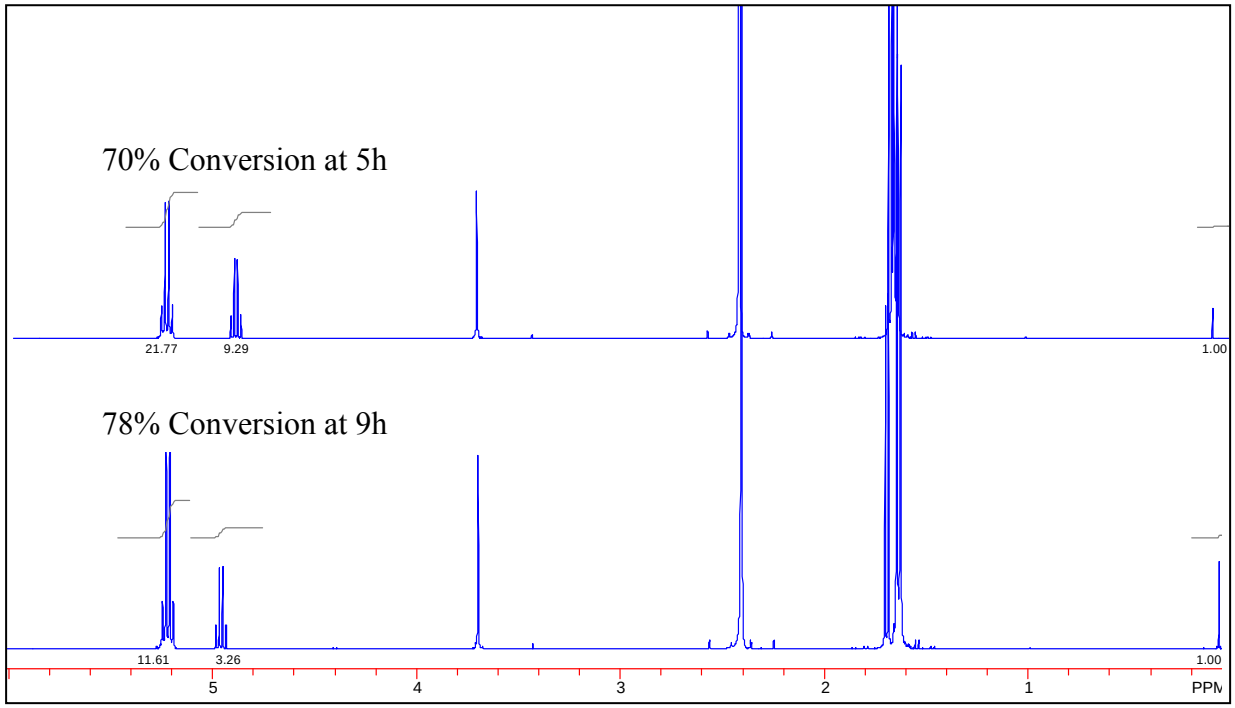

Figure 2.3.4 ^{1}H NMR spectra measuring progress of PEG-PLLA synthesis.

Analysis of the isolated and dried product (Figure 2.3.5) confirmed the absence of methanol and toluene and indicated that the PEG had successfully polymerized the L-lactide monomer. When the number of methoxy protons was set to 3, the number of chiral protons multiplied by the repeat unit weight of 72 g/mol indicated a M_n of 40,900 g/mol.

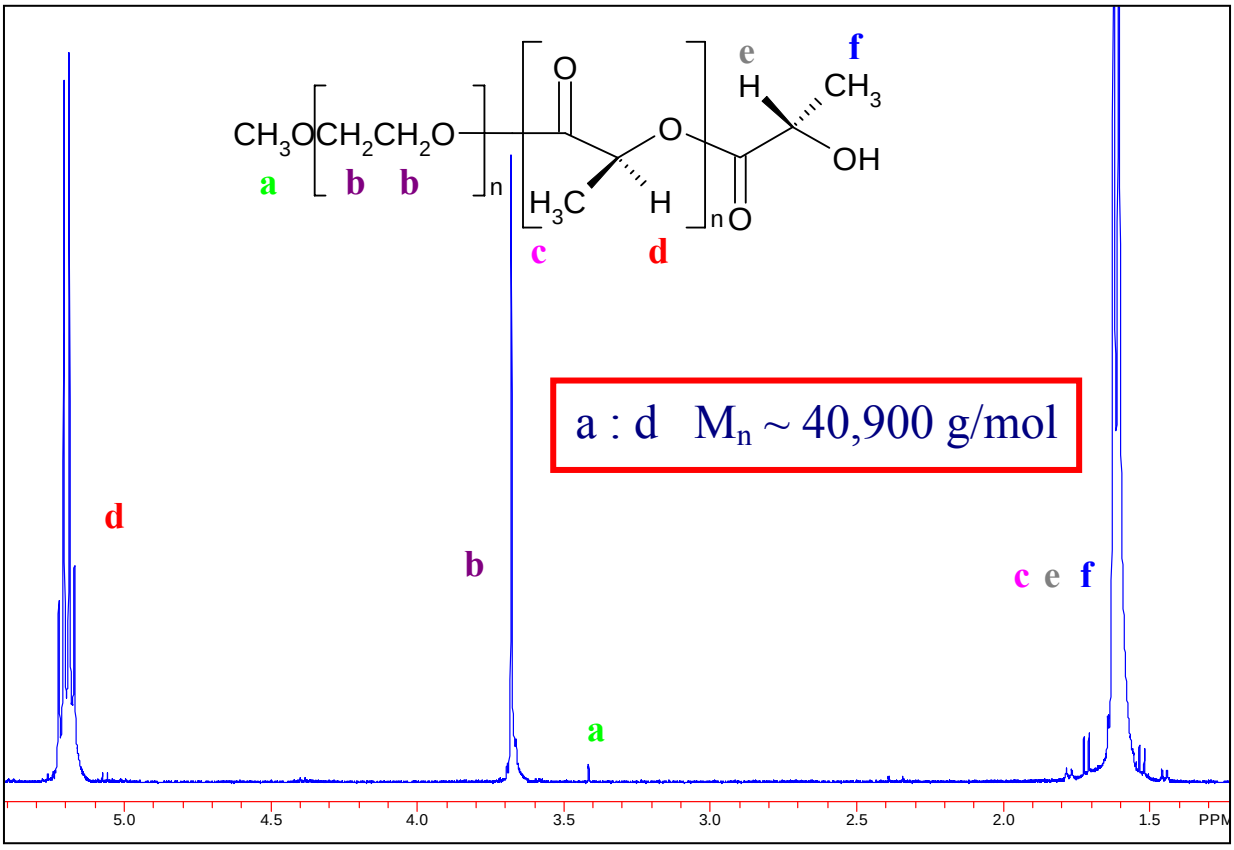

Figure 2.3.5 ^{1}H NMR spectrum of product of poly(ethylene glycol-b-L-lactide) (PEG-PLLA) diblock copolymer synthesis.

The actual M_n for the PEG-PLLA copolymer as determined by GPC results (Figure 2.3.6) was 10,500 g/mol with a polydispersity of 1.1 (Table 2.3.1). A very small high molecular weight shoulder is present in the GPC trace of the copolymer.

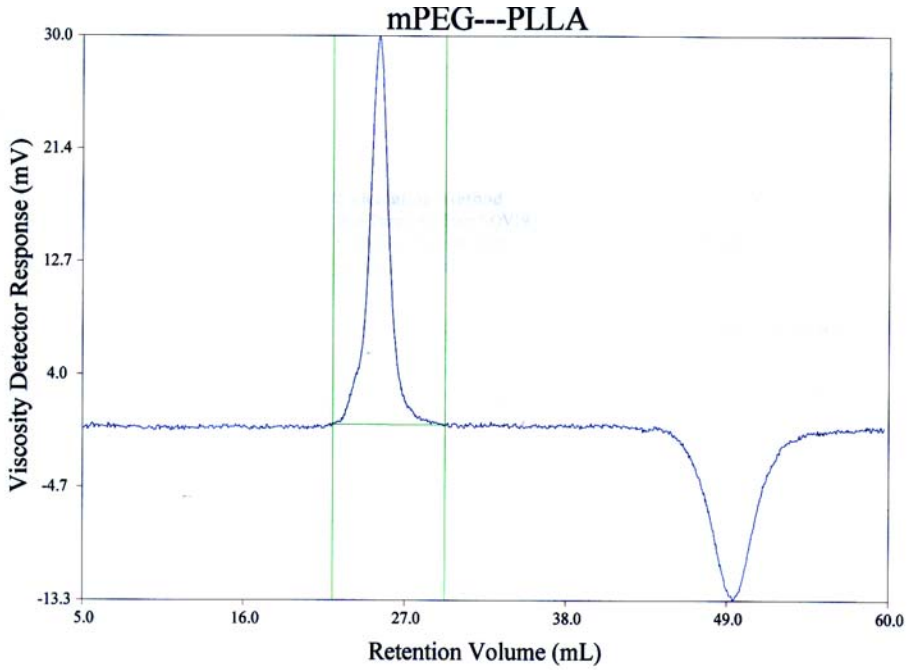

Figure 2.3.6 GPC trace of product of poly(ethylene glycol-b-L-lactide) (PEG-PLLA) diblock copolymer synthesis.

2.3.2 *Synthesis of PEG-PDLLA copolymer*

A ring-opening polymerization of D,L-lactide monomer initiated by monomethylether poly(ethylene glycol) (PEG; $M_n \approx 2000$ g/mol) with stannous octoate catalyst was successfully employed to synthesize a PEG-PDLLA copolymer. ^{1}H NMR analysis performed on the recrystallized monomer after drying (Figure 2.3.7) confirmed the absence of ethyl acetate and water relative to the $CDCl_3$ solvent (Figure 2.3.7 inset).

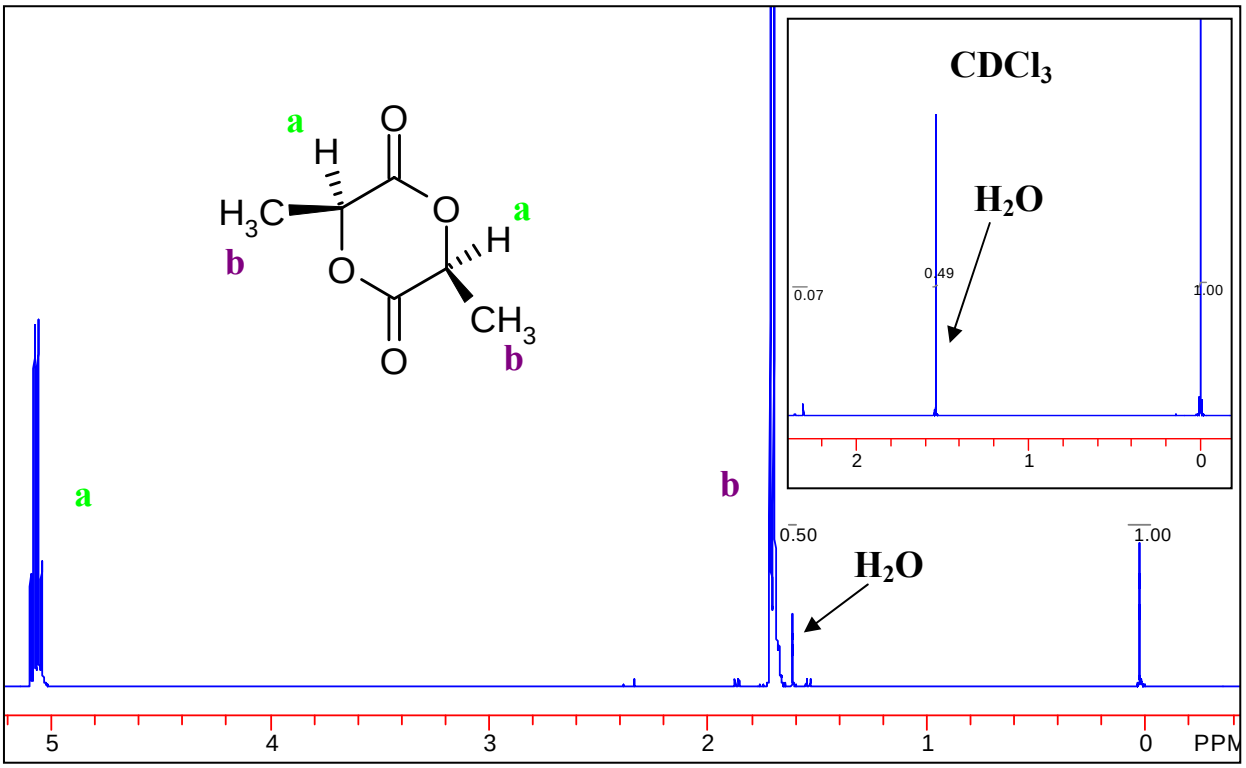

Figure 2.3.7 ^{1}H NMR spectrum of recrystallized D,L-lactide monomer after drying.

Reaction progress of the polymerization was monitored by ^{1}H NMR by observing the change in chemical shift of chiral protons from 4.95 to 5.25 ppm. The percent conversion calculated from these spectra (Figure 2.3.8) allowed the reaction speed to be estimated so that it could be terminated after ~90% conversion (7.75 h).

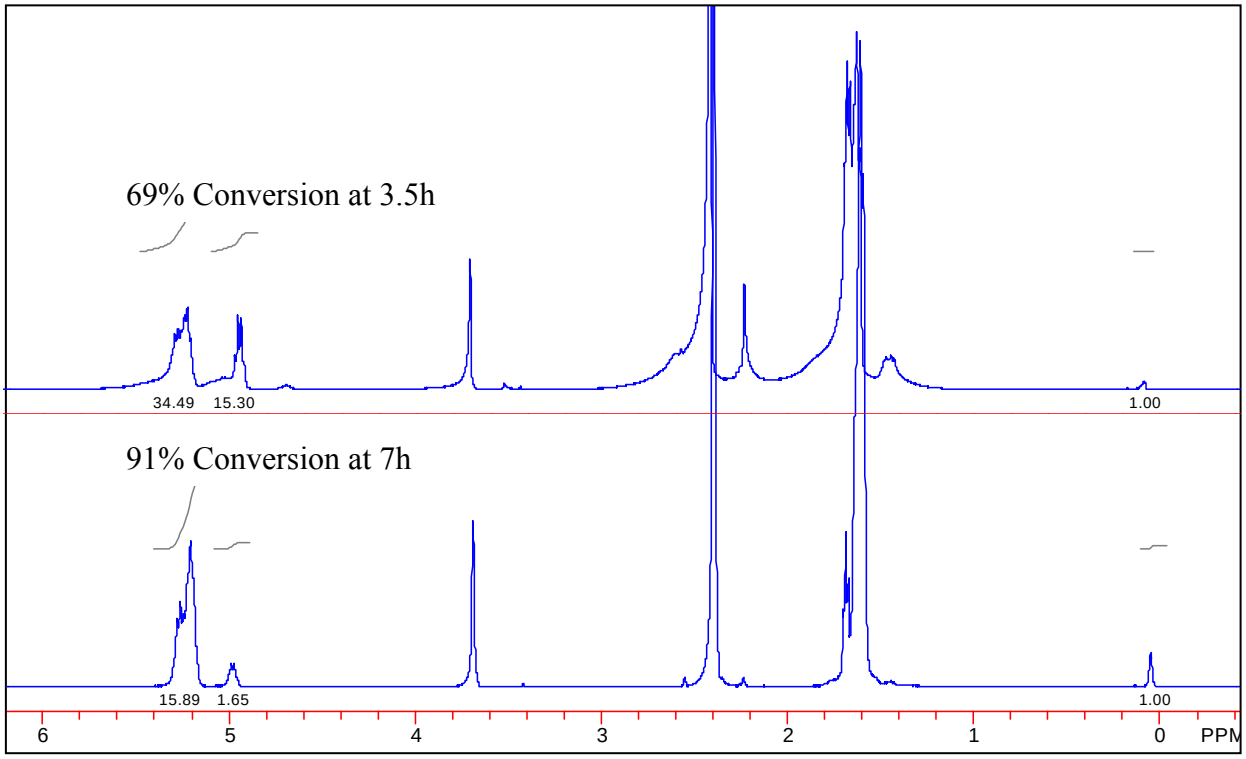

Figure 2.3.8 ^{1}H NMR spectra measuring progress of PEG-PDLLA synthesis.

Analysis of the isolated and dried product (Figure 2.3.9) indicated that the PEG had successfully polymerized the D,L-lactide monomer and confirmed the removal of much 2-propanol and toluene. When the number of methoxy protons was set to 3, the number of chiral protons multiplied by the repeat unit weight of 72 g/mol indicated a M_n of 44,100 g/mol.

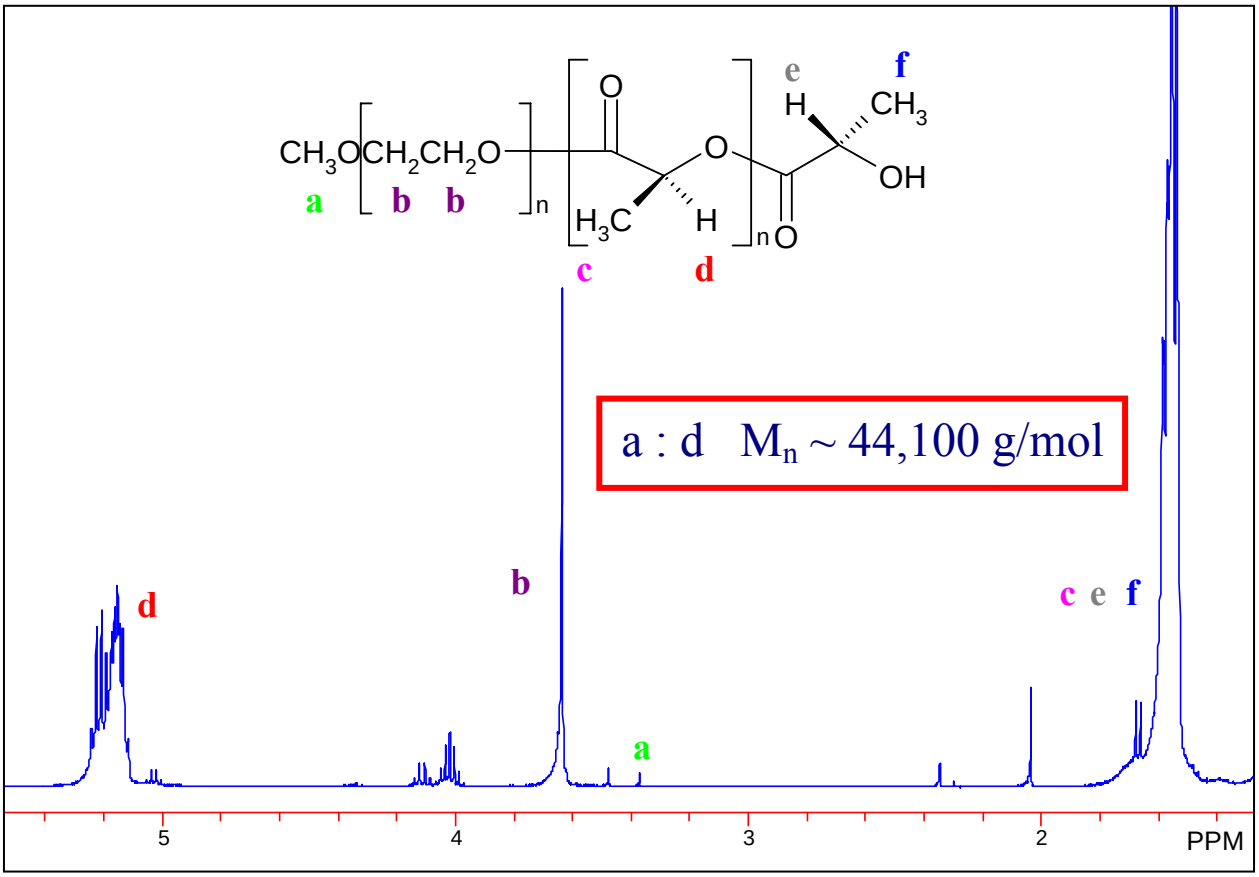

Figure 2.3.9 ^{1}H NMR spectrum of product of poly(ethylene glycol-b-D,L-lactide) (PEG-PDLLA) diblock copolymer synthesis.

The actual M_n for the PEG-PDLLA copolymer as determined by GPC results (Figure 2.10) was 19,600 g/mol with a polydispersity of 1.2. A small high molecular weight shoulder is present in the GPC trace of the copolymer.

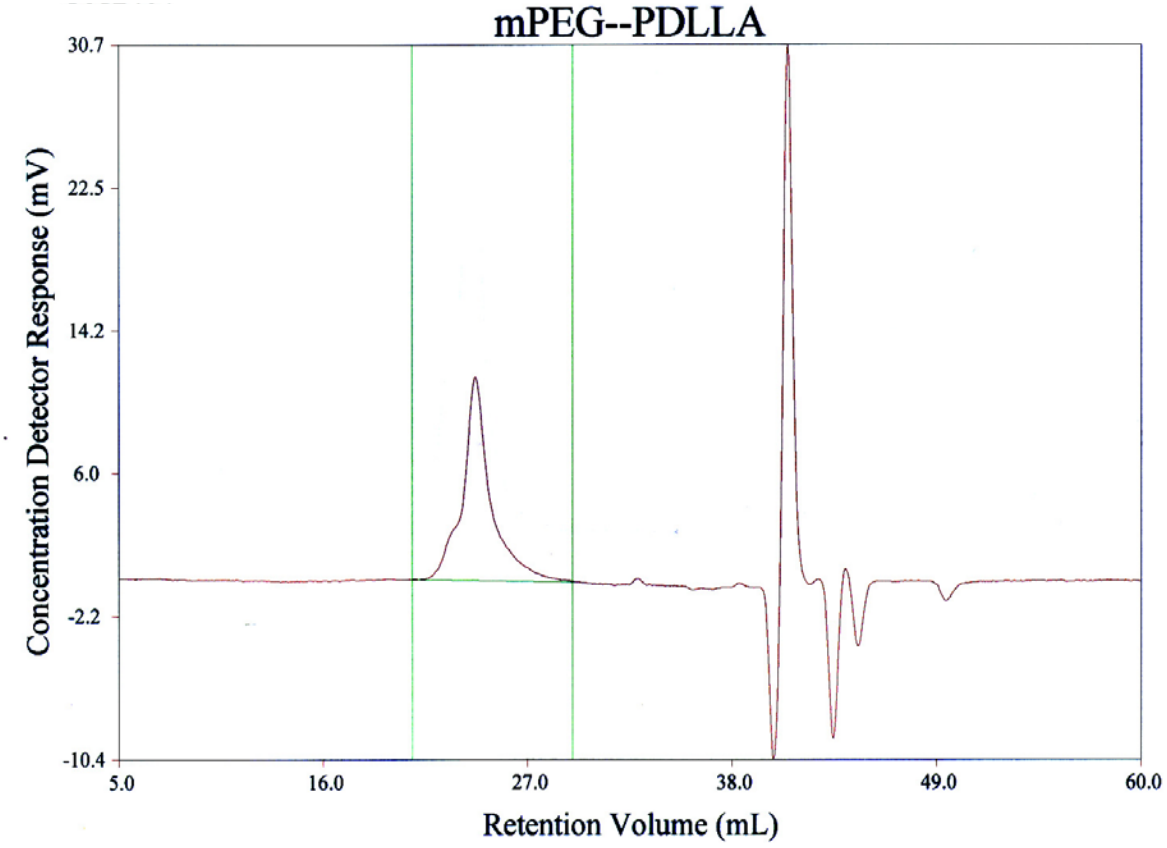

Figure 2.3.10 GPC trace of product of poly(ethylene glycol-b-D,L-lactide) (PEG-PDLLA) diblock copolymer synthesis.

2.3.3 Synthesis of PEG-PLLA copolymer (repeated)

A second ring-opening polymerization of L-lactide monomer initiated by monomethylether poly(ethylene glycol) (PEG; $M_n \approx 2000$ g/mol) with stannous octoate catalyst was successfully employed to synthesize a PEG-PLLA copolymer with a higher molecular weight than the first one. Reaction progress of the polymerization was monitored by ^{1}H NMR

by observing the change in chemical shift of chiral protons from 4.95 to 5.25 ppm (Figure 2.3.4) and the reaction was terminated after ~90% conversion (10.6 h).

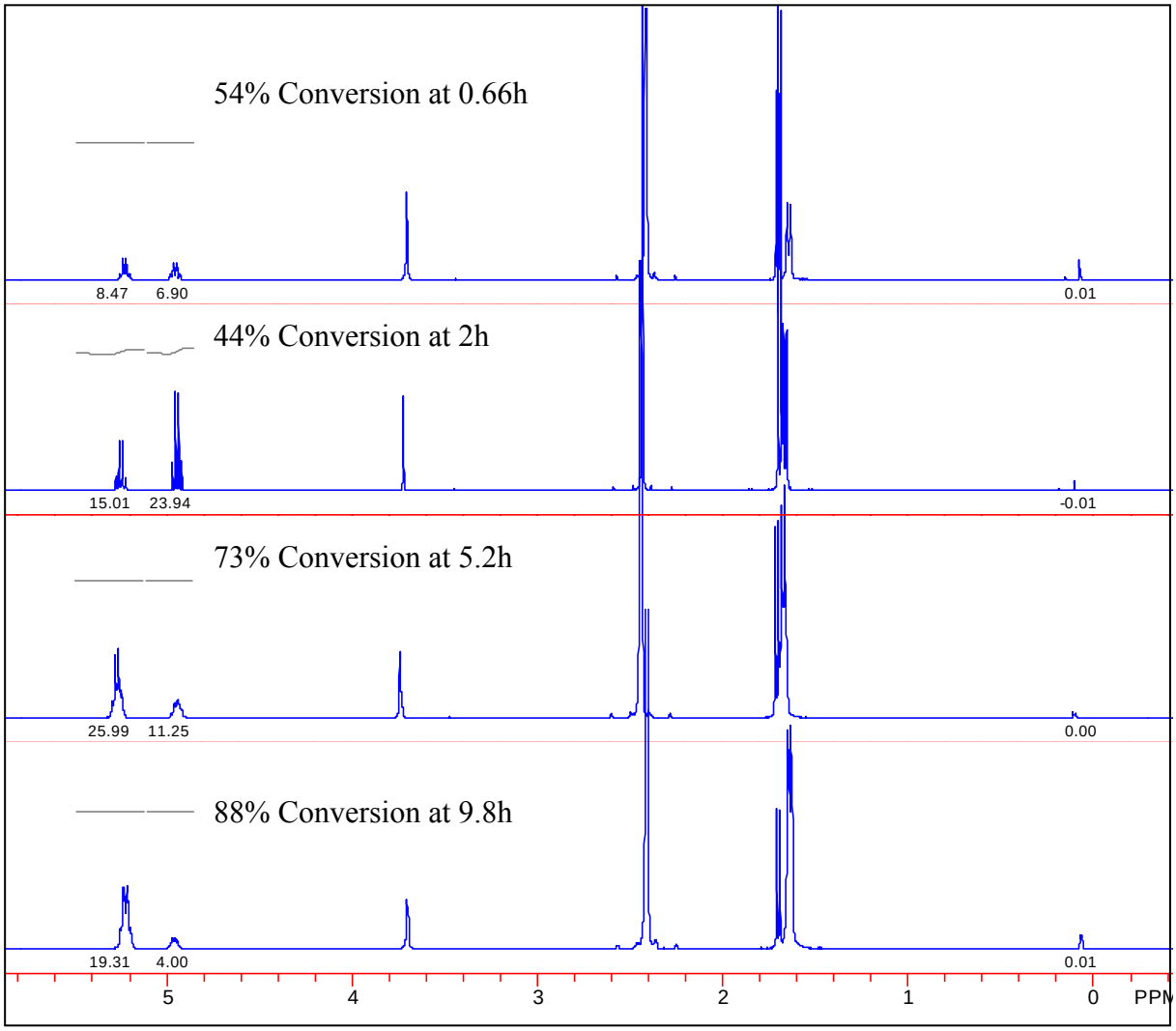

Figure 2.3.11 ^{1}H *NMR spectra measuring progress of PEG-PDLLA synthesis.*

Analysis of the isolated and dried product (Figure 2.12) confirmed the absence of methanol and toluene solvent and indicated that the PEG had successfully polymerized the L-lactide monomer. The peak at 2.36 ppm is from toluene which had contaminated the $CDCl_3$ solvent, and not from the reaction. When the number of methoxy protons was set to 3, the number of chiral protons multiplied by the repeat unit weight of 72 g/mol indicated an M_n of 52,450 g/mol.

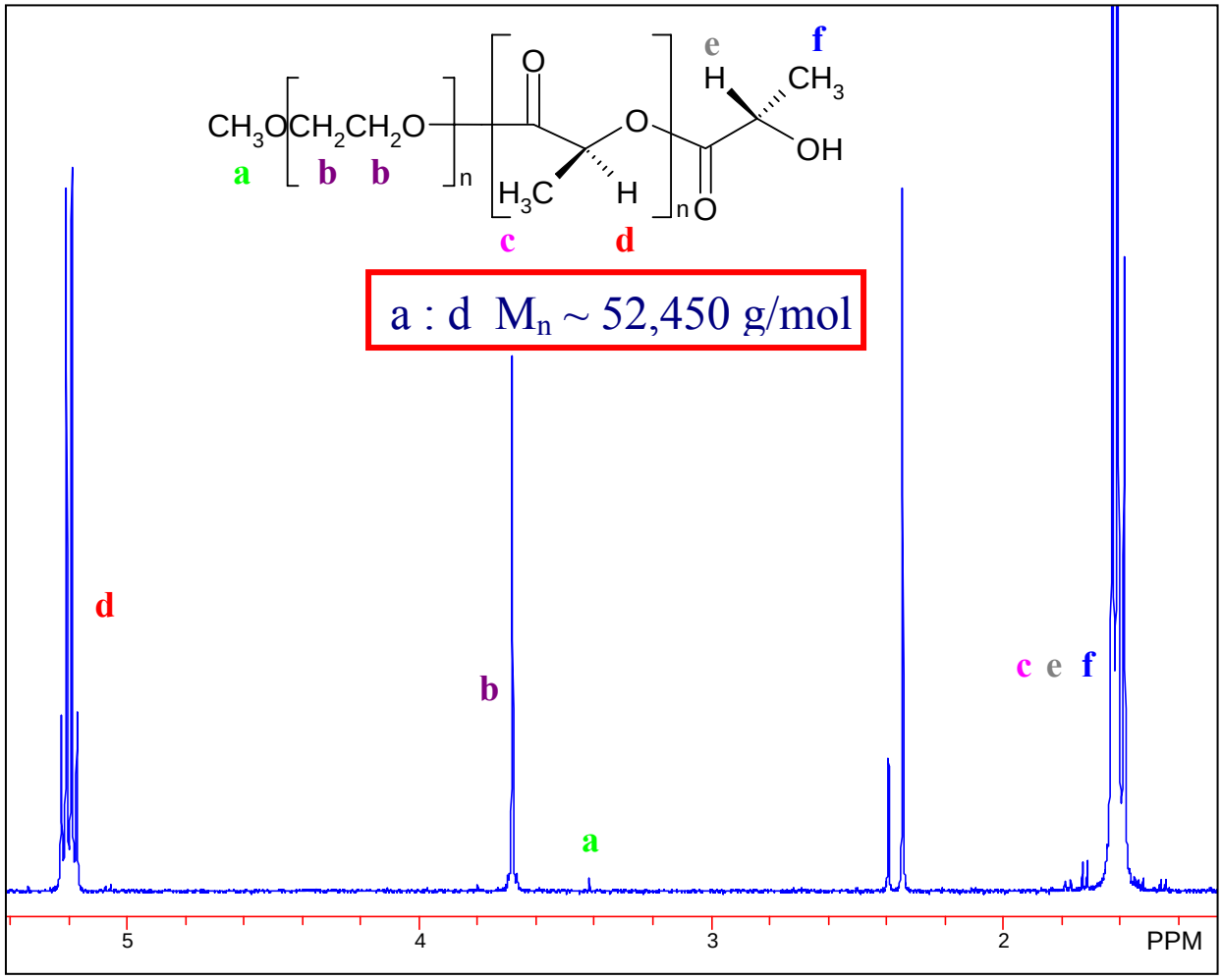

Figure 2.3.12 ^1H NMR spectrum of product of second poly(ethylene glycol-b-D,L-lactide) (PEG-PDLLA) diblock copolymer synthesis.

The actual M_n for the PEG-PLLA copolymer as determined by GPC results (Figure 2.3.13) was 22,100 g/mol with a polydispersity of 1.2. A small high molecular weight shoulder is present in the GPC trace of the copolymer.

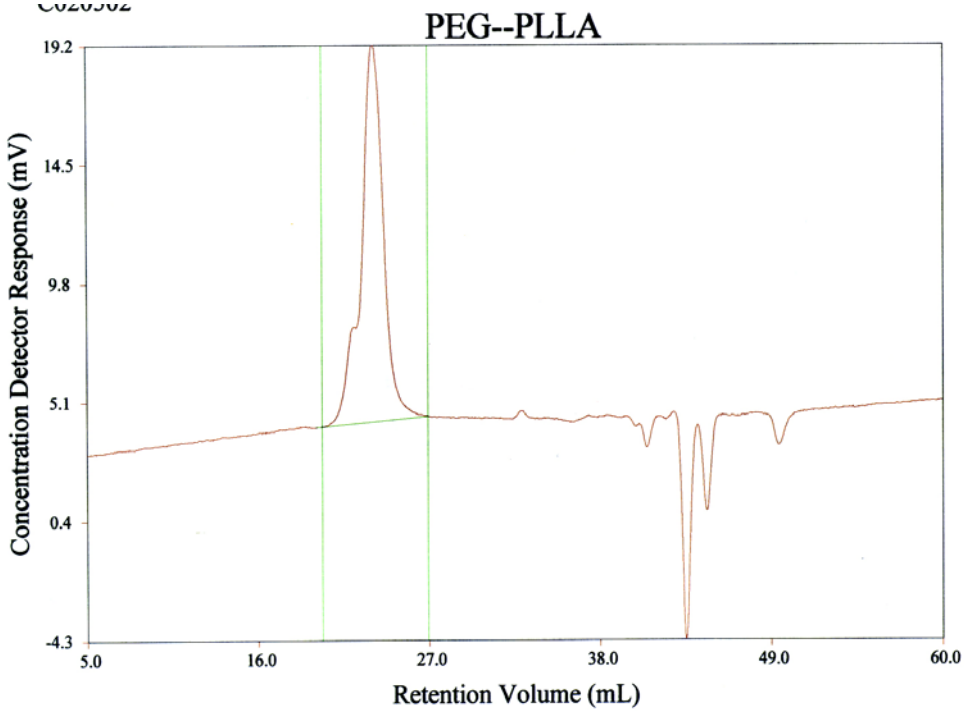

Figure 2.3.13 GPC trace of product of second poly(ethylene glycol-b-L-lactide) (PEG-PLLA) diblock copolymer synthesis.

2.3.4 Synthesis of PEG-PDLLA copolymer (repeated)

A second ring-opening polymerization of D,L-lactide monomer initiated by monomethylether poly(ethylene glycol) (PEG; $M_n \approx 2000$ g/mol) with stannous octoate catalyst was successfully employed to synthesize a PEG-PDLLA copolymer with a higher molecular weight than the first one. ^{1}H NMR analysis performed on the recrystallized monomer after drying (Figure 2.3.14) confirmed the absence of ethyl acetate and water relative to the $CDCl_3$ solvent.

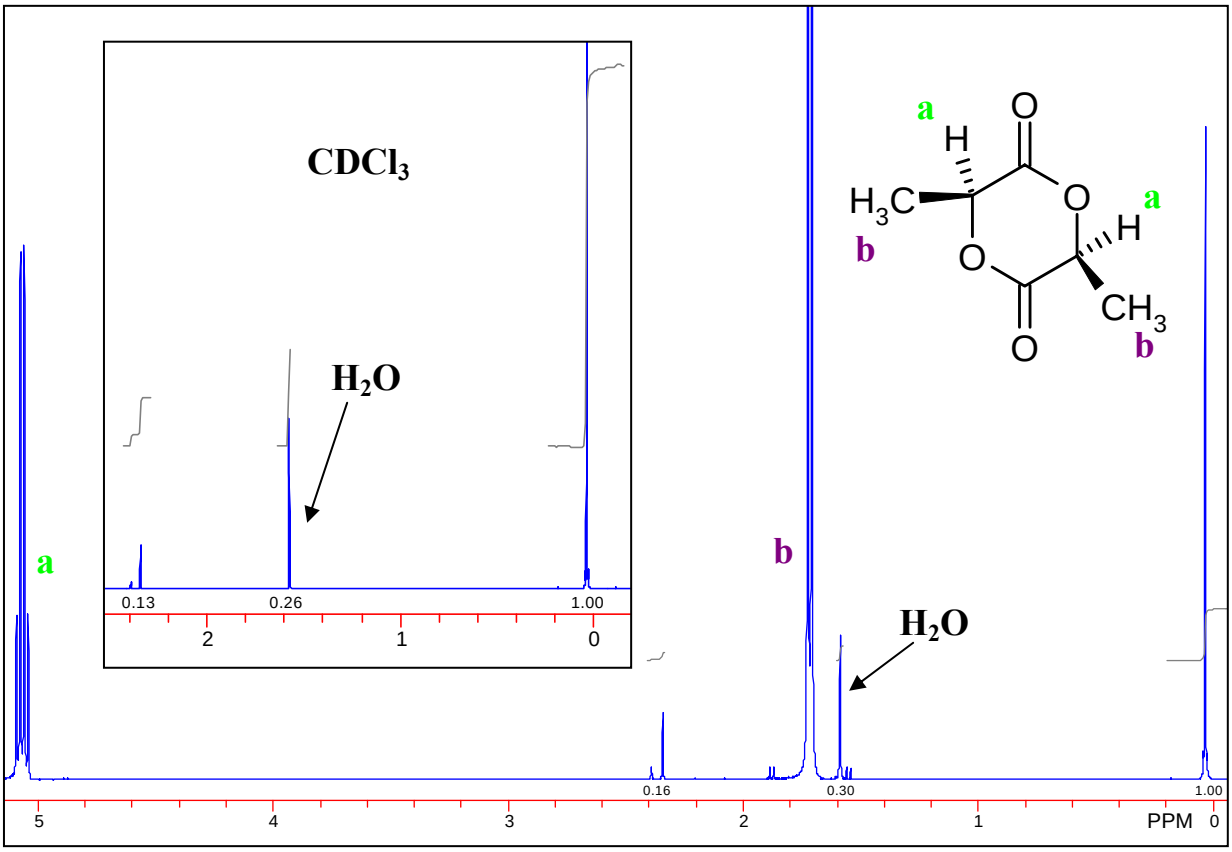

Figure 2.3.14 ^{1}H NMR spectrum of recrystallized D,L-lactide monomer after drying.

Reaction progress of the polymerization was monitored by ^{1}H NMR by observing the change in chemical shift of chiral protons from 4.95 to 5.25 ppm (Figure 2.3.15) and the reaction was terminated after ~90% conversion (4.2 h).

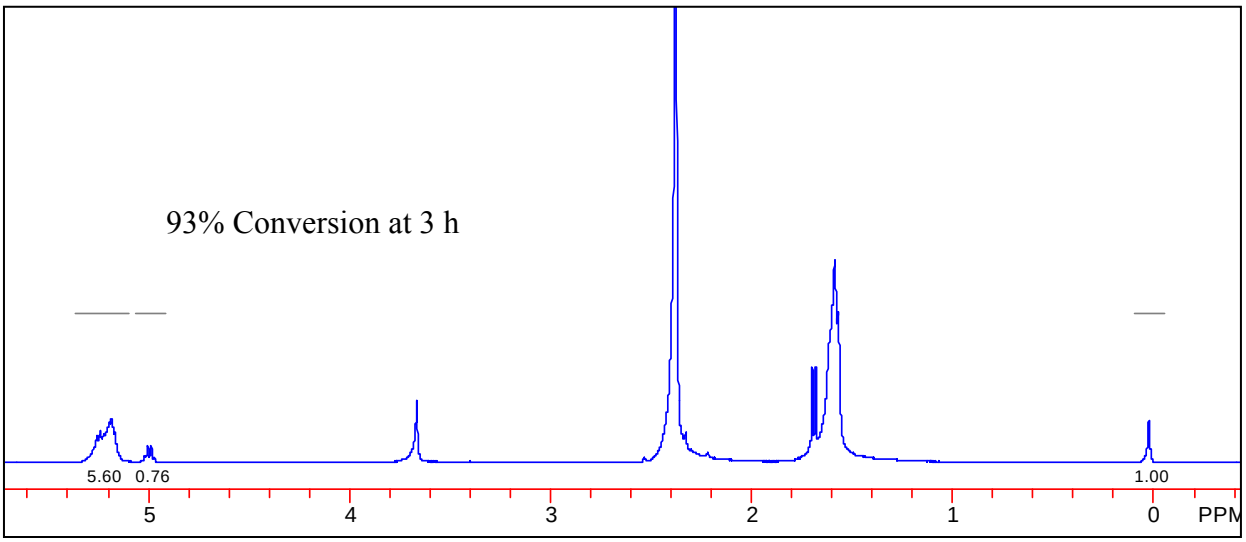

Figure 2.3.15 ^{1}H NMR spectrum measuring progress of second PEG-PDLLA synthesis.

Analysis of the isolated and dried product (Figure 2.3.16) confirmed the absence of methanol, toluene, and chloroform and indicated that the PEG had successfully polymerized the D,L-lactide monomer. When the number of methoxy protons was set to 3, the number of chiral protons multiplied by the repeat unit weight of 72 g/mol indicated a M_n of 42,100 g/mol.

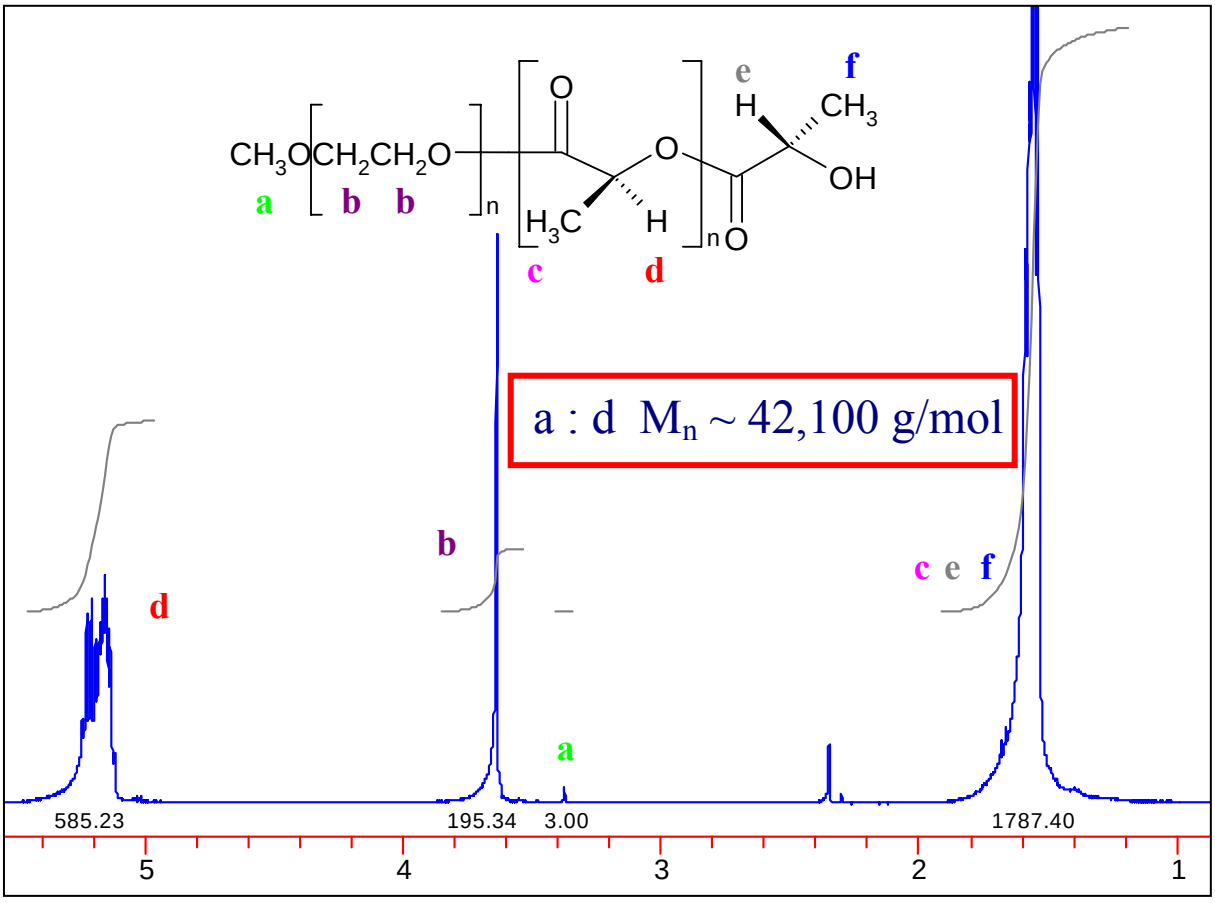

Figure 2.3.16 ^{1}H NMR spectrum of product of second poly(ethylene glycol-b-d,l-lactide) (PEG-PDLLA) diblock copolymer synthesis.

The actual M_n for the PEG-PDLLA copolymer as determined by GPC results (Figure 2.3.17) was 36,900 g/mol with a polydispersity of 1.1. A small high molecular weight shoulder is present in the GPC trace of the copolymer.

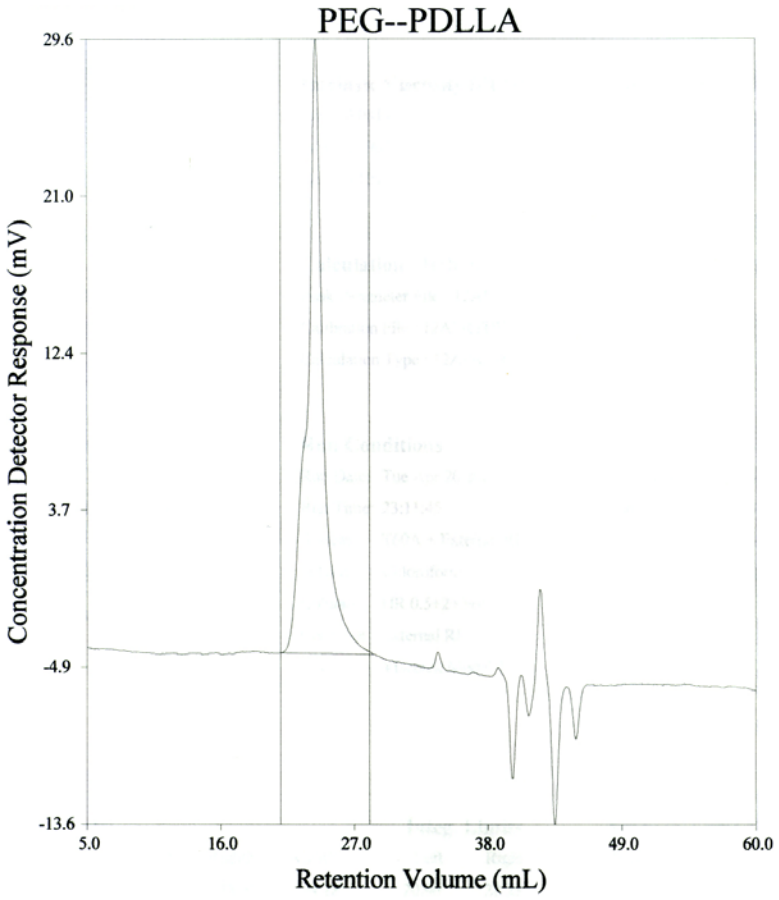

*Figure 2.3.17 GPC trace of product of second poly(ethylene glycol-*b*-D,L-lactide) (PEG-PDLLA) diblock copolymer synthesis.*

Table 2.3.1 Molecular weights of poly(ethylene glycol-*b*-lactide) diblock copolymers.

	PEG-PLLA 1	**PEG-PDLLA 1**	**PEG-PLLA 2**	**PEG-PDLLA 2**
M_n	10,500	19,600	22,100	36,900
PDI	1.1	1.2	1.2	1.1

2.4 Discussion

Two sets of ring-opening polymerizations of L- and D,L-lactide monomers were successfully initiated by PEG to synthesize PEG-PLLA and PEG-PDLLA diblock copolymers, respectively (Table 2.3.1). The narrow polydispersities of the materials suggest that little to no transesterification occurred during polymerization of the polylactide blocks. The use of dry toluene during the drying of the PEG and copolymer synthesis proved very successful in reducing the amount of water in the system, as seen in the increase in molecular weight of the products of the repeated syntheses (Table 2.3.1). The molecular weight of the second PEG-PDLLA copolymer was very close to the target molecular weight of 42,000 g/mol (2000 g/mol PEG and 40,000 g/mol PDLLA), demonstrating that this polymerization method is a viable one for synthesizing PEG-PDLLA diblock copolymers of this size. Dry toluene also helped to double the molecular weight of the PEG-PLLA when it was synthesized the second time.

The low molecular weight of both PEG-PLLA diblock copolymers (compared to the target molecular weight) was likely due to their decreased solubility in toluene as molecular weight increased during synthesis. It is possible that higher molecular weights for the PEG-PLLA diblock copolymers may have been achieved if more than 2 mL toluene/1g monomer had been used during synthesis. Lucke et al. [35] synthesized PEG-PLLA diblock copolymers of a similar size (PEG:2000, PLLA:40,000) using the same solution ring-opening polymerization, but they used 8 mL toluene for each gram of monomer. This would result in a lower copolymer concentration during synthesis, possibly improving the solubility of the product. Another strategy to obtain higher molecular weights of PEG-PLLA may be to conduct the ring-opening polymerization in the melt (bulk polymerization).

GPC results for each diblock copolymer returned a lower M_n than that calculated from the ^1H NMR spectrum for each product. A small high molecular weight shoulder on the peak in each of the GPC traces (Figures 2.3.6, 2.3.10, 2.3.13, and 2.3.17) may explain the disparity between these values. The presence of a shoulder in the GPC traces of every one of the polymers suggests that the cause is systematic. One explanation is the presence of a small amount of difunctional PEG, which could initiate a polymerization in two directions and form triblock copolymers. Because water can initiate ring-opening polymerization, the presence of residual water may explain for the lower than expected molecular weights. Increases in M_n following increased efforts to eliminate water during the second set of syntheses support this hypothesis.

2.5 Conclusions

The use of monomethylether PEG to initiate a ring-opening polymerization of D,L-lactide monomer with stannous octoate catalyst is a viable method for synthesizing PEG-PDLLA diblock copolymers with target molecular weights of 42,000 g/mol (PEG:2000, PDLLA:40,000). This method may also be practical for the synthesis of PEG-PLLA diblock copolymers using L-lactide if additional toluene is added to reduce the copolymer concentration during synthesis, preventing early precipitation of the product from the reaction solution. The use of dry toluene when drying the PEG initiator is an extremely effective way of reducing the amount of water present during the polymerization. High molecular weight shoulders on the GPC peaks of each copolymer indicate that a small amount of the PEG initiator may be difunctional.

Chapter 3 Electrospinning Bioresorbable Tissue Scaffolds

3.1 Introduction

For tissue engineering, the method by which the biomaterial is processed into a scaffold is important for achieving a surface topography and an architecture (e.g. porosity, pore size) suited to the desired tissue. The surface topography influences cell adhesion and spreading, while the porosity permits cell infiltration into the scaffold interior. Electrospinning is a novel method of processing polymers into porous tissue scaffolds comprised of fused nanoscale fibers [27]. A broad range of polymers can be electrospun and through careful selection of electrospinning conditions (e.g., [28, 110, 114]) fiber diameter can be adjusted from 50 nm to 5 μm [27]. Importantly, the range from 1 to 5 μm corresponds to the length scale reported to increase cell attachment and spreading in many cell types [26]. Specifically, it has been shown using surfaces with parallel grooves that increases in groove depth [165] and ridge width (below 4 μm) [166] increase attachment and orientation. Therefore, I hypothesize that manipulating scaffold topography by varying fiber diameter will alter cell adhesion, proliferation, and potentially phenotypic behavior.

The goals of this research are twofold. First I will demonstrate that the polymers PLLA, PDLLA, PEG-PLLA, and PEG-PDLLA can be electrospun to form fused fiber mats whose fiber morphology is neither beaded nor melted. Second, I will determine electrospinning conditions that achieve a broad range of fiber diameters for a single polymer, PDLLA.

3.2 Materials and Methods

3.2.1 Materials

Poly(L-lactide) (PLLA) was donated by Ethicon (Somerville, NJ) and used as received. Poly(D,L-lactide) (PDLLA; Birmingham Polymers, Birmingham, AL) was used as received. Poly(ethylene glycol-*b*-lactide) diblock copolymers (PEG-PLLA and PEG-PDLLA) were synthesized as described in Chapter 2. Ethanol (AAPER Alcohol and Chemical Co., Shelbyville, KY) and 1,1,1,3,3,3-hexafluoro-2-propanol (HFIP; Sigma-Aldrich, St. Louis, MO) were used as received. Dichloromethane (Mallinckrodt Baker, Paris, KY) and *N*,*N*-dimethylformamide (DMF; EM Science, Gibbstown, NJ) were used as received.

3.2.2 Electrospinning PDLLA using DMF as a solvent

3.2.2.1 Coverslip preparation

Glass microscope coverslips (18 mm dia.; Fisher) were sonicated in ethanol for 10 min and dried at 40 °C in a Fisher Isotemp oven. PDLLA was dissolved in DMF to make a 5.0 wt % solution. PDLLA solution (265 μL) was pipetted onto each cleaned coverslip after it was mounted onto a spincoater (Model 1-EC101D-R485; Headway Research, Garland, TX). Each coverslip was spun at 2500 rpm for 30 s. Spincoated coverslips were placed in a vacuum desiccator at room temperature overnight to remove residual solvent.

3.2.2.2 Scaffold preparation

Fiber scaffolds were created by electrospinning solutions of PDLLA in DMF onto the spincoated coverslips (Figure 3.2.1).

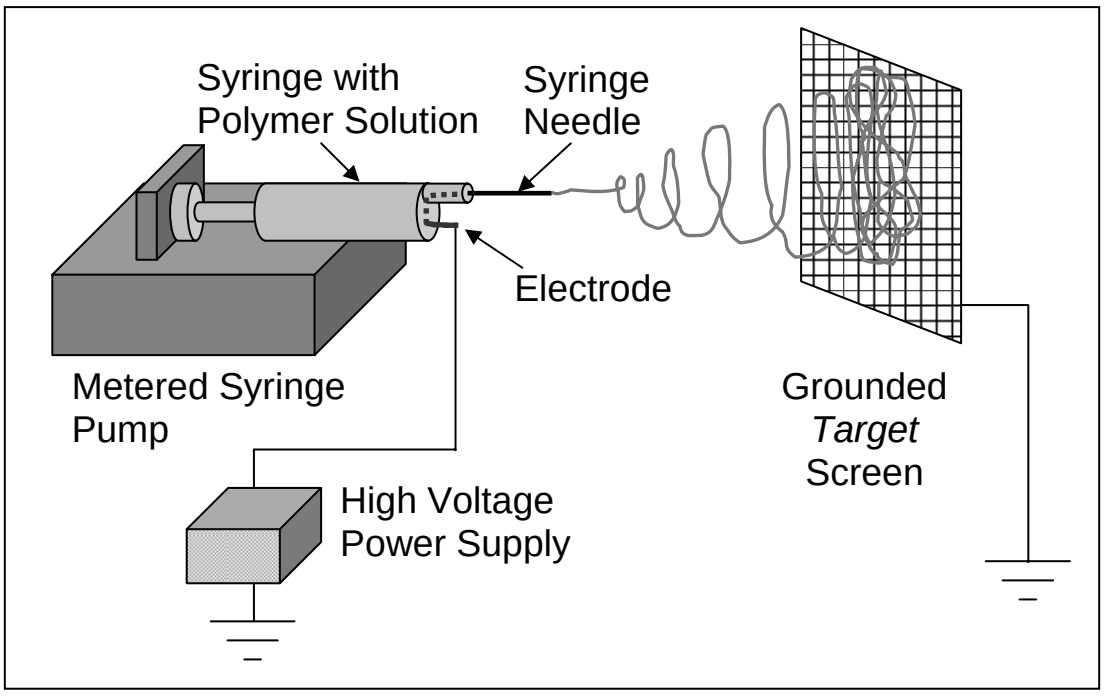

Figure 3.2.1 Electrospinning apparatus.

PDLLA was dissolved in DMF to make 21 wt%, 30 wt%, and 38 wt% solutions. Each solution was drawn into a 30-mL syringe fitted with a 20-gauge needle. An electrode was mounted inside the base of the needle. PDLLA spincoated coverslips were arranged on a grounded metal screen 15 cm away from the syringe needle. As a syringe pump (Model KDS100; kdScientific, New Hope, PA) dispensed solution from the syringe at a fixed rate (Table 3.2.1), an electric potential (Table 3.2.1) from a high voltage power source (Model CZE1000R; Spellman High Voltage Electronics Corp., Hauppauge, NY) was applied to the solution in the syringe via its electrode.

Table 3.2.1 Electrospinning parameters for PDLLA in DMF solutions

Solution (wt %)	**Flow Rate (mL/hr)**	**Voltage (kV)**
21	1.5	15
30	0.5	15
38	1.5	10

Under the electric potential the polymer was ejected from the syringe tip as a nanofiber polymer toward the grounded metal screen. Each solution was electrospun for 2 min. Electrospun samples were placed in a vacuum desiccator at ambient temperature overnight to remove residual solvent.

3.2.3 Electrospinning PDLLA, PLLA, PEG-PDLLA, and PEG-PLLA using HFIP as a solvent

3.2.3.1 Coverslip preparation

Glass microscope coverslips (18 mm dia.; Fisher) were sonicated in ethanol for 10 min and dried at 40 °C in a Fisher Isotemp oven. PDLLA and PEG-PDLLA were separately dissolved in CH_2Cl_2 to make two 3.6 wt % solutions. PDLLA solution (270 μL) was pipetted onto each cleaned coverslip after it was mounted onto the spincoater (Model 1-EC101D-R485; Headway Research, Garland, TX). Each coverslip was spun at 2500 rpm for 30 s. Half of the PDLLA spincoated coverslips were spincoated a second time with PEG-PDLLA solution in the same manner. Spincoated coverslips were placed in a vacuum desiccator at room temperature overnight to remove residual solvent.

3.2.3.2 Scaffold preparation

Fiber scaffolds were created by electrospinning solutions of polymers in HFIP onto the spincoated coverslips. PDLLA, PLLA, PEG-PDLLA, and PEG-PLLA were dissolved in HFIP to make 15, 8.2, 26, and 26 wt % solutions, respectively. Different concentrations were required for the different polymers in order to achieve electrospun fibers because the fibers had different molecular weights. Solution concentration increases as polymer molecular weight decreases because the polymer chains in solution must have a certain degree of entanglement in order to electrospin into a fiber [167]. Electrospinning of the four polymers was performed as described

in section 3.2.2.2, except that a 22-gauge needle was used. For all polymers, the electrospinning conditions were a flow rate of 1.5 mL/h, a voltage of 15 kV, and a throw distance of 15 cm. PDLLA and PLLA solutions were electrospun onto PDLLA spincoated coverslips while PEG-PDLLA and PEG-PLLA solutions were electrospun onto PEG-PDLLA spincoated coverslips. Solutions were electrospun until the surfaces of the coverslips were no longer transparent. Electrospinning time ranged from 10 min to 1 h. Electrospun samples were placed in a vacuum desiccator at ambient temperature overnight to remove residual solvent.

3.2.4 Electrospinning Different PDLLA Fiber Diameters

3.2.4.1 Coverslip Preparation

Glass microscope coverslips (18 mm dia.; Fisher) were sonicated in ethanol for 10 min and dried at 40 °C in a Fisher Isotemp oven. PDLLA was dissolved in CH_2Cl_2 to make a 3.6 wt% solution. PDLLA solution (270 μL) was pipetted onto each cleaned coverslip after it was mounted onto the spincoater (Model 1-EC101D-R485; Headway Research, Garland, TX). Each coverslip was spun at 2500 rpm for 30 s. Spincoated coverslips were placed in a vacuum desiccator at room temperature overnight to remove residual solvent.

3.2.4.2 Scaffold Preparation

Fiber scaffolds having different fiber diameters were created by electrospinning solutions with varied concentrations of PDLLA (5.0, 7.5, 15, 25, and 30 wt%) in HFIP onto the spincoated coverslips. Electrospinning was performed as described in section 3.2.3.2. The parameters used to electrospin the various concentrations of PDLLA in HFIP are listed below (Table 3.2.2).

Table 3.2.2 Electrospinning parameters for PDLLA in HFIP solutions

Solution (wt %)	Flow Rate (mL/hr)	Voltage (kV)	Distance (cm)
5.0	1.5	15	15
7.5	1.5	8, 15, 25	15
15	1.5	15	15
25	1.5	15, 20	6.5, 15
30	2.0	22, 24	15

Solutions were electrospun until the surfaces of the coverslips were no longer transparent. Electrospinning time ranged from 30 min to over 2.5 h. Electrospun samples were placed in a vacuum desiccator at ambient temperature overnight to remove residual solvent.

3.2.5 Instrumentation and Characterization

3.2.5.1 Scanning Electron Microscopy (SEM)

Electrospun fiber size was characterized using SEM. Electrospun samples were mounted onto SEM sample studs and coated with an 8-μm layer of palladium in a sputter coater (Model 208HR; Cressington Scientific Instruments, Cranberry Township, PA) equipped with a thickness controller (Model MTM20; Cressington). SEM images were obtained using a LEO 1550 Field Emission SEM (Carl Zeiss SMT**,** Thornwood, NY) operating at 5 kV with a secondary electron detector. Images were imported into ImagePro (I-Cube, Crofton, MD) and analyzed for fiber diameter.

3.2.5.2 Differential Scanning Calorimetry (DSC)

Thermal analysis was performed on electrospun PLLA and PEG-PLLA fibers using DSC. Samples (5-7 mg) were sealed in aluminum pans (Seiko Instruments Inc.) and run using a Seiko DSC 220C with a nitrogen purge. The samples were heated from 25 to 220 °C at a rate of 20

°C/min and the data were normalized to a 1 mg sample mass. Data analysis was performed using Origin (OriginLab Corp., Northampton, MA).

3.2.5.3 Light Microscopy

To estimate fiber diameter quickly, phase contrast images of the PDLLA fibers electrospun from various solution concentrations were collected using a Hamamatsu camera (I-Cube, Crofton, MD) mounted on an Olympus IX50 inverted microscope (Opelco, Sterling, VA) with a Prior motorized stage and analyzed using ImagePro.

3.2.5.4 Gel Permeation Chromatography (GPC)

Molecular weights and polydispersities were estimated using a Waters 2690 Gel Permeation Chromatograph (GPC; Waters Corporation, Milford, MA) equipped with four Waters Styragel® HR columns (Models HR 0, HR 2, HR 3, and HR 4), an online Viscotek 100 differential viscometric detector (Viscotek, Houston, TX), and a Viscotek laser refractometer. Chloroform was the mobile phase with a flow rate of 1.0 mL/min at 25 °C. A calibration plot constructed from polystyrene standards was used to determine the molecular weights of the samples via a universal calibration.

3.3 Results and Discussion

3.3.1 Electrospinning using DMF as a solvent

Four different concentrations of PDLLA (17, 21, 30, and 38 wt%) were electrospun onto glass microscope coverslips spincoated with PDLLA. The 17 wt% solution was too dilute and resulted in electrospraying of nanoparticles. The other three solutions electrospun into fibers.

SEM images taken of each electrospun polymer revealed the fiber sizes and shape (Figure 3.3.1). Smoothness appears to increase with concentration.

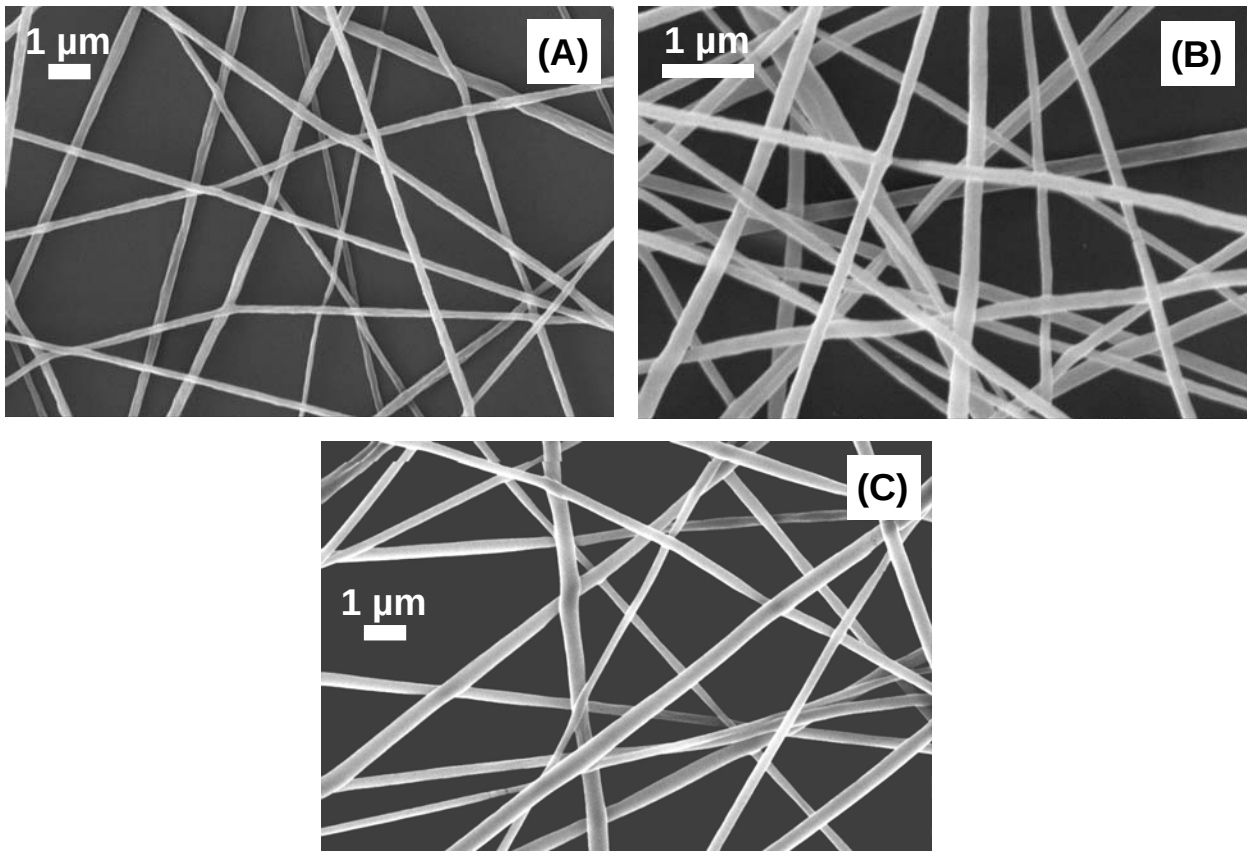

Figure 3.3.1 SEM images of PDLLA electrospun from DMF: (A) 21 wt%, (B) 30 wt%, (C) 38 wt%.

Analysis of fiber diameter indicated that the 30 wt% fibers were smaller than the 21 and 38 wt% fibers (Table 3.3.1). Although diameter typically increases with concentration [114, 168], the lack of a trend between the three groups may reflect changes in flow rate (Table 3.2.1). Fiber diameter has been shown to increase with flow rate [28], and therefore the smaller diameter for the intermediate concentration may be a consequence of the lower flow rate used. In addition, because fiber diameter decreases as voltage decreases [28], the lower voltage used for the 38 wt% solution (Table 3.2.1) may have reduced fiber diameter and further diluted the expected concentration-dependent trend.

Table 3.3.1 Average diameters of the PDLLA fibers electrospun from DMF

wt% of PDLLA in DMF	Fiber Diameter (μm)
21	0.240 ± 0.057
30	0.199 ± 0.059
38	0.310 ± 0.099

3.3.2 Electrospinning using HFIP as a solvent

The copolymers (i.e., PEG-PLLA, PEG-PDLLA) and homopolymers (i.e., PLLA, PDLLA) were individually electrospun onto glass microscope coverslips spincoated with PEG-PDLLA or PDLLA, respectively. SEM images taken of each electrospun polymer revealed the fiber sizes and shape (Figure 3.3.2). All four polymers electrospun into fibers with smooth surfaces. The distortion observed in the images of the PLLA fibers (Figure 3.3.2B) was an artifact of SEM; at lower resolutions this distortion was not observed. The PEG-PLLA fibers (Figure 3.3.2D) appeared to have fused together into a fibrous network, most likely a result of residual solvent. Table 3.3.2 contains the average diameters of the electrospun polymer fibers. Differences in fiber diameters may reflect differences in polymer molecular weight (Table 2.3.1) and solution concentration, since fiber diameter increases with molecular weight and concentration [168]. The significantly higher molecular weight for PEG-PDLLA may explain the larger fiber diameter relative to PEG-PLLA for the same solution concentration. The significantly higher solution concentration for PDLLA may explain the larger fiber diameter relative to PLLA for polymers of similar molecular weight. Gel Permeation Chromatography (GPC) analysis of PLLA before and after dissolution in HFIP returned number average molecular weights of 39,800 g/mol and 42,100 g/mol, respectively, with polydispersity indices of

1.1 for each. These data indicate that the HFIP did not affect the molecular weight of the polymers in electrospinning solution.

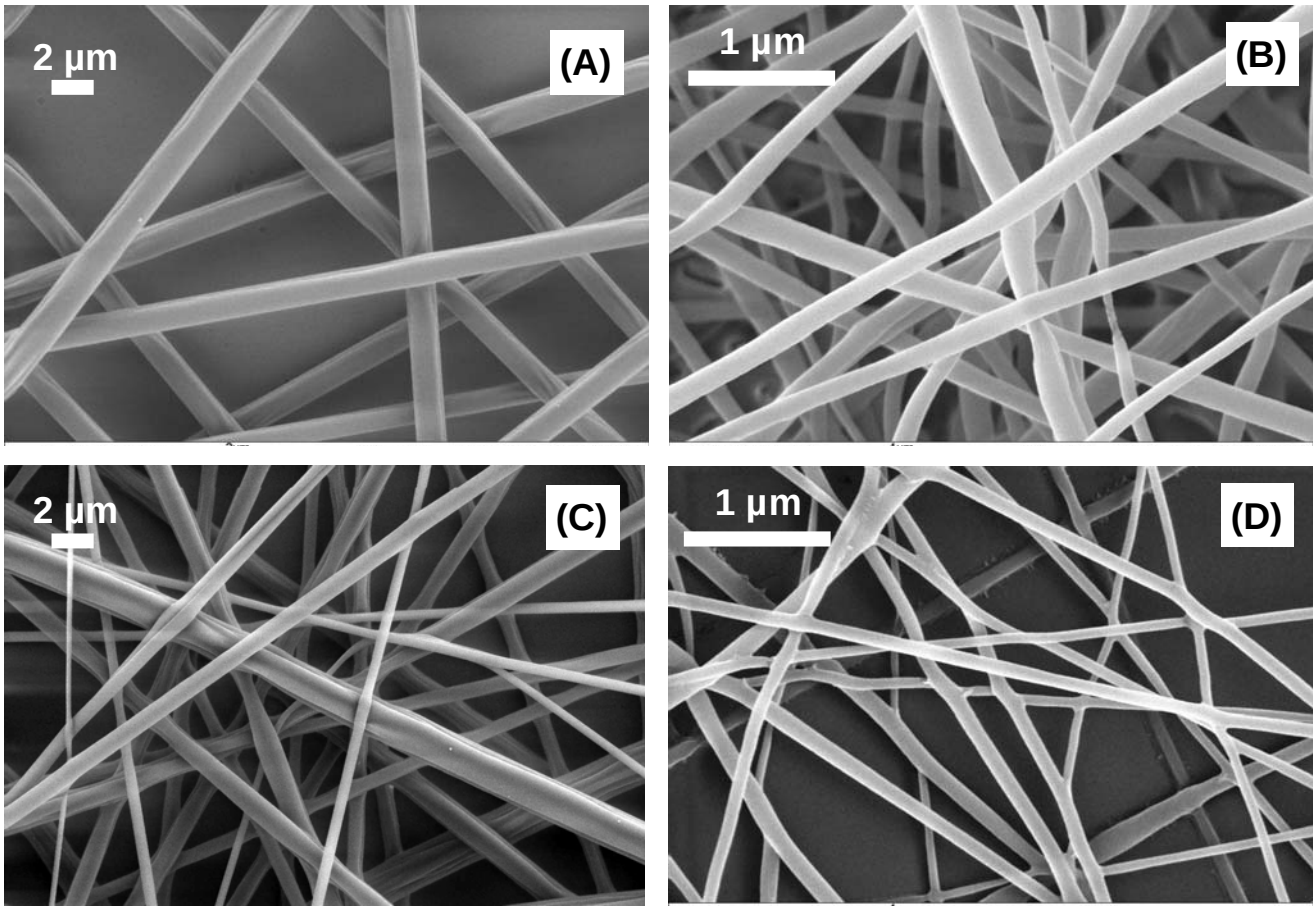

Figure 3.3.2 SEM micrographs of polymers electrospun from 1,1,1,3,3,3-hexafluoro-2-propanol (HFIP): (A) PDLLA, (B) PLLA, (C) PEG-PDLLA, and (D) PEG-PLLA. Fiber diameters are listed in Table 3.3.2.

Table 3.3.2 Average diameters of the polymer fibers electrospun from HFIP.

Electrospun Polymer	**wt% in HFIP**	**Fiber Diameter (µm)**
PDLLA	15	2.14 ± 0.35
PLLA	8.2	0.246 ± 0.079
PEG-PDLLA	26	0.889 ± 0.446
PEG-PLLA	26	0.171 ± 0.066
PDLLA	5.0	0.141 ± 0.039

Differential scanning calorimetry (DSC) was performed on the electrospun PLLA fibers (Figure 3.3.3) and the electrospun PEG-PLLA fibers (Figure 3.3.4) to determine if their respective polymers displayed any level of crystallinity that had been induced during the electrospinning process. The glass transition temperature (T_g) for each sample was taken as the temperature at which the physical aging peak of the sample reached a maximum. The PEG present in the diblock copolymer depressed its T_g, resulting in a lower T_g for PEG-PLLA (59 °C) relative to PLLA alone (67 °C). Likewise, PEG also depressed the melting temperature (T_m) of the copolymer, evident by the T_m of PLLA at 180 °C and the T_m of PEG-PLLA at 159 °C. These values indicate that the PLLA fibers had a slightly larger window for crystallization (the difference between T_m and T_g) than the PEG-PLLA (i.e. 111 °C vs. 100 °C). For both the PLLA and the PEG-PLLA materials, the areas of their crystallization peaks are smaller than their melting peak areas (Table 3.3.3), indicating that they possessed some crystallinity before DSC was performed and that both of the polymers crystallized to some degree during electrospinning. GPC results for the PEG-PLLA indicated a M_n of 10,500 g/mol, which includes a 2000 g/mol PEG block, resulting in 81 wt% PLLA in the diblock copolymer sample. When the difference between the melting peak area (ΔH_f) and the crystallization peak area (ΔH_c) for the PEG-PLLA material was corrected to account for the weight percent of PLLA, $\Delta H_f - \Delta H_c$ for the PLLA blocks of the PEG-PLLA material was 11,783 μW·°C/g PLLA compared to 9082 μW·°C/g PLLA for the PLLA material. These data show that there was 29.7% more crystallinity per gram of PLLA in the electrospun PEG-PLLA material compared to the electrospun PLLA material. This disparity may be attributed to the differences in molecular weight (M_n) of the PLLA (39,800 g/mol) and the PEG-PLLA (10,500 g/mol) materials because low molecular weight polymers may crystallize more easily than polymers with much higher molecular weights.

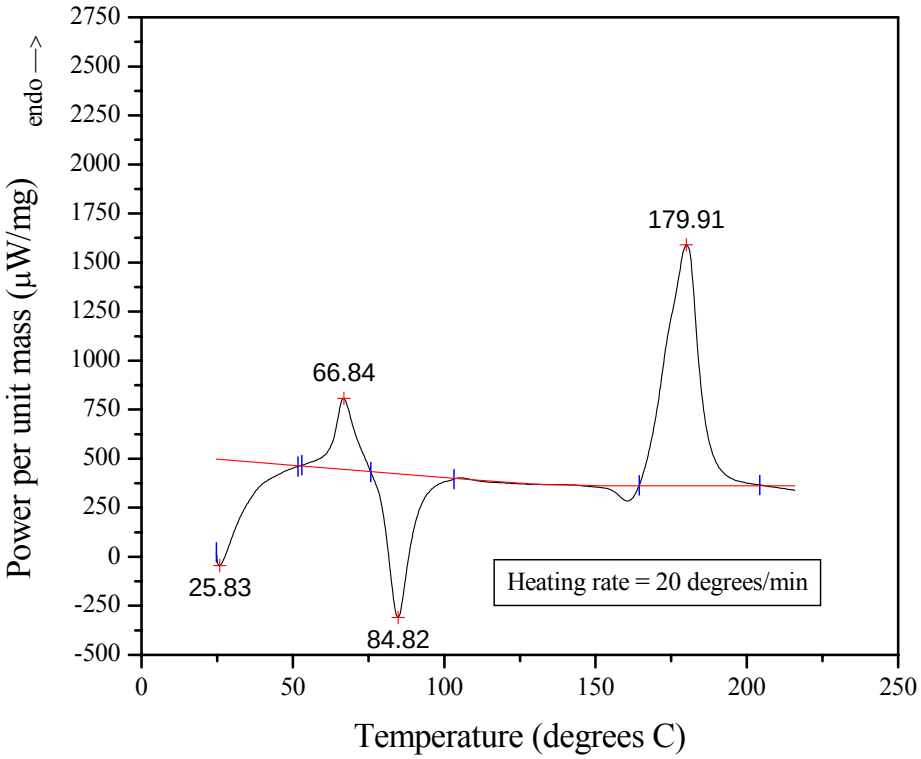

Figure 3.3.3 DSC curve of electrospun PLLA

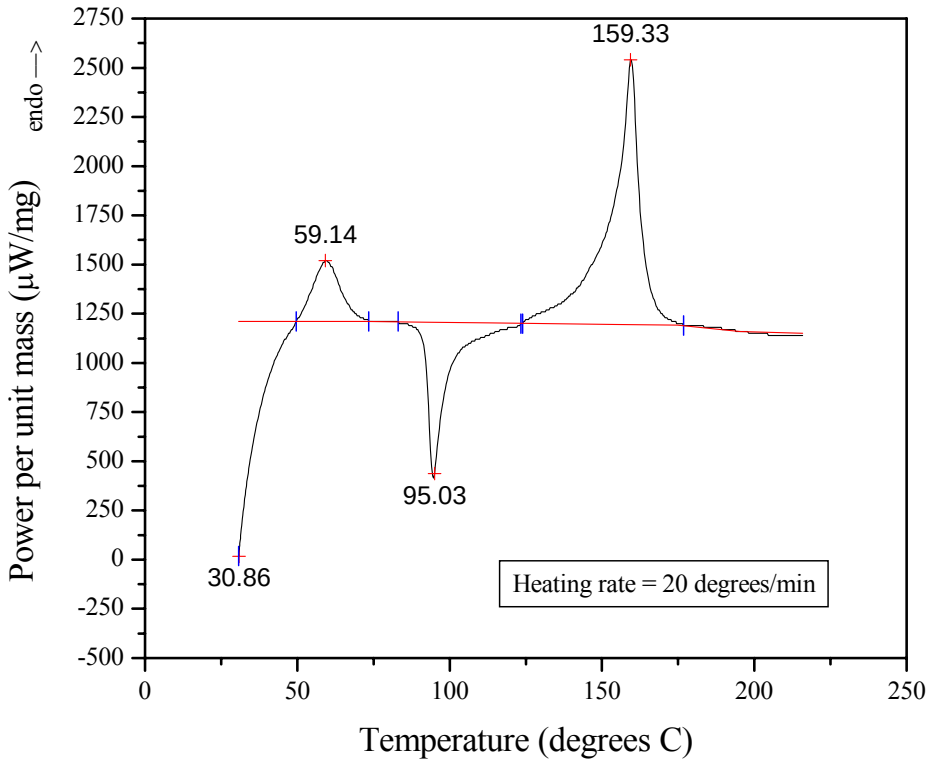

Figure 3.3.4 DSC curve of electrospun PEG-PLLA

Table 3.3.3 Integration values for peaks from PLLA and PEG-PLLA DSC curves

Sample	Total Peak Areas (μW·°C/mg)		Difference between peaks ($\Delta H_f - \Delta H_c$)/g sample	Wt% PLLA	Corrected difference between peaks ($\Delta H_f - \Delta H_c$)/g PLLA
	Crystallization (ΔH_c)/g sample	Melting (ΔH_f)/g sample			
PLLA	6586	15668	9082	100	9082
PEG-PLLA	6114	15658	9544	81	11,783

3.3.3 Electrospinning Different PDLLA Fiber Diameters

In an effort to obtain electrospun PDLLA fibers with significantly different diameters, a series of PDLLA in HFIP solutions were created and electrospun. Solution concentration was decreased below 15 wt% in an attempt to electrospin fibers at least half an order of magnitude smaller than 2.14 ± 0.35 μm. A 7.5 wt% PDLLA solution was electrospun at three different voltages (Table 3.2.2), but phase contrast light microscopy indicated the resultant fibers were of the same order of magnitude as the 15 wt% fibers. A 5.0 wt% PDLLA in HFIP was electrospun at the same conditions as the 15 wt% solution and fibers of 0.141 ± 0.039 μm were obtained (Table 3.3.2). Phase contrast light microscopy revealed bright spots periodically along the fibers, suggesting that lower solution concentrations may electrospin into fibers possessing "pearls on a string" morphology. Zong et al. [28] demonstrated that inconsistencies in fiber structure such as beads along the fiber can be caused by polymer concentrations that are too low and voltages that are too high to maintain a consistent fiber morphology. Based on my results and the observations of Zong et al., I felt that polymer concentrations below 5.0 wt% would not produce useful fiber scaffolds.

Solution concentration was increased above 15 wt% in an attempt to electrospin fibers at least half an order of magnitude larger than 2.14 ± 0.35 μm. A solution of 30 wt% PDLLA in HFIP was electrospun at two separate voltages to create large fibers, but the fibers obtained were

so thick that the fiber instability – the whip-like motion of the ejected fiber during spinning that leads to the distribution of randomly-oriented fibers on the target [109] – was diminished significantly. Consequently, the syringe pump had to be repeatedly slid back and forth parallel to the target screen so that the electrospun fiber would overlap the coverslips instead of continuously depositing in the same location. Less than half of the total surface area of the coverslips was covered after over 2.5 hours. In addition, the viscous polymer solution caused the syringe needle to repeatedly detach during electrospinning. Consequently, despite the approximate 10-20 μm fiber diameter obtained, the process of fabricating scaffolds with fibers of this size was considered impractical and a less concentrated solution (25 wt%) was tried instead. The 25 wt% PDLLA in HFIP solution was electrospun at two different voltages, each at a different distance (Table 3.2.2), but neither set of conditions was conducive to achieving sufficiently consistent fiber deposition on the coverslips even with moving the syringe pump. At one point multiple polymer jets were observed emanating from the syringe tip, but the distribution of polymer across the coverslips was poor. Phase contrast light microscopy indicated the fibers were roughly 6 μm in diameter, but fabricating them into scaffolds was not feasible. As a result of these poor initial results, efforts to create large diameter fibers were abandoned.

3.4 Conclusions

In this study, spinning parameters were identified and scaffolds were formed from PEG-PLLA, PEG-PLLA, PLLA, and PDLLA with various fiber diameters. Concentrations of 21 to 38 wt% PDLLA in DMF resulted in fiber diameters of 0.20 to 0.31 μm, but no systematic trend was observed, possibly because of the effects of varied flowrate and voltage. When polymers in HFIP were electrospun, fiber diameter increased with solution concentration and molecular

weight. Both PLLA and PEG-PLLA crystallized to some degree during electrospinning, with the PEG-PLLA material crystallizing 29.7% more per gram of PLLA than the PLLA material. PDLLA in HFIP solutions with concentrations ranging from 5.0 to 30 wt% were electrospun into fibers whose diameters increased with concentration. Only solutions between 5.0 and 15 wt % were successfully electrospun into fiber scaffolds suitable for tissue engineering applications. Efforts to electrospin at higher concentrations to obtain PDLLA fibers statistically larger than those from a 15 wt% solution demonstrated it was possible, but impractical. This study demonstrated that polymer, solvent, and solution characteristics influence electrospinning ability and fiber diameter.

Chapter 4 Cell Culture on Electrospun Polymer Scaffolds

4.1 Introduction

The name "contact guidance" has been given to the phenomenon in which topographical features of biomaterial interfaces influence cell adhesion, morphology, and function. [26] Topographical features in the range of 1 to 5 μm have been reported to increase cell attachment and spreading in many cell types [26]. Specifically, increases in groove depth [165] and ridge width (below 4 μm) [166] increase attachment and orientation, as demonstrated in studies using surfaces with parallel grooves. Therefore, I hypothesize that manipulating scaffold topography by varying fiber diameter will alter cell adhesion, proliferation, and potentially phenotypic behavior. The objective of this research was to identify systematic behavioral differences in cell response to surface topography as fiber diameter is varied from 0.1 to 10 μm. To test this two sets of studies were performed. In the first study MC3T3-El osteoblastic cells were cultured onto electrospun tissue scaffolds fabricated from poly(D,L-lactide) (PDLLA), poly(L-lactide) (PLLA), and poly(ethylene glycol-*b*-lactide) diblock copolymers (i.e. PEG-PDLLA and PEG-PLLA). Fluorescent staining was used to assess cell morphology on the substrates and to confirm the integrity of the electrospun fibers in cell culture. Cell number for MC3T3-E1 cells in a primitive, proliferative state was measured on electrospun scaffolds of the four different polymers and compared to spincoated PDLLA and PEG-PDLLA controls. In the second study, MC3T3-E1 cells were cultured on electrospun PDLLA scaffolds of two different fiber diameters and the cells were induced to differentiate. Cell number and alkaline phosphatase activity were measured.

4.2 Materials and Methods

4.2.1 Materials

Materials were obtained from Sigma-Aldrich (St. Louis, MO) unless otherwise specified. Phosphate-buffered saline (PBS), trypsin/EDTA (ethylenediamine tetraacetic acid), and minimum essential medium alpha modification (αMEM) were purchased from Invitrogen (Gaithersburg, MD). Fetal bovine serum (FBS; Gemini Bioproducts, Calabasas, CA) and antibiotic/antimycotic (penicillin, streptomycin, neomycin, fungizone; Invitrogen) were used as received. L-ascorbic acid 2-phosphate and β-glycerolphosphate were used as received. Fibronectin (in 0.05M Tris buffered saline, pH 7.5) was diluted with PBS to a working concentration of 1 μg/mL before use. Ethylenediamine tetraacetic acid (EDTA), potassium phosphate, bisbenzimide (Hoechst 33258 dye), Trizma® hydrochloride (Tris), sodium chloride, glycine, and Triton X-100 were used as received. Protease inhibitors aproptinin, leupeptin, and pepstatin were purchased from Calbiochem (La Jolla, CA). Alkaline phosphatase (ALP) reagent (17 mM *p*-nitrophenyl phosphate, 4 mM magnesium with buffer, pH 10.2 ± 0.2) was purchased from BioTron Diagnostics, Inc. (Hemet, CA). Monoclonal anti-human vinculin (hVIN-1) antibody, FITC conjugated goat anti-mouse antibody, 1,1'-Dioctadecyl-3,3,3',3'-tetramethylindocarbocyanine perchlorate (DiI; $DiIC_{18}(3)$), Calcein-AM, and blocking buffer solution were obtained from Molecular Probes (Eugene, OR) and used as received. *N*,*N*-Dimethylformamide (DMF; EM Science, Gibbstown, NJ) was used as received.

4.2.2 Substrate preparation

Substrates were formed as described in sections 3.2.3 and 3.2.4. Control surfaces were prepared by spincoating as described in sections 3.2.3.1 and 3.2.4.1. Scaffolds were prepared by

electrospinning PLLA, PDLLA, PEG-PLLA, and PEG-PDLLA onto spincoated surfaces as described in sections 3.2.3.2 and 3.2.4.2. Resultant fiber diameters for electrospun scaffolds are listed in Table 3.3.2. Electrospun and control substrates were placed into 12-well plates (Fisher) and sterilized under ultraviolet light overnight. Substrates were incubated with 1 mL of 1 μg/mL fibronectin for 1 h to promote cell adhesion and rinsed twice with PBS before seeding.

4.2.3 Cell culture

Cell studies were performed with a mouse calvaria-derived osteoprogenitor cell line (MC3T3-E1) donated by Dr. A. J. García (Georgia Institute of Technology). Cells were grown in culture medium (αMEM with 10% FBS and 1% antibiotic/antimycotic) and used at passages below 21. A quantity of 5×10^4 cells in 2 mL of culture medium was added into each well. In the first study, only culture medium was used and cells remained in a primitive, proliferative state without any alkaline phosphatase (ALP) activity. Cells were allowed to grow for 3, 7, and 14 days, and then substrates were analyzed for cell number. Culture medium was changed on days 3, 7, and 10. In the second study, cells were seeded onto the PDLLA fibers of different diameters and maintained in culture medium supplemented with L-ascorbic acid 2-phosphate (37.5 μg/mL) and β-glycerolphosphate (2 mM). This medium transformed them to a more mature state in which there are capable of differentiating. Cells were allowed to grow for 3, 7, and 14 days, and then substrates were analyzed for cell number and alkaline phosphatase activity. Culture medium was changed on days 3, 7, and 10.

4.2.4 Cell number

Fluorometric analysis of DNA content was used to determine the total number of cells on each substrate [157, 169]. Substrates were rinsed twice with PBS and cells were lifted

mechanically with cell scrapers (Fisher). Two 0.5-mL aliquots of 10 mM EDTA (pH 12.3) pipetted into each well were collected into corresponding 1.5-mL microcentrifuge caps. Caps were vortexed and stored at -70 °C until analysis. Prior to analysis, samples were thawed, sonicated on ice for 10 min, and 0.2 mL of 1 M KH_2PO_4 was added to neutralize pH. DNA standards (1 mL each) were created by adding known volumes of DNA solution (0-140 μL) of a 50 μg/mL DNA solution to varying volumes of EDTA (pH 12.3) (50 μg/mL corresponds to an absorbance of 1.00 through a path of 1 cm at 260 nm). These standards were sonicated on ice for 10 min and 0.2 mL of 1 M KH_2PO_4 was added. Aliquots of 0.4 mL DNA standard or homogenized supernatant were combined with 1.6 mL of a 100 ng/mL solution of Hoechst 33258 dye in 100 mM NaCl and 10 mM Tris buffer to perform fluorescence measurements. Measurements were made in duplicate with a DyNAQuant 200 (Hoefer, San Francisco, CA). A linear relationship between fluorescence and the concentrations of the DNA standards was used to calculate DNA concentrations. Cell number was calculated using a conversion factor of 9.1 pg DNA/cell (determined experimentally).

4.2.5 Alkaline phosphatase (ALP) activity

The hydrolysis of *p*-nitrophenyl phosphate was used to assay ALP activity, an early indicator of osteoblastic phenotype. Substrates were rinsed twice with PBS and cells were lifted mechanically with cell scrapers (Fisher). Two 0.5-mL aliquots of 1% protease inhibitors (0.2 mg/mL aproptinin, 0.2 mg/mL leupeptin, 0.1 mg/mL pepstatin in TG solution [50 mM Tris, 100 mM glycine, pH 10.5]) in TGT solution (50 mM Tris, 100 mM glycine, and 0.1% Triton X-100, pH 10.5) were added to each well and collected into 1.5-mL microcentrifuge caps [161, 170]. Caps were vortexed and stored at -70 °C until analysis. Prior to analysis, samples were thawed and sonicated in a bath sonicator for 10 min. For each sample, a 200 μL volume was combined

with 1 mL of ALP reagent equilibrated at 30 °C. A Genesis 5 spectrophotometer (Spectronic Instruments, Rochester, NY) was used to measure absorbance at 405 nm at one minute intervals for four minutes. Activity was calculated using the slope of absorbance versus time and normalized by cell number.

4.2.6 Fluorescence microscopy

Fluorescent staining was used to determine whether the copolymer electrospun fibers persist throughout two weeks of cell culture. $DiIC_{18}(3)$ was added to the PEG-PDLLA and PEG-PLLA electrospinning solutions (but not the spincoating solutions) at a concentration of 1 μg/mL prior to electrospinning. Fluorescence images of the fibers were obtained at 3, 7, and 14 days in cell culture.

Immunofluorescent staining was performed to visualize focal adhesion plaques and to determine cell morphology. $DiIC_{18}(3)$ was added to the PDLLA in DMF electrospinning solutions at a concentration of 1 μg/mL prior to electrospinning. Electrospun substrates were placed into 12-well plates (Fisher) and sterilized under ultraviolet light for 2 h. Aspirated substrates were incubated with 300 μL of 1 μg/mL fibronectin for 1 h to promote cell adhesion and rinsed twice with PBS before seeding. A quantity of 5×10^4 cells in 2 mL of culture medium was added into each well, and allowed to attach for 18 h at 37 °C. Half of the seeded substrates were stained with Calcein-AM to determine cell morphology, and half were immunofluorescently stained with an antibody against vinculin to visualize focal adhesion contacts. To stain for vinculin, cells were fixed in formalin for 10 min at room temperature and then rinsed twice with PBS. Blocking buffer (1 mL) was added and substrates were incubated at room temperature for 1.5 h. Following aspiration, the substrates were incubated for 45 min at room temperature with 0.5 mL of a 1:100 dilution of hVIN-1 in blocking buffer solution, and

then rinsed three times with PBS. Each of these substrates was incubated for 15 min at room temperature with 0.5 mL of a 1:20 dilution of FITC conjugated antibody in PBS, and then rinsed three times with PBS. To determine cell morphology, culture medium was replaced with fresh growth medium containing a 1:500 dilution of Calcein-AM stock solution. Substrates were incubated at 37 °C for 30 min before each was rinsed three times with PBS.

All fluorescence microscopy images of the fibers or cells on the fibers were obtained using a Hamamatsu camera (I-Cube, Crofton, MD) mounted on an Olympus IX50 inverted microscope (Opelco, Sterling, VA) with a 60X objective and a Prior motorized stage. Fluorescence images of calcein-labeled cells or FITC-labeled focal adhesion plaques were separately acquired using a wide blue filter cube, and images of DiI stained fibers were acquired using a wide green filter cube.

4.2.7 Contact angles

A Ramé-Hart goniometer (model 100-06, Mountain Lakes, NJ) was used to measure static contact angles. Substrates were clean glass microscope coverslips spincoated with 3.6 wt % solutions of PDLLA, PLLA, PEG-PDLLA, or PEG-PLLA. For each polymer, contact angles of 3-μL drops of deionized water were measured at four locations on each of two substrates. One pair of each of the copolymer substrates was immersed in deionized water for 24 hours then dried with nitrogen before contact angles were measured.

4.2.8 Statistics

Values are presented as mean ± standard deviation. Statistical analyses were performed using Origin® 6.1 (OriginLab, Northampton, MA). A one-way analysis of variance (ANOVA)

procedure with a significance level (α) of 0.05 was used to determine significant differences between groups.

4.3 Results

4.3.1 Coverslip preparation

The chemistry of the polymers spincoated onto the coverslips and the environmental conditions during electrospinning proved to be important considerations during substrate preparation. When spincoated directly onto the cleaned coverslip, the diblock copolymers (PEG-PLLA and PEG-PDLLA) were observed to gradually lift off the coverslip over time in culture, but the homopolymers remained on the coverslips. Consequently, the PEG-PDLLA spincoated controls were fabricated by spincoating PEG-PDLLA onto coverslips already spincoated with PDLLA. This process prevented the diblock copolymer from lifting off the coverslip in culture. Spincoated coverslips fabricated on rainy days, however, tended to delaminate in culture over two weeks regardless of the polymer(s) used. As a result, a concerted effort was made to only spincoat coverslips on days with low humidity.

4.3.2 Substrate sterilization/Fluorescence microscopy

Ultraviolet (UV) light sterilized coverslip samples of electrospun polymer were seeded with MC3T3-E1 cells and cultured for two weeks. (Initially, electrospun substrates were each sterilized with 1 mL ethanol for one hour, but fluorescent microscopy indicated that sterilization by ethanol dissolved the fibers. Consequently, electrospun substrates were sterilized by UV light for at least two hours as recommended by Fischbach et al. [171].) Calcein-AM staining of cells on these substrates indicated that cells on electrospun surfaces extended along fibers (Fig. 4.3.1) but had reduced projected cell area relative to smooth surfaces (not shown). Fluorescence

images of FITC-stained focal adhesion plaques revealed significant non-specific fluorescence (not shown), resulting in pictures very similar to the calcein-AM stain pictures. Only two hours of UV light exposure proved to be an insufficient length of sterilization time, however, because the majority of the culture wells became contaminated after several days.

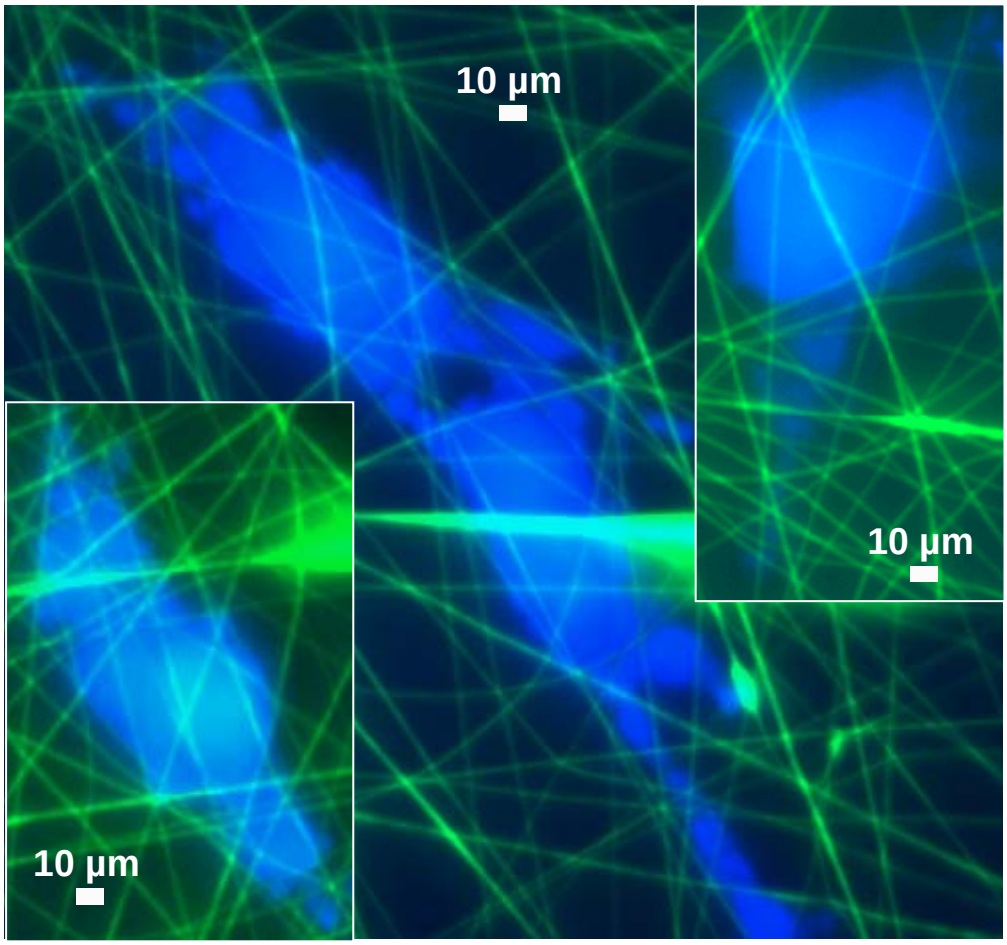

Figure 4.3.1 Fluorescence microscopy images of Calcein-AM stained live cells on fibers electrospun from 21.4% PDLLA in DMF.

Ultimately, UV sterilization overnight (at least 8 hours) resulted in sufficient sterility without degrading the electrospun fibers. Fluorescent micrographs of the two copolymer samples in culture confirmed that their fibers maintained their structure without degrading over 14 days (Fig. 4.3.2). It is expected that the homopolymers also should persist over 14 days in culture because they formed larger fibers.

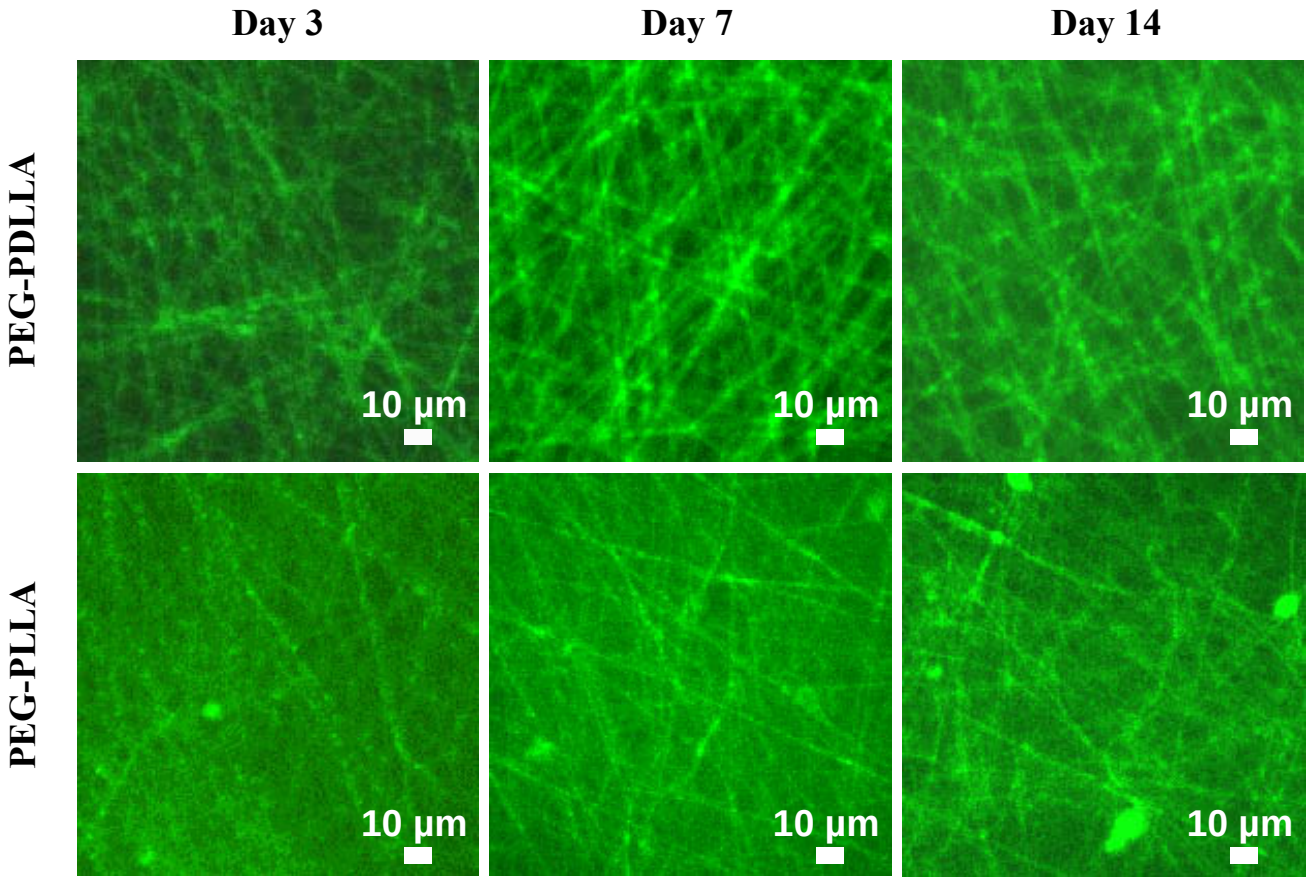

Figure 4.3.2 Fluorescence micrographs of fibers after 3, 7, and 14 days in cell culture. PEG-PDLLA fiber diameter is 0.889 ± 0.446 µm, and PEG-PLLA fiber diameter is 0.171 ± 0.066 µm.

4.3.3 First cell culture study: Cell density on homopolymer and copolymer substrates

To assess how each surface affects cell proliferation, cell density on each substrate was determined at 3, 7 and 14 days after seeding (Fig. 4.3.3). In this study cells were maintained in regular growth medium, which allows the cells to proliferate but does not induce osteoblastic maturation. The results indicate that cells proliferate on all electrospun and spincoated polymer surfaces. At 14 days, cell density on the spincoated control surfaces was comparable to that on tissue culture polystyrene (TCPS). A significant difference in density between the PDLLA spincoated surfaces and the electrospun surfaces of similar chemical composition (PDLLA and

PLLA) was observed at both days 7 and 14. In addition, the electrospun homopolymer and copolymer scaffolds comprised of PDLLA supported higher cell densities than their PLLA-containing counterparts. Because the PDLLA-containing fibers were larger in diameter than their PLLA-containing counterparts, the differences in cell density is likely an effect of fiber diameter.

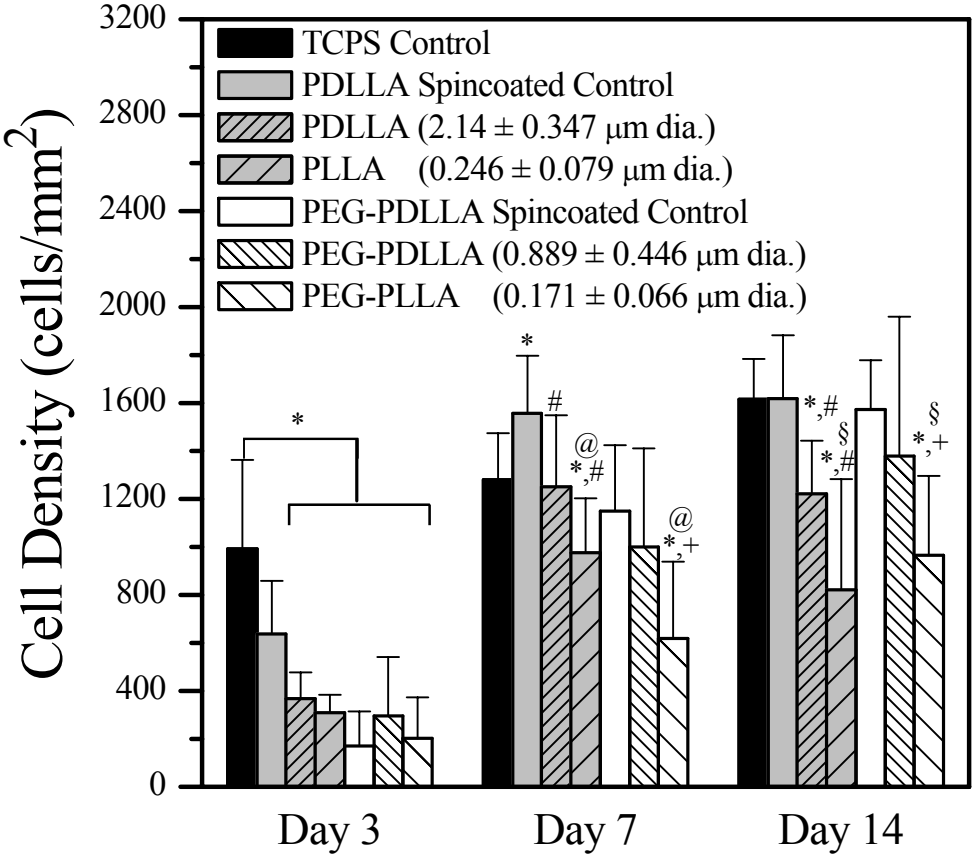

*Figure 4.3.3 Cell number on electrospun polymer fibers, spincoated controls, and TCPS controls as a function of culture duration. n=8, except TCPS n=4; error bars correspond to the standard deviation. * denotes significant difference from TCPS; # denotes significant difference from spincoated PDLLA control; + denotes significant difference from spincoated PEG-PDLLA control; @ denotes significant difference from electrospun PDLLA; § denotes significant difference from electrospun PEG-PDLLA.*

4.3.4 Contact angle measurements

Contact angle measurements were performed on coverslips spincoated with each polymer (Table 4.3.1) to determine if differences in surface chemistry might contribute to measured differences in cell density on the four electrospun materials. Advancing water contact angles were similar for PDLLA and PEG-PDLLA polymers, and similar for PLLA and PEG-PLLA polymers. Contact angles between PDLLA-containing polymers and their PLLA-containing counterparts were moderately, but statistically different. However, following immersion in water for 24 hrs, contact angles were similar among the four materials.

Table 4.3.1 Water contact angles on spincoated polymer films. Mean ± standard deviation for n=8.

Spincoated Surface	**Contact Angle (degrees) Before Hydration**	**Contact Angle (degrees) After Hydration**
PDLLA	63 ± 2	66 ± 2
PLLA	71 ± 5	66 ± 1
PEG-PDLLA	66 ± 3	66 ± 4
PEG-PLLA	70 ± 3	65 ± 1

4.3.5 Second cell culture study: PDLLA fiber diameter study

In the second culture study, electrospun PDLLA substrates were formed with two different fiber diameters (2.14 and 0.14 μm) and MC3T3-E1 cells were cultured on these surfaces to determine how fiber diameter affects osteoblastic differentiation (Fig. 4.3.4). In this study cells were maintained in culture medium containing L-ascorbic acid 2-phosphate and β-glycerolphosphate to stimulate synthesis of an extracellular matrix and osteoblastic differentiation. The results indicate that at day 3 cell densities on spincoated controls and both electrospun fiber sizes was significantly less than on the TCPS controls. Also on day 3, the cell densities for both electrospun surfaces were significantly lower than that on the spincoated

control. By day 7, the four different groups were not statistically different, but by day 14, the mean cell densities of both electrospun fiber samples were significantly larger than the TCPS controls. In addition, on day 14 the cell density for the largest diameter fibers was significantly larger than that of the PDLLA spincoated controls. However, cell density on the 2.14 μm PDLLA fibers was not statistically different from the density on the 0.14 μm PDLLA fibers.

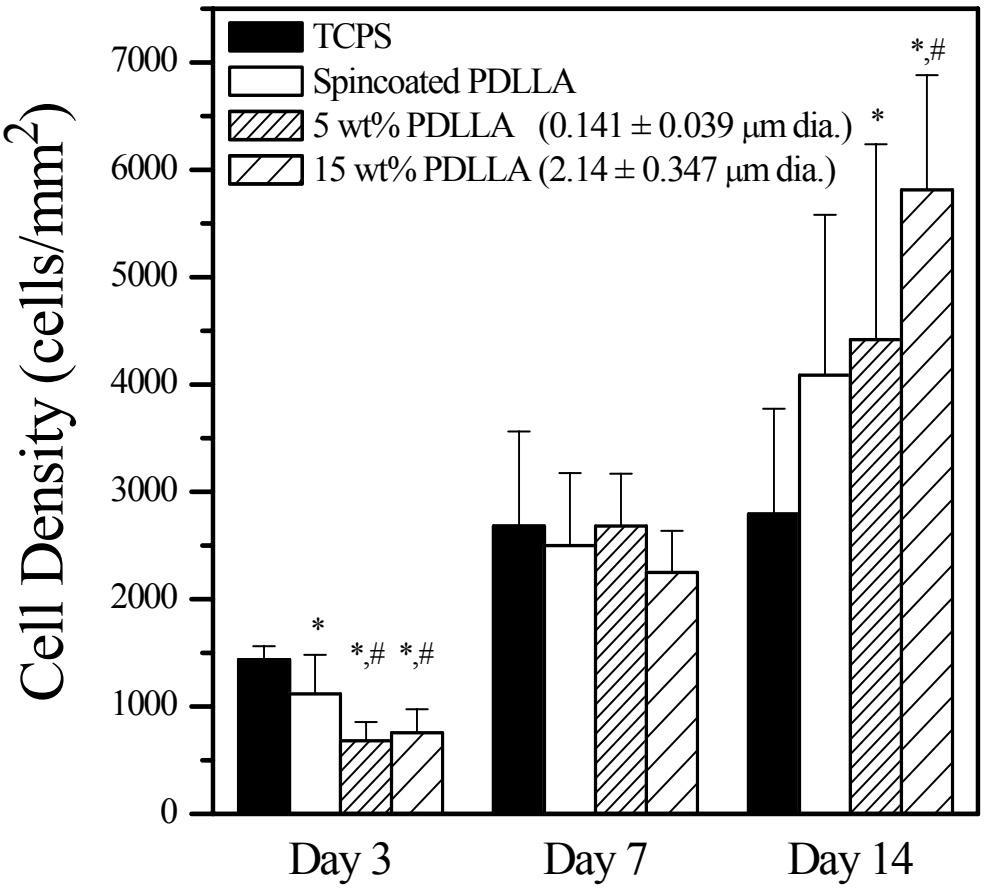

*Figure 4.3.4 Cell number on the electrospun PDLLA polymer fibers, spincoated controls, and TCPS controls over 14 days. n=8. Error bars correspond to the standard deviation. * denotes significant difference from TCPS; # denotes significant difference from spincoated PDLLA control.*

Measurements of ALP activity were performed at days 7 and 14 to characterize the effect of fiber diameter on osteoblastic differentiation. Although ALP activity was not detectable on all substrates at day 7 (not shown), activities were measured for all conditions at day 14 (Fig. 4.3.5).

These measurements reveal comparable activities for all three PDLLA substrates. In addition, they were statistically lower than ALP activity for cells grown on TCPS surfaces.

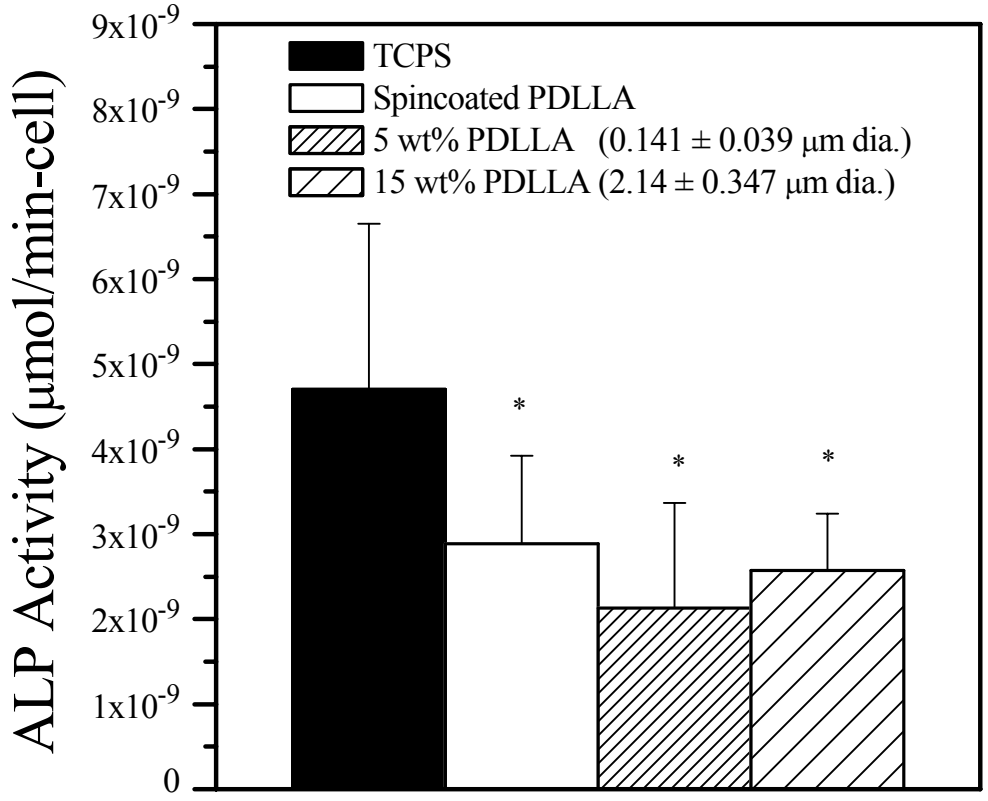

*Figure 4.3.5 ALP activity of cells on the electrospun polymer fibers, spincoated controls, and TCPS controls for 14 days. n=8. Error bars correspond to the standard deviation. * denotes significant difference from TCPS.*

4.4 Discussion

4.4.1 Cell density assays

The results of several groups indicate that various cell types preferentially adhere to microgrooved surfaces [165, 166, 172], roughened surfaces [63], textured surfaces [173], and electrospun fibers [112] all within the same size range as the fibers in this study. Britland et al. cultured nerve cells on periodic ridges separated by 25-μm grooves of varying depth with laminin chemically bound to the groove surfaces in tracks parallel or orthogonal to the grooves

[165]. As the depth of the grooves increased past 1 μm, the neurites aligned themselves more with the topographical groove patterns and less with the chemical patterns [165]. Jansen and coworkers determined that only the width of ridges in microgrooved surfaces, not groove width or depth, affected the size, shape, and orientation of rat dermal fibroblasts incubated on the surfaces [166]. They also observed attachment of the lamellapodia of osteoblasts cultured on grooved surfaces with 1 and 2 μm-wide ridges [172], which are the same order of magnitude in size as the PEG-PDLLA and PDLLA fibers, respectively. Lampin et al. observed that vascular and corneal cells cultured on PMMA secrete thicker extracellular matrices and adhere more as surface roughness increased, showing that increases in surface roughness lead to increases in cell adhesion [63]. Mata et al. observed that osteoblast-like cells sense and adhere to textured surfaces, with optimal adhesion on textures with maximum depths ranging from 500 nm to 2 μm [173]. Li et al. demonstrated that human bone-marrow-derived mesenchymal stem cells (hMSCs) attach to and proliferate on electrospun scaffolds of PLGA with fiber diameters between 500 and 800 nm [112]. In addition, it is plausible that topographies that influence cell attachment will also influence cell proliferation since attachment is a prerequisite for proliferation.

The cell density data, in addition to the contact angle measurements, suggest that cell number increases with an increase in fiber diameter. This would agree with evidence that cell attachment (required for proliferation) and orientation increase with substrate groove depth [165]. An increase in cell number with fiber diameter was not only observed for cells in a proliferative state (Fig. 4.3.3), but also observed for cells in a more mature differentiating state seeded on different sized PDLLA fibers (Fig. 4.3.4). It is important to note that the cells cultured on the electrospun fibers in this second study proliferated more than the cells cultured on the

TCPS controls. This is opposite to the results in Figure 4.3.3, and is likely due to the presence of L-ascorbic acid 2-phosphate and β-glycerolphosphate in the latter study. These compounds stimulate collagen deposition and osteoblastic maturation [155], which could significantly alter cell interaction with the fiber substrates. The significant difference in cell density between the 15 wt% PDLLA fibers and the spincoated PDLLA control, but not the 5.0 wt% PDLLA fibers and the spincoated PDLLA control may be a result of cell infiltration into the fibers. Cells have been observed to migrate into the interior of electrospun scaffolds [117], resulting in higher cell density for a scaffold. Because the vertical gap between fibers should increase with fiber diameter, one would expect that cell infiltration would increase with increasing fiber diameter. However, below a certain fiber diameter one would expect the gap to be too small to permit cell infiltration, and cell density would be similar to that on smooth surfaces.

4.4.2 Contact angle measurements

The statistical difference between the contact angle measurements of the PDLLA-containing polymers and their PLLA-containing counterparts suggests a difference in the hydrophilicity of the polymer surfaces. This is important because significant increases in surface hydrophilicity may reduce cell attachment and consequently cell proliferation [63]. Given the similarity in contact angles once the polymers became wetted, I hypothesize that differences in cell proliferation (Figure 4.3.3) were more a consequence of differences in fiber diameter than of surface chemistry.

4.4.3 ALP activity assays

No significant differences in ALP activity were observed with changes in surface topography (i.e. fiber diameter). Previous work has shown a decrease in ALP activity with

roughness [174, 175], but an increase on regularly textured surfaces [174, 175]. Martin et al. [174] observed a general decrease in ALP activity of osteoblast-like cells as surface roughness increased, but this trend was not universal for all of the roughened substrate types tested . Rosa et al. [175] reported a decrease in ALP activity of rat bone marrow cells cultured on irregularly textured hydroxyapatite (HA), but an increase in ALP activity of the same cells cultured on more regularly textured HA with no more than 15% microporosity. These studies along with the results in Figure 4.3.5 suggest that while surface topography may have some effect on cellular differentiation, surface chemistry may have a greater effect on differentiation than surface topography.

The hypothesis that surface chemistry influences differentiation is supported by previous studies [176, 177]. Bruinink and Wintermantel [176] observed an increase in the ALP activity of primary adult rat bone marrow cells when cultured on TCPS treated with sulfuric acid compared to untreated TCPS. Liao et al. [177] concluded that differentiation of rat calvaria osteoblasts (as evidenced by ALP activity) is more likely to occur on hydrophilic silicone surfaces than hydrophobic silicone surfaces.

4.5 Conclusions

Diblock copolymers of PEG-PDLLA and PEG-PLLA were compared with PDLLA and PLLA for their ability to act as cell-supporting electrospun fiber scaffolds for osteoblastic cells. Fluorescence microscopy revealed that electrospun fiber scaffolds limit cell spreading and that cells primarily extended along the fibers. In addition, these scaffolds persisted in cell culture for two weeks and analysis of the cells cultured over 14 days revealed that cell density increases with fiber diameter. L-ascorbic acid 2-phosphate and β-glycerolphosphate were demonstrated to

have a significant positive effect on cell density. In contrast to cell density, ALP activity, an indicator of osteoblastic differentiation, was unaffected by fiber diameter.

Chapter 5 Conclusions and Future Work

5.1 Conclusions

The overall goal of this research was to evaluate resorbable biocompatible electrospun scaffolds as supports for tissue engineering. To accomplish this, PEG-PLLA and PEG-PDLLA diblock copolymers were synthesized with target molecular weights of 42,000 g/mol. Next these two polymers and commercially available PLLA and PDLLA were electrospun to form scaffolds with fibers of diameters 0.14 to 2.1 μm. Finally, cell culture studies were performed to characterize cell morphology, proliferation, and osteoblastic differentiation.

A number of important conclusions can be drawn from the results of the research described in chapters two through four. The use of monomethylether PEG to initiate a ring-opening polymerization of D,L-lactide monomer with stannous octoate catalyst was found to be a viable method for synthesizing PEG-PDLLA diblock copolymers with target molecular weights of 42,000 g/mol (PEG:2000, PDLLA:40,000). This method may also be practical for the synthesis of PEG-PLLA diblock copolymers using L-lactide if additional toluene is added to reduce the copolymer concentration during synthesis, preventing early precipitation of the product from the reaction solution. The use of dry toluene was an extremely effective way of reducing the amount of water present during the polymerization. A small amount of the PEG initiator may be difunctional as indicated by high molecular weight shoulders on the GPC peaks of each copolymer. Electrospinning parameters were identified and used to successfully form scaffolds from PEG-PLLA, PEG-PDLLA, PLLA, and PDLLA with various fiber diameters. When these polymers were electrospun from solution in HFIP while flowrate and voltage were held constant, fiber diameter increased with solution concentration and molecular weight. No systematic trend in diameter was observed when concentrations of 21 to 38 wt% PDLLA in

DMF were electrospun, possibly because of the effects of varied flowrate and voltage. Large diameter fibers were obtained with concentrated PDLLA in HFIP solutions, but scaffold fabrication was impractical with solution concentrations of 25 wt% or higher. Polymer, solvent, and solution characteristics were demonstrated to influence electrospinning ability and fiber diameter. Diblock copolymers of PEG-PDLLA and PEG-PLLA were compared with PDLLA and PLLA for their ability to act as cell-supporting electrospun fiber scaffolds for osteoblastic cells. Fluorescence microscopy revealed that electrospun fiber scaffolds limit cell spreading and that cells primarily extended along the fibers. In addition, these scaffolds persisted in cell culture for two weeks and analysis of the cells cultured over 14 days revealed that cell density increases with fiber diameter. L-ascorbic acid 2-phosphate and β-glycerolphosphate were demonstrated to have a significant positive effect on cell density. In contrast to cell density, ALP activity, an indicator of osteoblastic differentiation, was unaffected by fiber diameter.

5.2 Future work

Natural extensions of the work presented here could involve 1) expanding the breadth of materials and conditions that are examined, and 2) applying the materials to bone tissue engineering. With regard the first point, more syntheses, electrospinning, and cell culture assays could be performed in the future to complement the work done on this project to date. More PEG-PLA diblock copolymers could be synthesized with varying ratios of PEG to PLA. This would allow a greater range of data to determine more precisely how surface chemistry (i.e. the amount of PEG copolymerized with PLA) affects cell behavior. The accuracy of the stoichiometric calculations for each copolymerization might be increased if the molecular weight of the PEG was determined by GPC in addition to ^{1}H NMR alone. With more time, a range of solution concentrations could be created from each of the polymers used in the initial cell culture

study. These solutions could then be electrospun into fiber scaffolds with a range of fiber diameters for each polymer. Cell culture studies performed on these scaffolds may help to confirm the effects of fiber diameter upon cell behavior independent of polymer chemistry. Fluorescence microscopy could be performed to quantitatively evaluate the effect of different fiber diameters on cell spreading. It would be of particular interest to perform ALP activity assays on cells cultured on PEG-PDLLA scaffolds with different fiber diameters. Results of these assays could be compared to the ALP activity data from the second cell culture study above on different PDLLA fiber diameters to test the hypothesis that osteoblastic differentiation is more influenced by surface chemistry than by surface topography. Future work on this project should also include additional assays for later markers of osteoblastic maturation (e.g. osteopontin, osteocalcin, and bonesialoprotein).

In terms of applying this work to bone tissue engineering, once the most successful combinations of polymer chemistry and fiber diameter are identified, electrospun fiber meshes with these attributes should be fabricated for in vitro and in vivo testing. Additional in vitro assays using bone marrow stromal cells from adult rats would be beneficial to perform to complement the data already obtained from the studies using MC3T3-E1 osteoblastic mouse cells. Finally, it would be desirable to perform in vivo testing by implanting seeded electrospun meshes into laboratory animals with critical sized bone defects. The ability of seeded electrospun meshes to heal critical sized defects in laboratory animals by developing into bone tissue is necessary before electrospun scaffolds are a viable tissue engineering option for humans.

References

[1] Holland SJ, Tighe BJ. Advances in Pharmaceutical Sciences. San Diego, CA: Academic; 1992. p. 101.

[2] Rehm KE. Clinical application of resorbable biomaterials in reconstructive surgery. In: Plank H, Dauner M, Renardy M, editors. Degradation Phenomena on Polymeric Biomaterials. New York: Springer-Verlag; 1992. p. 163-176.

[3] Yaszemski MJ, Payne RG, Hayes WC, Langer R, Mikos AG. Evolution of bone transplantation: molecular, cellular and tissue strategies to engineer human bone. Biomaterials 1996;17:175-185.

[4] Christel PS, Vert M, Chabot F, Abols Y, Leary JL. Polylactic acid for intramedullary plugging. In: P. D, editor. Biomaterials and Biomechanics. Amsterdam: Elsevier Science Publishers; 1983.

[5] Matsusue Y, Yamamuro T, Oka M, Shikinami Y, Hyon SH, Ikada Y. Invitro and invivo studies on bioabsorbable ultrahigh-strength poly(L-lactide) rods. J Biomed Mater Res 1992;26:1553-1567.

[6] Hakkarainen M, Albertsson AC, Karlsson S. Weight losses and molecular weight changes correlated with the evolution of hydroxyacids in simulated in vivo degradation of homo- and copolymers of PLA and PGA. Polymer Degradation and Stability 1996;52:283-291.

[7] Harris LD, Kim BS, Mooney DJ. Open pore biodegradable matrices formed with gas foaming. J Biomed Mater Res 1998;42:396-402.

[8] Hutmacher DW. Scaffold design and fabrication technologies for engineering tissues - state of the art and future perspectives. J Biomat Sci-Polym Ed 2001;12:107-124.

[9] Gogolewski S, Pennings AJ. An artificial skin based on biodegradable mixtures of polylactides and polyurethanes for full-thickness skin wound covering. Makromol. Chem. Rapid. Commun. 1983;4:675-680.

[10] Zoppi RA, Contant S, Duek EAR, Marques FR, Wada MLF, Nunes SP. Porous poly(L-lactide) films obtained by immersion precipitation process: morphology, phase separation and culture of VERO cells. Polymer 1999;40:3275-3289.

[11] Lo H, Kadiyala S, Guggino SE, Leong KW. Poly(L-lactic acid) foams with cell seeding and controlled-release capacity. J Biomed Mater Res 1996;30:475-484.

[12] Schugens C, Maquet V, Grandfils C, Jerome R, Teyssie P. Biodegradable and macroporous polylactide implants for cell transplantation .1. Preparation of macroporous polylactide supports by solid-liquid phase separation. Polymer 1996;37:1027-1038.

[13] Schugens C, Maquet V, Grandfils C, Jerome R, Teyssie P. Polylactide macroporous biodegradable implants for cell transplantation .2. Preparation of polylactide foams by liquid-liquid phase separation. J Biomed Mater Res 1996;30:449-461.

[14] Gutsche AT, Lo HN, Zurlo J, Yager J, Leong KW. Engineering of a sugar-derivatized porous network for hepatocyte culture. Biomaterials 1996;17:387-393.

[15] Whang K, Thomas CH, Healy KE, Nuber G. A novel method to fabricate bioabsorbable scaffolds. Polymer 1995;36:837-842.

[16] Coombes AGA, Heckman JD. Gel casting of resorbable polymers.1. Processing and applications. Biomaterials 1992;13:217-224.

[17] Hu YH, Grainger DW, Winn SR, Hollinger JO. Fabrication of poly(a-hydroxy acid) foam scaffolds using multiple solvent systems. J Biomed Mater Res 2002;59:563-572.

[18] Tsuji H, Smith R, Bonfield W, Ikada Y. Porous biodegradable polyesters. I. Preparation of porous poly(L-lactide) films by extraction of poly(ethylene oxide) from their blends. J Appl Polym Sci 2000;75:629-637.

[19] Wake MC, Gupta PK, Mikos AG. Fabrication of pliable biodegradable polymer foams to engineer soft tissues. Cell Transpl 1996;5:465-473.

[20] Mooney DJ, Baldwin DF, Suh NP, Vacanti LP, Langer R. Novel approach to fabricate porous sponges of poly(D,L-lactic-co-glycolic acid) without the use of organic solvents. Biomaterials 1996;17:1417-1422.

[21] Goldstein AS, Zhu GM, Morris GE, Meszlenyi RK, Mikos AG. Effect of osteoblastic culture conditions on the structure of poly(DL-lactic-co-glycolic acid) foam scaffolds. Tissue Eng 1999;5:421-433.

[22] Nam YS, Yoon JJ, Park TG. A novel fabrication method of macroporous biodegradable polymer scaffolds using gas foaming salt as a porogen additive. J Biomed Mater Res 2000;53:1-7.

[23] Cooke MN, Fisher JP, Dean D, Rimnac C, Mikos AG. Use of stereolithography to manufacture critical-sized 3D biodegradable scaffolds for bone ingrowth. Journal of Biomedical Materials Research Part B-Applied Biomaterials 2003;64B:65-69.

[24] Zein I, Hutmacher DW, Tan KC, Teoh SH. Fused deposition modeling of novel scaffold architectures for tissue engineering applications. Biomaterials 2002;23:1169-1185.

[25] Mikos AG, Bao Y, Cima LG, Ingber DE, Vacanti JP, Langer R. Preparation of poly(glycolic acid) bonded fiber structures for cell attachment and transplantation. J Biomed Mater Res 1993;27:183-189.

[26] Curtis A, Wilkinson C. New depths in cell behaviour: reactions of cells to nanotopography. Cell Behaviour: Control and Mechanism of Motility; 1999. p. 15-26.

[27] Doshi J, Reneker DH. Electrospinning process and applications of electrospun fibers. J Electrostat 1995;35:151-160.

[28] Zong XH, Kim K, Fang DF, Ran SF, Hsiao BS, Chu B. Structure and process relationship of electrospun bioabsorbable nanofiber membranes. Polymer 2002;43:4403-4412.

[29] Zeng J, Chen XS, Xu XY, Liang QZ, Bian XC, Yang LX, Jing XB. Ultrafine fibers electrospun from biodegradable polymers. J Appl Polym Sci 2003;89:1085-1092.

[30] Athanasiou KA, Niederauer GG, Agrawal CM. Sterilization, toxicity, biocompatibility and clinical applications of polylactic acid/ polyglycolic acid copolymers. Biomaterials 1996;17:93-102.

[31] Klompmaker J, Jansen HWB, Veth RPH, de Groot JH, Nijenhuis AJ, Pennings AJ. Porous polymer implant for repair of meniscal lesions: A preliminary study in dogs. Biomaterials 1991;12:810-816.

[32] Feng L, Andrade JD. Protein adsorption on low-temperature isotropic carbon: I. Protein conformational change probed by differential scanning calorimetry. J Biomed Mater Res 1994;28:735-743.

[33] Elbert DL, Hubbell JA. Surface treatments of polymers for biocompatibility. Polymers; Annual Review of Materials Science 1996;26:365-394.

[34] Koegler WS, Griffith LG. Osteoblast response to PLGA tissue engineering scaffolds with PEO modified surface chemistries and demonstration of patterned cell response. Biomaterials 2004;25:2819-2830.

[35] Lucke A, Tessmar J, Schnell E, Schmeer G, Göpferich A. Biodegradable poly(D,L-lactic acid)-poly(ethylene glycol)-monomethyl ether diblock copolymers: structures and surface properties relevant to their use as biomaterials. Biomaterials 2000;21:2361-2370.

[36] Södergård A, Stolt M. Properties of lactic acid based polymers and their correlation with composition. Progress in Polymer Science 2002;27:1123-1163.

[37] Kricheldorf HR. Syntheses and application of polylactides. Chemosphere 2001;43:49-54.

[38] Enomoto K, Ajioka M, Yamaguchi A. Polyhydroxycarboxylic acid and preparation process thereof. 1994, Mitsui Toatsu Chemicals, Incorporated: USA.

[39] Lewis DH. Controlled release of bioactive agents from lactide/glycolide polymers. In: Chasin M, Langer R, editors. Biodegradable Polymers as Drug Delivery Systems. New York: Marcel Dekker; 1990. p. 1-41.

[40] Chabot F, Vert M, Chapelle S, Granger P. Configurational structures of lactic acid stereocopolymers as determined by C-13-labeled (H-1)-NMR. Polymer 1983;24:53-59.

[41] Zhang X, McDonald M, Goosen FA, Auley KB. Mechanism of lactide polymerization in the presence of stannous octoate: The effect of hydroxy and carboxylic acid substances. J Polym Sci 1994;32:2965-2970.

[42] Tsuji H, Ikada Y. Crystallization from the melt of poly(lactide)s with different optical purities and their blends. Macromolecular Chemistry and Physics 1996;197:3483-3499.

[43] Kricheldorf HR, Kreisersaunders I. Polylactones.19. Anionic-polymerization of L-lactide in solution. Makromolekulare Chemie-Macromolecular Chemistry and Physics 1990;191:1057-1066.

[44] Jedlinski Z, Walach W, Kurcok P, Adamus G. Polymerization of lactones.12. Polymerization of L-dilactide and L,D-dilactide in the presence of potassium methoxide. Makromolekulare Chemie-Macromolecular Chemistry and Physics 1991;192:2051-2057.

[45] Kricheldorf HR, Dunsing R. Polylactones.8. Mechanism of the cationic polymerization of L,L-dilactide. Makromolekulare Chemie-Macromolecular Chemistry and Physics 1986;187:1611-1625.

[46] Ouhadi T, Stevens C, Teyssie P. Mechanism of e-caprolactone polymerization by aluminum alkoxides. Die Makromolekulare Chemie, Suppl. 1975;1:191-201.

[47] Kricheldorf HR, Berl M, Scharnagl N. Poly(lactones).9. Polymerization mechanism of metal alkoxide initiated polymerizations of lactide and various lactones. Macromolecules 1988;21:286-293.

[48] Kricheldorf HR, Lee SR. Polylactones.32. High-molecular-weight polylactides by ring-opening polymerization with dibutylmagnesium or butylmagnesium chloride. Polymer 1995;36:2995-3003.

[49] Nijenhuis AJ, Grijpma DW, Pennings AJ. Lewis acid-catalyzed polymerization of L-lactide - kinetics and mechanism of the bulk polymerization. Macromolecules 1992;25:6419-6424.

[50] Kricheldorf HR, Kreisersaunders I, Boettcher C. Polylactones.31. Sn(II)octoate-initiated polymerization of L-lactide - a mechanistic study. Polymer 1995;36:1253-1259.

[51] Kowalski A, Duda A, Penczek S. Kinetics and mechanism of cyclic esters polymerization initiated with tin(II) octoate. 3. Polymerization of L,L-dilactide. Macromolecules 2000;33:7359-7370.

[52] Dubois P, Jacobs C, Jerome R, Teyssie P. Macromolecular engineering of polylactones and polylactides.4. Mechanism and kinetics of lactide homopolymerization by aluminum isopropoxide. Macromolecules 1991;24:2266-2270.

[53] Bero M, Kasperczyk J, Jedlinski ZJ. Coordination polymerization of lactides.1. Structure determination of obtained polymers. Makromolekulare Chemie-Macromolecular Chemistry and Physics 1990;191:2287-2296.

[54] Stolt M, Sodergard A. Use of monocarboxylic iron derivatives in the ring-opening polymerization of L-lactide. Macromolecules 1999;32:6412-6417.

[55] Kricheldorf HR, Serra A. Polylactones.6. Influence of various metal-salts on the optical purity of poly(L-lactide). Polymer Bulletin 1985;14:497-502.

[56] Chamberlain BM, Jazdzewski BA, Pink M, Hillmyer MA, Tolman WB. Controlled polymerization of DL-lactide and e-caprolactone by structurally well-defined alkoxo-bridged di- and triyttrium(III) complexes. Macromolecules 2000;33:3970-3977.

[57] Tanzi MC, Verderio P, Lampugnani MG, Resnati M, Dejana E, Sturani E. Cytotoxicity of some catalysts commonly used in the synthesis of copolymers for biomedical use. Journal of Materials Science-Materials in Medicine 1994;5:393-396.

[58] Budavari S, O'Neil MJ, Smith A, Heckelman PE, Kinneary JF, eds. The Merck Index. 12 ed. Whitehouse Station, NJ: Merck & Co., Inc.; 1996.

[59] Desai NP, Hubbell JA. Solution technique to incorporate polyethylene oxide and other water-soluble polymers into surfaces of polymeric biomaterials. Biomaterials 1991;12:144-153.

[60] Desai NP, Hubbell JA. Surface physical interpenetrating networks of poly(ethylene-terephthalate) and poly(ethylene oxide) with biomedical applications. Macromolecules 1992;25:226-232.

[61] Zhu KJ, Lin XZ, Yang SL. Preparation, characterization, and properties of polylactide (PLA) poly(ethylene glycol) (PEG) copolymers - a potential drug carrier. J Appl Polym Sci 1990;39:1-9.

[62] Gopferich A, Peter SJ, Lucke A, Lu LC, Mikos AG. Modulation of marrow stromal cell function using poly(D,L-lactic acid)-block-poly(ethylene glycol)-monomethyl ether surfaces. Journal of Biomedical Materials Research 1999;46:390-398.

[63] Lampin M, Warocquier-Clerout R, Legris C, Degrange M, Sigot-Luizard MF. Correlation between substratum roughness and wettability, cell adhesion, and cell migration. J Biomed Mater Res 1997;36:99-108.

[64] Mooney D, Hansen L, Vacanti J, Langer R, Farmer S, Ingber D. Switching from differentiation to growth in hepatocytes - control by extracellular matrix. J Cell Physiol 1992;151:497-505.

[65] Chanda M, Advanced Polymer Chemistry: A Problem Solving Guide. 2000, New York: Marcel Dekker.

[66] Masson P, Beinert G, Franta E, Rempp P. Synthesis of Polyethylene Oxide Macromers. Polymer Bulletin 1982;7:17-22.

[67] Ishizu K, Furukawa T. Synthesis of functionalized poly(ethylene oxide) macromonomers. Polymer 2001;42:7233-7236.

[68] Zalipsky S. Functionalized poly(ethylene glycol) for preparation of biologically relevant conjugates. Bioconj Chem 1995;6:150-165.

[69] Cammas S, Nagasaki Y, Kataoka K. Heterobifunctional poly(ethylene oxide) - Synthesis of a-methoxy-w-amino and a-hydroxy-w-amino PEOs with the same molecular-weights. Bioconj Chem 1995;6:226-230.

[70] Nagasaki Y, Iijima M, Kato M, Kataoka K. Primary amino-terminal heterobifunctional poly(ethylene oxide) - facile synthesis of poly(ethylene oxide) with a primary amino group at one end and a hydroxyl group at the other end. Bioconj Chem 1995;6:702-704.

[71] Yokoyama M, Okano T, Sakurai Y, Kikuchi A, Ohsako N, Nagasaki Y, Kataoka K. Synthesis of poly(ethylene oxide) with heterobifunctional reactive groups at its terminals by an anionic initiator. Bioconj Chem 1992;3:275-276.

[72] Nagasaki Y, Kutsuna T, Iijima M, Kato M, Kataoka K, Kitano S, Kadoma Y. Formyl-ended heterobifunctional poly(ethylene oxide) - synthesis of poly(ethylene oxide) with a formyl group at one end and a hydroxyl group at the other end. Bioconj Chem 1995;6:231-233.

[73] Li SM, Vert M. Synthesis, characterization, and stereocomplex-induced gelation of block copolymers prepared by ring-opening polymerization of L(D)-lactide in the presence of poly(ethylene glycol). Macromolecules 2003;36:8008-8014.

[74] Zhu ZX, Xiong CD, Zhang LL, Yuan ML, Deng XM. Preparation of biodegradable polylactide-co-poly(ethylene glycol) copolymer by lactide reacted poly(ethylene glycol). European Polymer Journal 1999;35:1821-1828.

[75] Kissel T, Li YX, Unger F. ABA-triblock copolymers from biodegradable polyester A-blocks and hydrophilic poly(ethylene oxide) B-blocks as a candidate for in situ forming hydrogel delivery systems for proteins. Adv Drug Del Rev 2002;54:99-134.

[76] Younes H, Cohn D. Morphological study of biodegradable PEO/PLA block copolymers. J Biomed Mater Res 1987;21:1301-1316.

[77] Cohn D, Marom G, Younes H. Design and synthesis of biodegradable poly(ether-esters). In: Pizzoferrato A, Marchetti PG, Ravaglioli A, Lee AJC, editors. Advances in Biomaterials: Biomaterials and Clinical Applications. Amsterdam: Elsevier Science Publishers B.V.; 1987. p. 503-510.

[78] Cohn D, Younes H. Biodegradable PEO/PLA block copolymers. J Biomed Mater Res 1988;22:993-1009.

[79] Deng XM, Xiong CD, Cheng LM, Xu RP. Synthesis and characterization of block copolymers from D,L-lactide and poly(ethylene glycol) with stannous chloride. Journal of Polymer Science Part C-Polymer Letters 1990;28:411-416.

[80] Kricheldorf HR, Meierhaack J. Polylactones.22. ABA triblock copolymers of L-lactide and poly(ethylene glycol). Makromolekulare Chemie-Macromolecular Chemistry and Physics 1993;194:715-725.

[81] Hu DSG, Liu HJ. Structural-analysis and degradation behavior in polyethylene-glycol poly(L-lactide) copolymers. J Appl Polym Sci 1994;51:473-482.

[82] Sakurai K, Nakada Y, Nakamura T, Tudomi R, Matumoto J, Takahashi Y. Preparation and characterization of polylactide-poly(ethylene glycol)-polylactide triblock polymers and a preliminary in vivo examination of the blood circulation time for the nanoparticles made therefrom. J Macromol Sci-Pure Appl Chem 1999;36:1863-1877.

[83] Rashkov I, Manolova N, Li SM, Espartero JL, Vert M. Synthesis, characterization, and hydrolytic degradation of PLA/PEO/PLA triblock copolymers with short poly(L-lactic acid) chains. Macromolecules 1996;29:50-56.

[84] Jedlinski Z, Kurcok P, Walach W, Janeczek H, Radecka I. Polymerization of lactones.17. Synthesis of ethylene glycol-L-lactide block-copolymers. Makromolekulare Chemie-Macromolecular Chemistry and Physics 1993;194:1681-1689.

[85] Kricheldorf HR, Boettcher C. Polylactones.27. Anionic-polymerization of L-lactide - Variation of endgroups and synthesis of block-copolymers with poly(ethylene oxide). Makromolekulare Chemie-Macromolecular Symposia 1993;73:47-64.

[86] Li Y, Kissel T. Synthesis, characteristics and in vitro degradation of star-block copolymers consisting of -lactide, glycolide and branched multi-arm poly(ethylene oxide). Polymer 1998;39:4421-4427.

[87] Choi YK, Kim SW, Bae YH. Thermoplastic biodegradable hydrogels: Star-shaped block copolymer for polypeptide drug delivery. Abstracts of Papers of the American Chemical Society 1996;212:8-POLY.

[88] Kwon GS, Okano T. Polymeric micelles as new drug carriers. Adv Drug Del Rev 1996;21:107-116.

[89] Göpferich A, Peter SJ, Lucke A, Lu LC, Mikos AG. Modulation of marrow stromal cell function using poly(D,L-lactic acid)-block-poly(ethylene glycol)-monomethyl ether surfaces. J Biomed Mater Res 1999;46:390-398.

[90] Lieb E, Tessmar J, Hacker M, Fischbach C, Rose D, Blunk T, Mikos AG, Göpferich A, Schulz MB. Poly(D,L-lactic acid)-poly(ethylene glycol)-monomethyl ether diblock

copolymers control adhesion and osteoblastic differentiation of marrow stromal cells. Tissue Eng 2003;9:71-84.

[91] Hubbell JA. Bioactive biomaterials. Current Opinion in Biotechnology 1999;10:123-129.

[92] Lu L, Kam L, Hasenbein M, Nyalakonda K, Bizios R, Göpferich A, Young JF, Mikos AG. Retinal pigment epithelial cell function on substrates with chemically micropatterned surfaces. Biomaterials 1999;20:2351-2361.

[93] Kane RS, Takayama S, Ostuni E, Ingber DE, Whitesides GM. Patterning proteins and cells using soft lithography. Biomaterials 1999;20:2363-2376.

[94] Cook AD, Hrkach JS, Gao NN, Johnson IM, Pajvani UB, Cannizzaro SM, Langer R. Characterization and development of RGD-peptide-modified poly(lactic acid-co-lysine) as an interactive, resorbable biomaterial. Journal of Biomedical Materials Research 1997;35:513-523.

[95] Carlisle ES, Mariappan MR, Nelson KD, Thomes BE, Timmons RB, Constantinescu A, Eberhart RC, Bankey PE. Enhancing hepatocyte adhesion by pulsed plasma deposition and polyethylene glycol coupling. Tissue Eng 2000;6:45-52.

[96] Cima LG. Polymer substrates for controlled biological interactions. J Cell Biochem 1994;56:155-161.

[97] Klee D, Hocker H. Polymers for biomedical applications: Improvement of the interface compatibility. Biomedical Applications: Polymer Blends; 1999. p. 1-57.

[98] Gregorius K, Mouritsen S, Elsner HI. Hydrocoating: a new method for coupling biomolecules to solid phases. Journal of Immunological Methods 1995;181:65-73.

[99] Tessmar JK, Mikos AG, Göpferich A. Amine-reactive biodegradable diblock copolymers. Biomacromolecules 2002;3:194-200.

[100] Tessmar J, Mikos A, Göpferich A. The use of poly(ethylene glycol)-block-poly(lactic acid) derived copolymers for the rapid creation of biomimetic surfaces. Biomaterials 2003;24:4475-4486.

[101] Hollinger JO, Leong K. Poly(a-hydroxy acids): Carriers for bone morphogenetic proteins. Biomaterials 1996;17:187-194.

[102] Mikos AG, Thorsen AJ, Czerwonka LA, Bao Y, Langer R, Winslow DN, Vacanti JP. Preparation and characterization of poly(L-lactic acid) foams. Polymer 1994;35:1068-1077.

[103] Shastri VP, Martin I, Langer R. Macroporous polymer foams by hydrocarbon templating. PNAS 2000;97:1970-1975.

[104] Hacker M, Tessmar J, Neubauer M, Blaimer A, Blunk T, Göpferich A, Schulz MB. Towards biomimetic scaffolds: Anhydrous scaffold fabrication from biodegradable amine-reactive diblock copolymers. Biomaterials 2003;24:4459-4473.

[105] Widmer MS, Gupta PK, Lu L, Meszlenyi RK, Evans GRD, Brandt K, Savel T, Gurlek A, Patrick Jr CW, Mikos AG. Manufacture of porous biodegradable polymer conduits by an extrusion process for guided tissue regeneration. Biomaterials 1998;19:1945-1955.

[106] Aubert JH, Clough RL. Low-density, microcellular polystyrene foams. Polymer 1985;26:2047-2054.

[107] Hoffman AS. Hydrogels for biomedical applications. Adv Drug Del Rev 2002;54:3-12.

[108] Allin S, Payton E. in Chemical Engineering and Materials Science Engineering. 2003, Virginia Polytechnic Institute and State University: Blacksburg, VA.

[109] Shin YM, Hohman MM, Brenner MP, Rutledge GC. Experimental characterization of electrospinning: the electrically forced jet and instabilities. Polymer 2001;42:9955-9967.

[110] Boland ED, Wnek GE, Simpson DG, Pawlowski KJ, Bowlin GL. Tailoring tissue engineering scaffolds using electrostatic processing techniques: A study of poly(glycolic acid) electrospinning. J Macromol Sci-Pure Appl Chem 2001;38:1231-1243.

[111] Kenawy ER, Layman JM, Watkins JR, Bowlin GL, Matthews JA, Simpson DG, Wnek GE. Electrospinning of poly(ethylene-co-vinyl alcohol) fibers. Biomaterials 2003;24:907-913.

[112] Li WJ, Laurencin CT, Caterson EJ, Tuan RS, Ko FK. Electrospun nanofibrous structure: A novel scaffold for tissue engineering. J Biomed Mater Res 2002;60:613-621.

[113] Zong XH, Ran SF, Fang DF, Hsiao BS, Chu B. Control of structure, morphology and property in electrospun poly (glycolide-co-lactide) non-woven membranes via post-draw treatments. Polymer 2003;44:4959-4967.

[114] Deitzel JM, Kleinmeyer J, Harris D, Beck Tan NC. The effect of processing variables on the morphology of electrospun nanofibers and textiles. Polymer 2001;42:261-272.

[115] Gupta P, Wilkes GL. Some investigations on the fiber formation by utilizing a side-by-side bicomponent electrospinning approach. Polymer 2003;44:6353-6359.

[116] Reneker DH, Kataphinan W, Theron A, Zussman E, Yarin AL. Nanofiber garlands of polycaprolactone by electrospinning. Polymer 2002;43:6785-6794.

[117] Yoshimoto H, Shin YM, Terai H, Vacanti JP. A biodegradable nanofiber scaffold by electrospinning and its potential for bone tissue engineering. Biomaterials 2003;24:2077-2082.

[118] Ohgo K, Zhao CH, Kobayashi M, Asakura T. Preparation of non-woven nanofibers of Bombyx mori silk, Samia cynthia ricini silk and recombinant hybrid silk with electrospinning method. Polymer 2003;44:841-846.

[119] Li SM, Garreau H, Vert M. Structure property relationships in the case of the degradation of massive aliphatic poly-(a-hydroxy acids) in aqueous-media .1. poly(DL-lactic acid). Journal of Materials Science-Materials in Medicine 1990;1:123-130.

[120] Li SM, Garreau H, Vert M. Structure property relationships in the case of the degradation of massive poly(a-hydroxy acids) in aqueous-media .2. Degradation of lactide-glycolide copolymers - PLA37.5GA25 and PLA75GA25. Journal of Materials Science-Materials in Medicine 1990;1:131-139.

[121] Pitt CG, Gratzl MM, Kimmel GL, Surles J, Schindler A. Aliphatic polyesters.2. The degradation of poly(DL-lactide), poly(e-caprolactone), and their copolymers in vivo. Biomaterials 1981;2:215-220.

[122] Reed AM, Gilding DK. Biodegradable polymers for use in surgery - poly(glycolic)-poly(lactic acid) homo and co-polymers .2. In vitro degradation. Polymer 1981;22:494-498.

[123] Hakkarainen M. Aliphatic polyesters: Abiotic and biotic degradation and degradation products. Degradable Aliphatic Polyesters; 2002. p. 113-138.

[124] von Burkersroda F, Schedl L, Göpferich A. Why degradable polymers undergo surface erosion or bulk erosion. Biomaterials 2002;23:4221-4231.

[125] Vert M, Li S, Garreau H, Mauduit J, Boustta M, Schwach G, Engel R, Coudane J. Complexity of the hydrolytic degradation of aliphatic polyesters. Angewandte Makromolekulare Chemie 1997;247:239-253.

[126] Griffith LG. Polymeric biomaterials. Acta Materialia 2000;48:263-277.

[127] Li S. Hydrolytic degradation characteristics of aliphatic polyesters derived from lactic and glycolic acids. J Biomed Mater Res (Appl Biomater) 1999;48:342-353.

[128] Vert M, Mauduit J, Li SM. Biodegradation of PLA/GA polymers - increasing complexity. Biomaterials 1994;15:1209-1213.

[129] Amass W, Amass A, Tighe B. A review of biodegradable polymers: Uses, current developments in the synthesis and characterization of biodegradable polyesters, blends of biodegradable polymers and recent advances in biodegradation studies. Polymer International 1998;47:89-144.

[130] Pitt CG. Poly-e-caprolactone and its copolymers. In: Langer R, Chasin M, editors. Biodegradable Polymers and Drug Delivery Systems. New York: Marcel Dekker; 1990. p. 71-120.

[131] Schmitt EA, Flanagan DR, Linhardt RJ. Importance of distinct water environments in the hydrolysis of poly(DL-lactide-co-glycolide). Macromolecules 1994;27:743-748.

[132] Göpferich A. Mechanisms of polymer degradation and erosion. Biomaterials 1996;17:103-114.

[133] Schwach G, Coudane J, Engel R, Vert M. Influence of polymerization conditions on the hydrolytic degradation of poly(DL-lactide) polymerized in the presence of stannous octoate or zinc metal. Biomaterials 2002;23:993-1002.

[134] Li SM, Garreau H, Vert M. Structure-property relationships in the case of the degradation of massive poly(a-hydroxy acids) in aqueous-media .3. Influence of the morphology of poly(L-lactic acid). Journal of Materials Science-Materials in Medicine 1990;1:198-206.

[135] Grizzi I, Garreau H, Li S, Vert M. Hydrolytic degradation of devices based on poly(D,L-lactic acid) size-dependence. Biomaterials 1995;16:305-311.

[136] Chu CC. Hydrolytic degradation of polyglycolic acid - tensile-strength and crystallinity study. J Appl Polym Sci 1981;26:1727-1734.

[137] Mariette B, Vert M, Coudane J. Stereocopolymers for parenteral sustained-release of peptides - Release of GRF29NH(2) from a PLA/GA matrix. Journal of Controlled Release 1994;28:297-298.

[138] Therin M, Christel P, Li SM, Garreau H, Vert M. In vivo degradation of massive poly(a-hydroxy acids) - validation of in vitro findings. Biomaterials 1992;13:594-600.

[139] Cordewener FW, Rozema FR, Bos RRM, Boering G. Material properties and tissue reaction during degradation of poly(96L/4D-lactide) - a study in-vitro and in rats. Journal of Materials Science-Materials in Medicine 1995;6:211-217.

[140] Vert M, Christel P, Chabot F, Leray J. Bioresorbable plastic materials for bone surgery. In: Hastings GW, Ducheyne P, editors. Bacromolecular biomaterials. Boca Raton, FL: CRC Press; 1984. p. 119-142.

[141] Vert M, Chabot F, Leray J, Christel P. Stereoregular bioresorbable polyesters for orthopedic-surgery. Makromolekulare Chemie-Macromolecular Chemistry and Physics 1981:30-41.

[142] Nakamura T, Hitomi S, Watanabe S, Shimizu Y, Jamshidi K, Hyon SH, Ikada Y. Bioabsorption of polylactides with different molecular-properties. Journal of Biomedical Materials Research 1989;23:1115-1130.

[143] Christel P, Chabot F, Leray JL, Morin C, Vert M. Biodegradable composites for internal fixation. In: Winter GD, Gibbons DF, Plenk H, editors. Biomaterials 1980. New York: John Wiley and Sons; 1982. p. 271-280.

[144] Leenslag JW, Pennings AJ, Bos RRM, Rozema FR, Boering G. Resorbable materials of poly(L-lactide) .7. In vivo and in vitro degradation. Biomaterials 1987;8:311-314.

[145] Bianco P, Riminucci M, Gronthos S, Robey PG. Bone marrow stromal stem cells: Nature, biology, and potential applications. Stem Cells 2001;19:180-192.

[146] Sell S. Stem cells: What are they? Where do they come from? Why are they here? When do they go wrong? Where are they going? In: Sell S, editor. Stem Cells Handbook. Totowa, NJ: Humana Press Inc.; 2004. p. 1-17.

[147] Lian JB, Stein GS. Concepts of Osteoblast Growth and Differentiation - Basis for Modulation of Bone Cell-Development and Tissue Formation. Critical Reviews in Oral Biology & Medicine 1992;3:269-305.

[148] Lian JB, Stein GS. The developmental stages of osteoblast growth and differentiation exhibit selective responses of genes to growth factors (TGFβ1) and hormones (vitamin D and glucocorticoids. Journal of Oral Implantology 1993;19:95-105.

[149] Shi ST, Kirk M, Kahn AJ. The role of type I collagen in the regulation of the osteoblast phenotype. Journal of Bone and Mineral Research 1996;11:1139-1145.

[150] Aubin JE. Bone stem cells. Journal of Cellular Biochemistry Supplements 1998;30/31:73-82.

[151] Li IWS, Cheifetz S, McCulloch CAG, Sampath KT, Sodek J. Effects of osteogenic protein-1 (OP-1,BMP-7) on bone matrix protein expression by fetal rat calvarial cells are differentiation stage specific. J Cell Physiol 1996;169:115-125.

[152] Kawamura M, Hatanaka K, Saito M, Ogino M, Ono T, Ogino K, Matsuo S, Harada Y. Are the anti-inflammatory effects of dexamethasone responsible for inhibition of the induction of enzymes involved in prostanoid formation in rat carrageenin-induced pleurisy? European Journal of Pharmacology 2000;400:127-135.

[153] Maniatopoulos C, Sodek J, Melcher AH. Bone-formation in vitro by stromal cells obtained from bone-marrow of young-adult rats. Cell and Tissue Research 1988;254:317-330.

[154] Cheng SL, Yang JW, Rifas L, Zhang SF, Avioli LV. Differentiation of human bone-marrow osteogenic stromal cells in vitro - induction of the osteoblast phenotype by dexamethasone. Endocrinology 1994;134:277-286.

[155] Peter SJ, Liang CR, Kim DJ, Widmer MS, Mikos AG. Osteoblastic phenotype of rat marrow stromal cells cultured in the presence of dexamethasone, β-glycerolphosphate, and L-ascorbic acid. J Cell Biochem 1998;71:55-62.

[156] Ter Brugge PJ, Jansen JA. In vitro osteogenic differentiation of rat bone marrow cells subcultured with and without dexamethasone. Tissue Eng 2002;8:321-331.

[157] Porter RM, Huckle WR, Goldstein AS. Effect of dexamethasone withdrawal on osteoblastic differentiation of bone marrow stromal cells. J Cell Biochem 2003;90:13-22.

[158] Choong PFM, Martin TJ, Ng KW. Effects of ascorbic-acid, calcitriol, and retinoic acid on the differentiation of preosteoblasts. J Ortho Res 1993;11:638-647.

[159] Jaiswal N, Haynesworth SE, Caplan AI, Bruder SP. Osteogenic differentiation of purified, culture-expanded human mesenchymal stem cells in vitro. J Cell Biochem 1997;64:295-312.

[160] Ishaug SL, Yaszemski MJ, Bizios R, Mikos AG. Osteoblast function on synthetic biodegradable polymers. J Biomed Mater Res 1994;28:1445-1453.

[161] Ishaug SL, Crane GM, Miller MJ, Yasko AW, Yaszemski MJ, Mikos AG. Bone formation by three-dimensional stromal osteoblast culture in biodegradable polymer scaffolds. J Biomed Mater Res 1997;36:17-28.

[162] Ishaug-Riley SL, Crane-Kruger GM, Yaszemski MJ, Mikos AG. Three-dimensional culture of rat calvarial osteoblasts in porous biodegradable polymers. Biomaterials 1998;19:1405-1412.

[163] Goldstein AS, Juarez TM, Helmke CD, Gustin MC, Mikos AG. Effect of convection on osteoblastic cell growth and function in biodegradable polymer foam scaffolds. Biomaterials 2001;22:1279-1288.

[164] Bergsma JE, Rozema FR, Bos RRM, Boering G, Debruijn WC, Pennings AJ. In-vivo degradation and biocompatibility study of in-vitro pre-degraded as-polymerized polylactide particles. Biomaterials 1995;16:267-274.

[165] Britland S, Periidge C, Denyer M, Morgan H, Curtis A, Wilkinson C. Morphogenetic guidance cues can interact synergistically and hierarchically in steering nerve cell growth. Exp Biol Online 1996;1.

[166] den Braber ET, de Ruijter JE, Ginsel LA, von Recum AF, Jansen JA. Quantitative analysis of fibroblast morphology on microgrooved surfaces with various groove and ridge dimensions. Biomaterials 1996;17:2037-2044.

[167] Cosgrove T, Griffiths PC. The critical overlap concentration measured by pulsed-field gradient nuclear-magnetic-resonance techniques. Polymer 1994;35:509-513.

[168] Koski A, Yim K, Shivkumar S. Effect of molecular weight on fibrous PVA produced by electrospinning. Materials Letters 2004;58:493-497.

[169] West DC, Sattar A, Kumar S. A simplified in situ solubilization procedure for the determination of DNA and cell number in tissue cultured mammalian cells. Analyt Biochem 1985;147:289-295.

[170] Goldstein AS. Effect of seeding osteoprogenitor cells as dense clusters on cell growth and differentiation. Tissue Eng 2001;7:817-827.

[171] Fischbach C, Tessmar J, Lucke A, Schnell E, Schmeer G, Blunk T, Göpferich A. Does UV irradiation affect polymer properties relevant to tissue engineering? Surface Science 2001;491:333-345.

[172] Matsuzaka K, Walboomers XF, de Ruijter JE, Jansen JA. The effect of poly-L-lactic acid with parallel surface micro groove on osteoblast-like cells in vitro. Biomaterials 1999;20:1293-1301.

[173] Mata A, Su XW, Fleischman AJ, Roy S, Banks BA, Miller SK, Midura RJ. Osteoblast attachment to a textured surface in the absence of exogenous adhesion proteins. IEEE Trans Nanobiosci 2003;2:287-294.

[174] Martin JY, Schwartz Z, Hummert TW, Schraub DM, Simpson J, Lankford J, Dean DD, Cochran DL, Boyan BD. Effect of titanium surface-roughness on proliferation, differentiation, and protein-synthesis of human osteoblast-like cells (MG63). J Biomed Mater Res 1995;29:389-401.

[175] Rosa AL, Beloti MM, van Noort R. Osteoblastic differentiation of cultured rat bone marrow cells on hydroxyapatite with different surface topography. Dent Mater 2003;19:768-772.

[176] Bruinink A, Wintermantel E. Grooves affect primary bone marrow but not osteoblastic MC3T3-E1 cell cultures. Biomaterials 2001;22:2465-2473.

[177] Liao H, Andersson A-S, Sutherland D, Petronis S, Kasemo B, Thomsen P. Response of rat osteoblast-like cells to microstructured model surfaces in vitro. Biomaterials 2003;24:649-654.

Vita

Anand Shreyans Badami was born in the Lehigh Valley of Pennsylvania in the fall of 1977. He grew up there and graduated as valedictorian from Northampton Area Senior High School in 1995. Four years later he earned his Bachelor's degree in Chemical Engineering from Villanova University. After graduation Anand worked for Validation and Process Associates, Inc. in Willow Grove, PA as a consultant in the pharmaceutical industry. His passion for learning and science led him to enroll in the Macromolecular Science and Engineering Program at Virginia Polytechnic Institute and State University in the fall of 2002. During his first summer in graduate school, Anand worked at a research internship with 3M in St. Paul, MN as a 3M Engineering Scholar for 2003. After earning his M.S. degree, he plans to pursue a Ph.D. in Macromolecular Science and Engineering.